

Supplementary Information

The Yun/Prohibitin complex regulates adult *Drosophila* intestinal stem cell proliferation through the transcription factor E2F1

Hang Zhao, Lin Shi, Zhengran Li, Ruiyan Kong, Xuejing Ren, Rui Ma, Lemei Jia, Meifang Ma, Shan Lu, Ran Xu, Richard Binari, Jian-Hua Wang, Meng-qiu Dong, Norbert Perrimon, and Zhouhua Li

Index of Supplementary Information

1. Relationship between Supplementary Figures and Figures
2. Supplementary Figures
3. Supplementary methods
4. Supplementary references
5. Full genotypes of flies in Figures

1. Relationship between Supplementary Figures and Figures

Fig. S1-S14 relate to Fig. 1

Fig. S15 relates to Fig. 2

Fig. S16-S29 relate to Fig. 3

Fig. S30-S33 relate to Fig. 4

Fig. S34 relates to Fig. 5

Fig. S35-S41 relate to Fig. 6

Fig. S42 and S43 relate to Fig. 7

2. Supplementary Figures

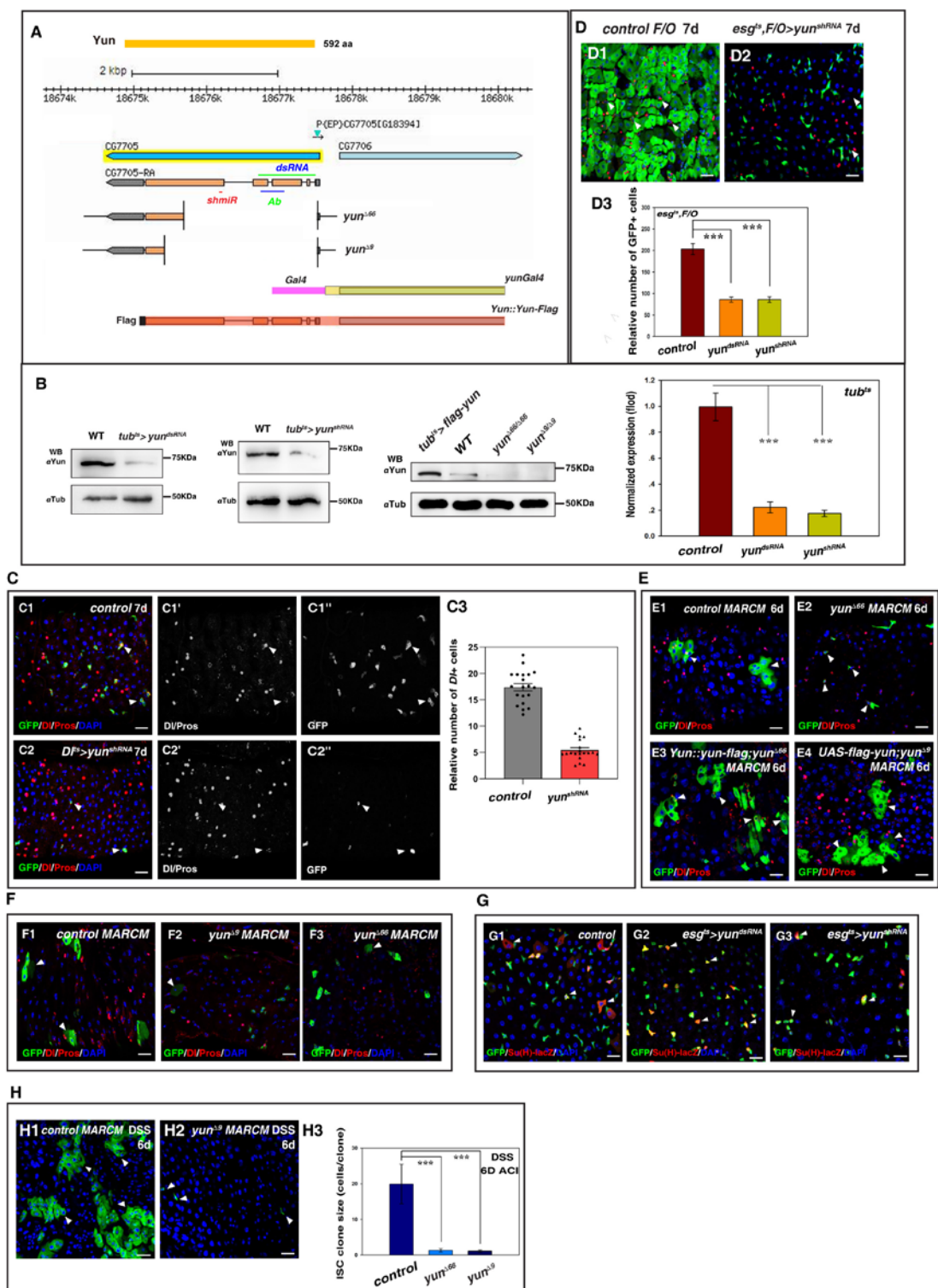


Fig. S1. Novel factor Yun is required for ISC proliferation.

(A) Schematic diagram of *yun* mutants and reagents generated in this study. See Methods for detailed information. (B) RNAi knockdown efficacy and Yun protein after

knockdown and in *yun* mutants. Yun protein levels are significantly reduced upon expression of *yun* RNAi constructs. Note that *tubGal4* is not expressed in female germline cells and ovaries are included in the samples. α Tubulin is used as a loading control. Yun protein in tissues with *yun* overexpression, WT, and *yun* homozygous mutant larva. α Tubulin is used as a loading control. The knockdown efficiency of two different *yun* RNAi lines used in this study was determined by qRT-PCR quantification from *tub^{ts}>yun^{RNAi}* flies (ovaries were not included). Ribosomal gene *RpL11* was used as a normalization control. Means \pm SD are shown. *** $P < 0.001$. (C) Yun is required for ISC proliferation. (C1) ISCs (green, by *Dl> GFP*) in control intestines at 29°C for 7 days (white arrowheads). Dl and Pros are in red. Split channel for Dl/Pros and GFP is shown separately (white arrowheads). (C2) The number of ISCs (*Dl>GFP* positive cells, green) is significantly decreased in *Dl^{ts}>yun^{shRNA}* intestines at 29°C for 7 days (white arrowheads). (C3) Quantification of the relative number of ISCs (*Dl>GFP* positive cells) in control and *yun*-depleted intestines. Mean \pm SD is shown. n=20-25 intestines. *** $P < 0.001$. (D) Yun is required for progenitor proliferation. (D1) Control *esg^{ts},F/O* midguts at 29°C for 7 days with Dl and Pros staining (red, progenitors are indicated by white arrowheads). (D2) *yun* knockdown in *esg^{ts},F/O* midguts at 29°C for 7 days with Dl and Pros staining (red, progenitors are indicated by white arrowheads). (D3) Quantification of the relative number of GFP-positive cells in different genotypes. Mean \pm SD is shown. n=20-30 intestines. *** $P < 0.001$. (E) Yun is required for ISC proliferation and regeneration. (E1) ISC MARCM clones (green) in the *FRT* control (6 days at 25°C, 6D ACI) (white arrowheads). (E2) *yun^{A66}* mutant ISC MARCM clones

(green) do not proliferate (6D ACI) (white arrowheads). (*E3* and *E4*) Restoring Yun function rescued ISC proliferation defects observed in *yun* mutants (6D ACI) (white arrowheads) (*E3*: *Yun::yun-flag; yun^{Δ66}*; *E4*: *UAS-flag-yun; yun^{Δ9}*). (*F*) Yun is not required for progeny differentiation. (*F1*) D1 and Pros staining of *FRT* control ISC MARCM clones, differentiated large ECs in the clones are indicated (white arrowheads). (*F2* and *F3*) *yun* mutant MARCM clones (*F2*: *yun^{Δ9}*, *F3*: *yun^{Δ66}*) (white arrowheads). Large D1⁻ *yun* mutant cells (GFP⁺) (putatively differentiating and mature ECs) can be observed. (*G*) EB identity and Notch activation are not affected in *yun*-depleted progenitors. (*G1*) EBs (by *GBE+Su(H)-lacZ* in red) in control intestines (white arrowheads). (*G2* and *G3*) Although the number of EB cells (by *GBE+Su(H)-lacZ* in red) is significantly decreased in *esg^{ts}>yun^{RNAi}* intestines at 29°C for 7 days (*G2*: *yun^{dsRNA}*, *G3*: *yun^{shRNA}*) (white arrowheads), EB cell identity (Notch signaling activation) is not affected. (*H*) Yun is required for regeneration. (*H1*) Control intestines with *FRT* ISC MARCM clones (green, arrowheads) can regenerate after treated with DSS (6D ACI). (*H2*) *yun* mutant MARCM clones (green, arrowheads) do not proliferate to regenerate the midgut after flies are fed with DSS (6D ACI). (*H3*) Quantification of the size of ISC clones in control and *yun* mutant intestines after DSS treatment. Mean ± SD is shown. n=15-25 intestines. ****P*<0.001. In all panels except graphs, GFP is in green and blue indicates DAPI staining of DNA. Scale bars: 20 μm.



Fig. S2. *yun* is essential for viability.

Representative images show wildtype, heterozygous and homozygous *yun*^{*Δ9*} larvae and pupa respectively. Scale bar: 0.1 mm.

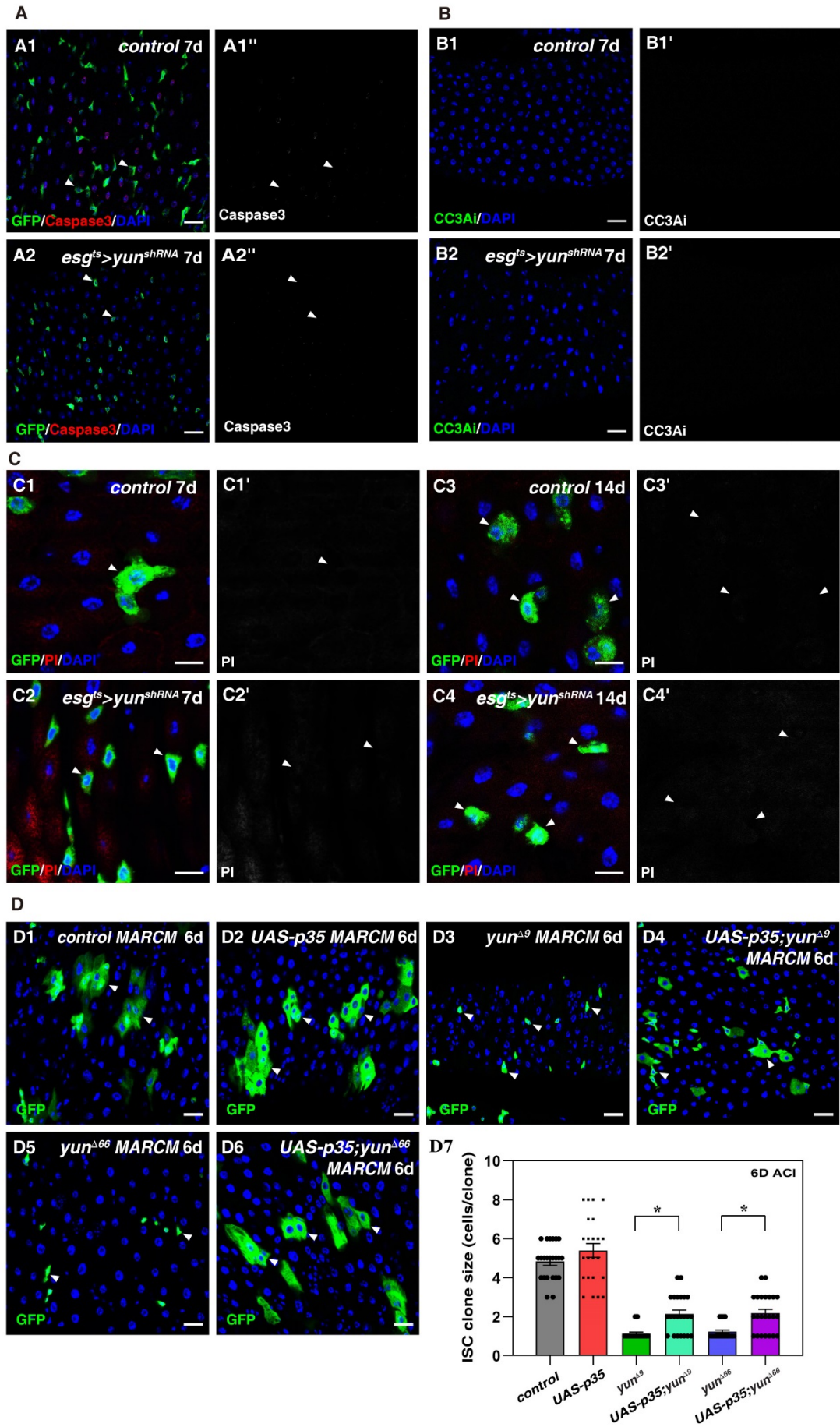


Fig. S3. Cell death is not the cause of ISC proliferation defects in the absence of Yun.

(A) No apoptosis (red, by active Caspase 3) was observed in *esg^{ts}>yun^{shRNA}* progenitors as well as in control progenitors at 29°C for 7 days (white arrowheads). Split channel for GFP and active Caspase 3 is shown separately (white arrowheads). (B) No apoptosis (green, by CC3Ai) was observed in *esg^{ts}>yun^{shRNA}* progenitors as well as in control progenitors at 29°C for 7 days (white arrowheads). Split channel for CC3Ai is shown separately. (C) No necrosis (red, by PI) was observed in *esg^{ts}>yun^{shRNA}* progenitors as well as in control progenitors at 29°C for 7 and 14 days (white arrowheads). Split channel for PI is shown separately (white arrowheads). (D) Ectopic expression of *UAS-p35* cannot rescue progenitor proliferation defects in *yun* mutants. ISC MARCM clones (white arrowheads) of different genotypes are shown. Quantification of the size of ISC clones in intestines with indicated genotypes. Mean \pm SD is shown. n=15-25 intestines. * $P<0.05$. In all panels except graphs, GFP is in green, blue indicates DAPI staining for DNA. Scale bars: 20 μ m.

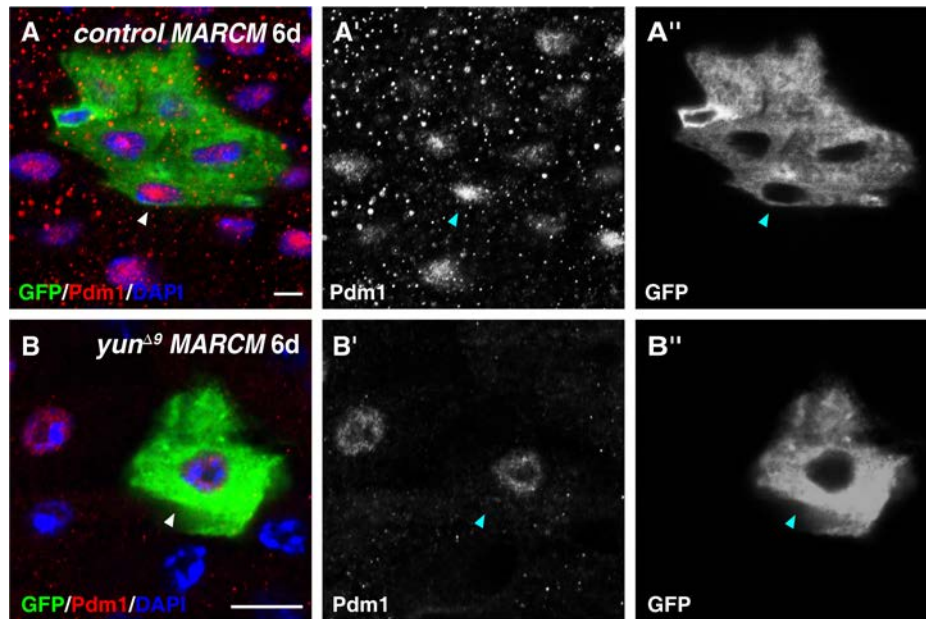


Fig. S4. EC differentiation is not affected in the absence of Yun.

(A and B) PDM1 (red) in MARCM clones (green) of control (A) and *yun*^{Δ9} (B) (white arrowheads). PDM1 and GFP channels are showed separately in black-white. GFP is in green, blue indicates DAPI staining for DNA. Scale bars: 10 μm.

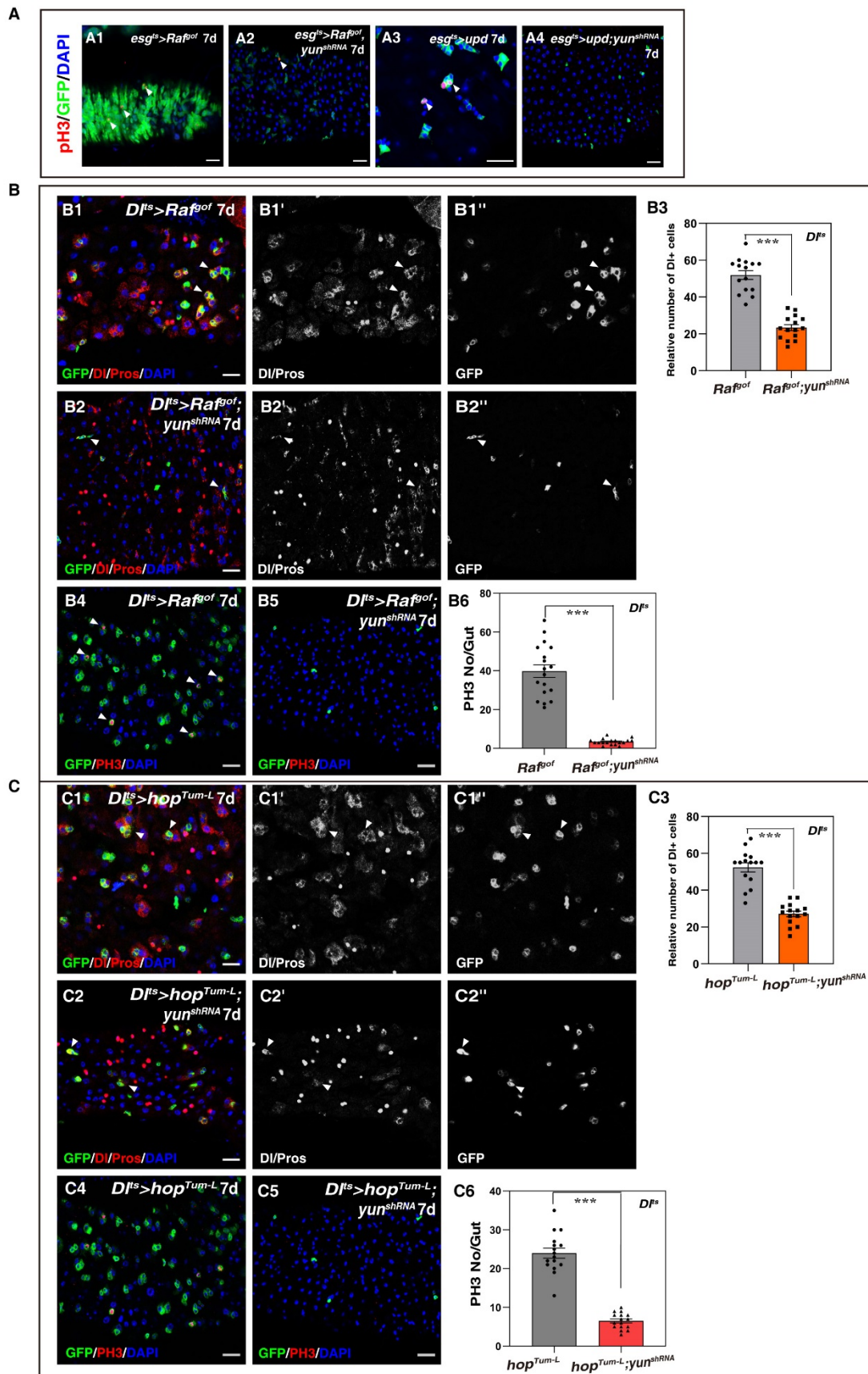


Fig. S5. *yun* is required for the proliferation of different transformed stem cells.

(A) Yun is required in progenitors for the proliferation of transformed stem cells. (A1) pH3 (red, white arrowheads) in $esg^{ts}>Raf^{gof}$ intestines at 29°C for 7 days (white arrowheads). (A2) pH3 in $esg^{ts}>yun^{RNAi}; Raf^{gof}$ intestines at 29°C for 7 days. (A3) pH3 (red, white arrowheads) in $esg^{ts}>upd$ intestines at 29°C for 7 days (white arrowheads). (A4) pH3 in $esg^{ts}>yun^{RNAi}; upd$ intestines at 29°C for 7 days. (B) Yun is required in ISCs for the proliferation of transformed stem cells that express constitutively active Raf. (B1) Activation of Raf^{gof} in ISCs (by Dl^{ts}) results in the accumulation of ISCs (by DI in red and $Dl>GFP$) at 29°C for 7 days (white arrowheads). Pros is in red. DI/Pros and GFP channels are shown separately in black-white. (B2) Simultaneous depletion of yun in $Dl^{ts}>Raf^{gof}$ intestines completely suppresses ISC accumulation at 29°C for 7 days (white arrowheads). (B3) Quantification of the relative number of ISCs in intestines with indicated genotypes. Mean \pm SD is shown. n=15 intestines. *** $P<0.001$. (B4) pH3 (red, white arrowheads) in $Dl^{ts}>Raf^{gof}$ intestines at 29°C for 7 days (white arrowheads). (B5) pH3 in $Dl^{ts}>yun^{RNAi}; Raf^{gof}$ intestines at 29°C for 7 days. (B6) Quantification of the number of PH3-positive cells per gut in intestines with indicated genotypes. Mean \pm SD is shown. n=18. *** $P<0.001$. (C) Yun is required in ISCs for the proliferation of transformed stem cells expressing constitutively active Hop. (C1) Activation of hop^{Tum-L} in ISCs (by Dl^{ts}) results in accumulation of ISCs (by DI in red and $Dl>GFP$) at 29°C for 7 days (white arrowheads). Pros is in red. DI/Pros and GFP channels are shown separately in black-white. (C2) Simultaneous depletion of yun in $Dl^{ts}>hop^{Tum-L}$ intestines completely suppresses ISC accumulation at 29°C for 7 days (white arrowheads). (C3) Quantification of the relative number of ISCs in intestines with

indicated genotypes. Mean \pm SD is shown. n=15 intestines. *** P <0.001. (C4) pH3 (red, white arrowheads) in $Dl^{ts}>hop^{Tum-L}$ intestines at 29°C for 7 days (white arrowheads). (C5) pH3 in $Dl^{ts}>yun^{RNAi}; hop^{Tum-L}$ intestines at 29°C for 7 days. (C6) Quantification of the number of PH3-positive cells per gut in intestines with indicated genotypes. Mean \pm SD is shown. n=16. *** P <0.001. In all panels except graphs, GFP is in green, blue indicates DAPI staining for DNA. Scale bars: 20 μ m.

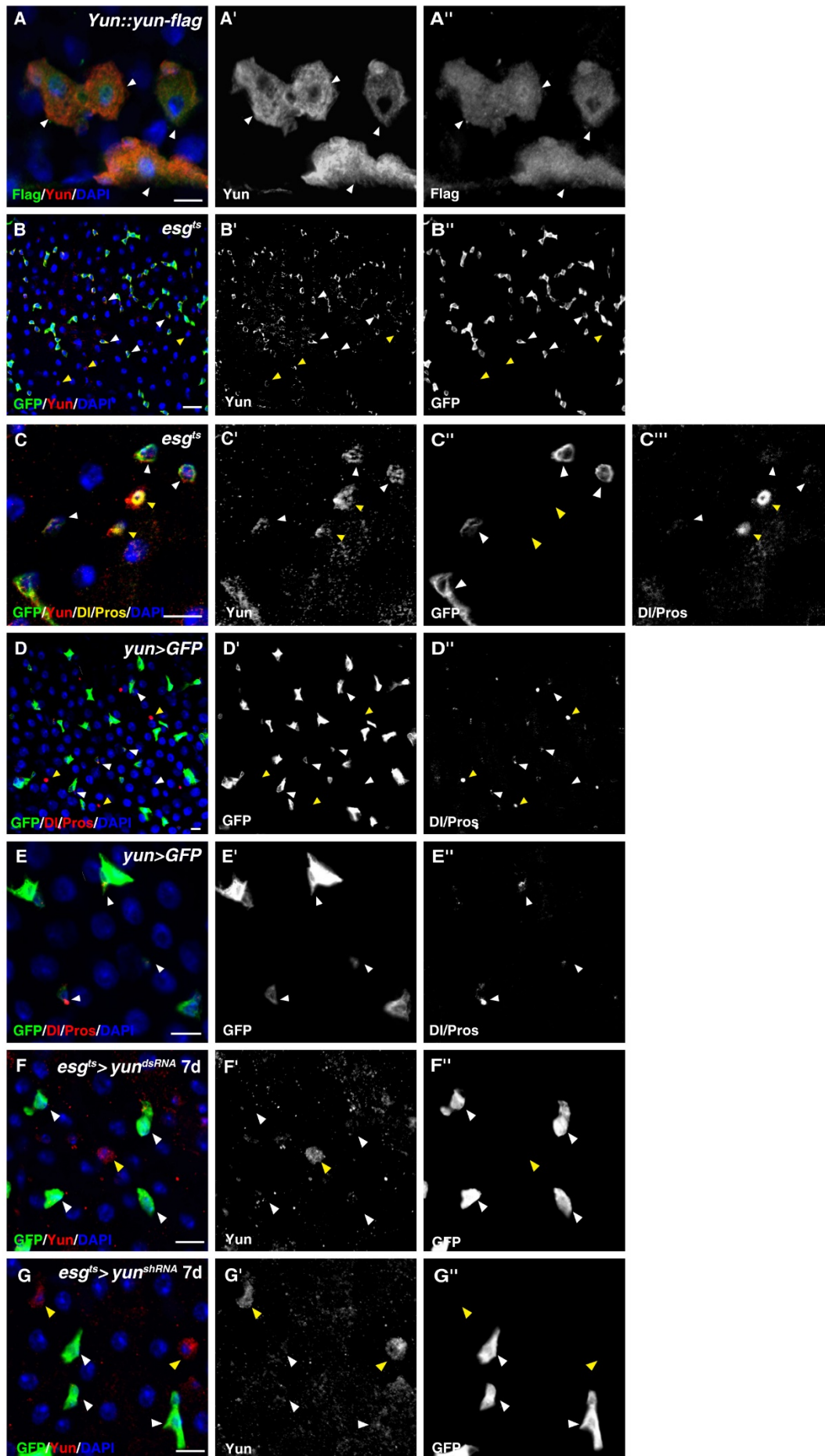


Fig. S6. Expression pattern and subcellular localization of Yun.

(A) Flag (green) and Yun (red) double labeling of *yun::yun-Flag* intestine showing co-localization. Yun is uniformly expressed in the cell, including in the cytosol and nucleus (white arrowheads). Flag and Yun channels are shown separately in black-white. (B) Yun (red) is mainly expressed in progenitors (green) and *esg>GFP* cells in intestine (white and yellow arrowheads respectively). Yun and GFP channels are shown separately in black-white. (C) Yun (red) is mainly expressed in progenitors (green, ISCs by D1 in yellow) and EE cells (by Pros in yellow) in intestine (white and yellow arrowheads, respectively). Yun, GFP, and D1/Pros channels are shown separately in black-white. (D and E) *yunGal4, UAS-GFP* cells (green) are mainly progenitors (by D1 in red), but rarely seen in EE cells (by Pros in red) (white and yellow arrowheads, respectively). GFP and D1/Pros channels are shown separately in black-white. (F and G) Knockdown of *yun* in progenitors effectively depletes Yun protein at 29°C for 7 days (white arrowheads), while Yun in EE cells is not affected (yellow arrowheads) (F: *yun^{dsRNA}*, G: *yun^{shRNA}*). GFP is in green, blue indicates DAPI staining for DNA. Scale bars: 10 μm except B and D (20 μm).

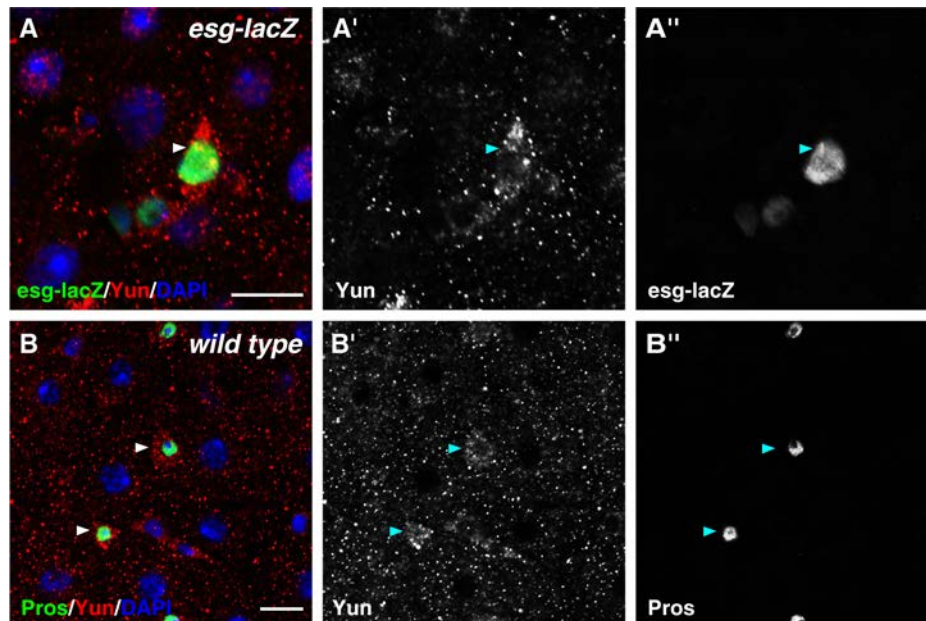


Fig. S7. Yun is expressed in progenitors and EEs.

(A) Yun (red) is expressed in progenitors (green) (white arrowheads). Yun and *esg-lacZ* channels are showed separately in black-white. (B) Yun (red) is expressed in EEs (green) (white arrowheads). Yun and Pros channels are showed separately in black-white. GFP is in green, blue indicates DAPI staining for DNA. Scale bars: 10 μ m.

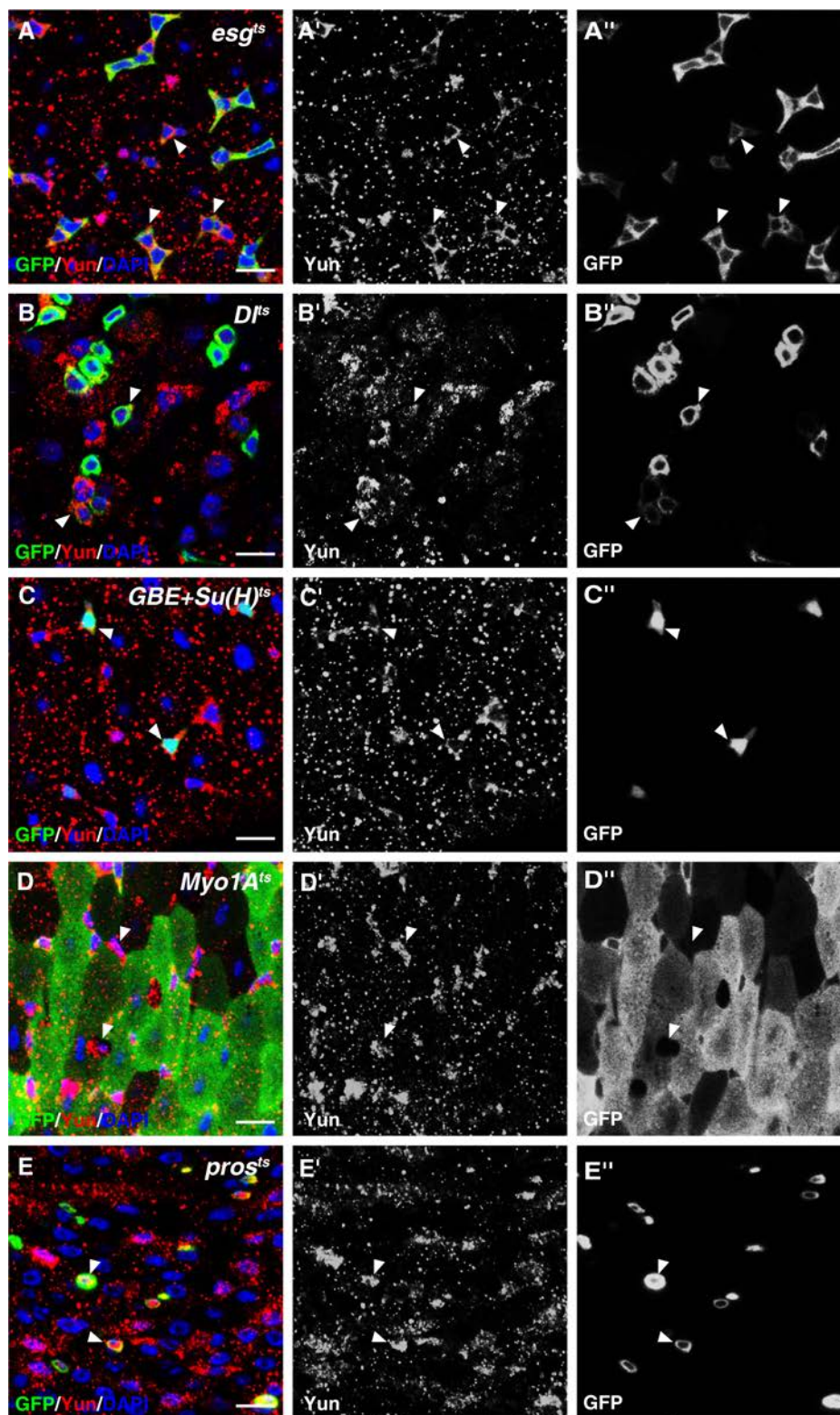


Fig. S8. Detailed examination of Yun expression pattern in intestine.

(A) Yun (red) is expressed in progenitors (green, by *esg*>*GFP*) (white arrowheads). Yun and GFP channels are showed separately in black-white. (B) Yun (red) is expressed in

ISCs (green, by *Dl>GFP*) (white arrowheads). Yun and GFP channels are showed separately in black-white. (C) Yun (red) is expressed in EBs (green, by *Gbe+Su(H)>GFP*) (white arrowheads). Yun and GFP channels are showed separately in black-white. (D) Yun (red) is not expressed in ECs (green, by *Myo1A>GFP*) (white arrowheads). Yun and GFP channels are showed separately in black-white. (E) Yun (red) is expressed in ee cells (green, by *pros>GFP*) (white arrowheads). Yun and GFP channels are showed separately in black-white. GFP is in green, blue indicates DAPI staining for DNA. Scale bars: 10 μ m.

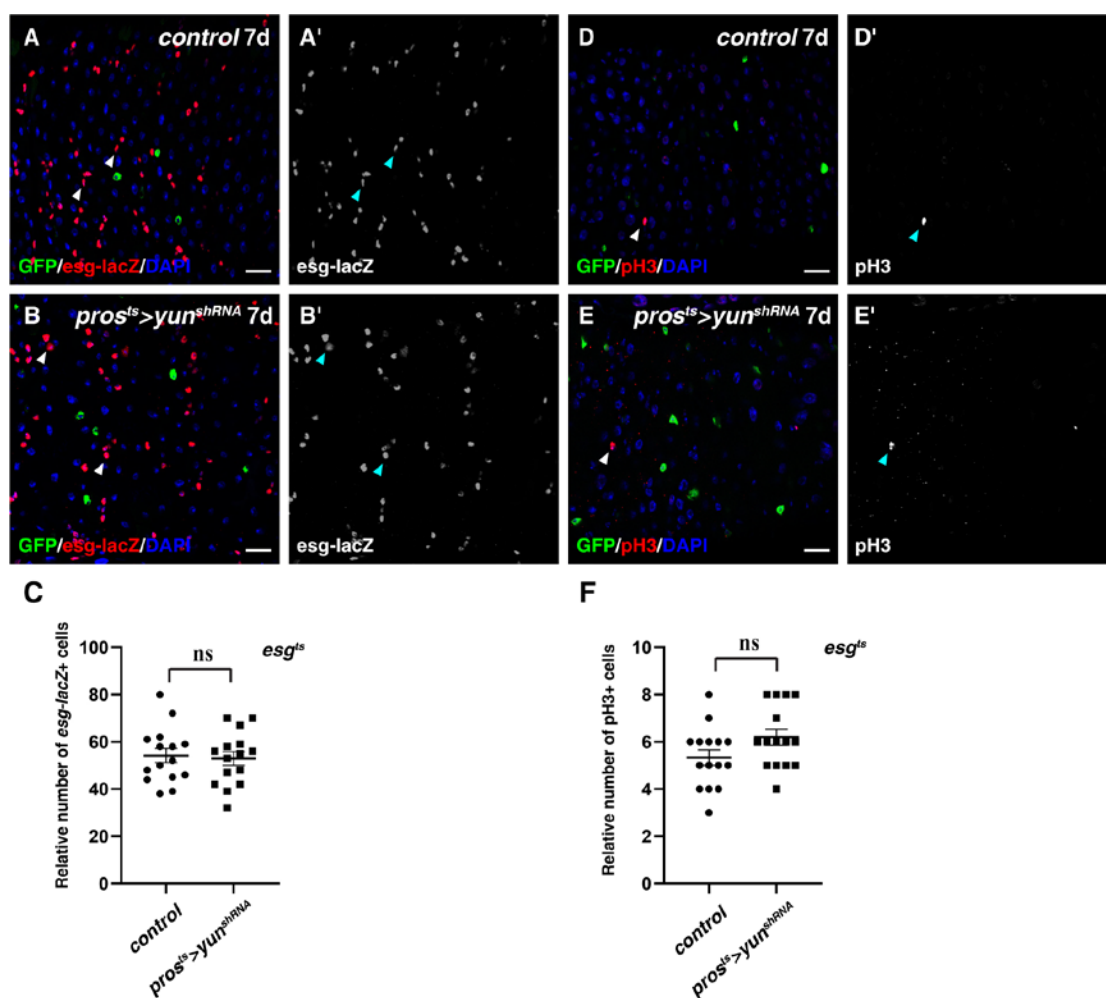


Fig. S9. Yun is dispensable in EEs for intestinal homeostasis.

(A-C) Yun in EEs is not required for intestinal homeostasis. (A) Progenitors (red, *esg-lacZ*) in control intestines at 29°C for 7 days (white arrowheads). (B) Progenitors (red, *esg-lacZ*) in *pros^{ts}>yun^{shRNA}* at 29°C for 7 days (white arrowheads). (C) Quantification of the relative number of progenitors in intestines with indicated genotypes. Mean \pm SD is shown. n=15 intestines. ^{ns}*P* >0.05. (D-F) Mitosis is not affected in the absence of Yun in EEs. (D) pH3-positive cells (red) in control at 29°C for 7 days (white arrowheads). (E) pH3-positive cells (red) in *pros^{ts}>yun^{shRNA}* at 29°C for 7 days (white arrowheads). (F) Quantification of the relative number of pH3-positive cells in intestines with indicated genotypes. Mean \pm SD is shown. n=15 intestines. ^{ns}*P* >0.05. In all panels except graphs, GFP is in green and blue indicates DAPI staining for DNA. Scale bars: 20 μ m.

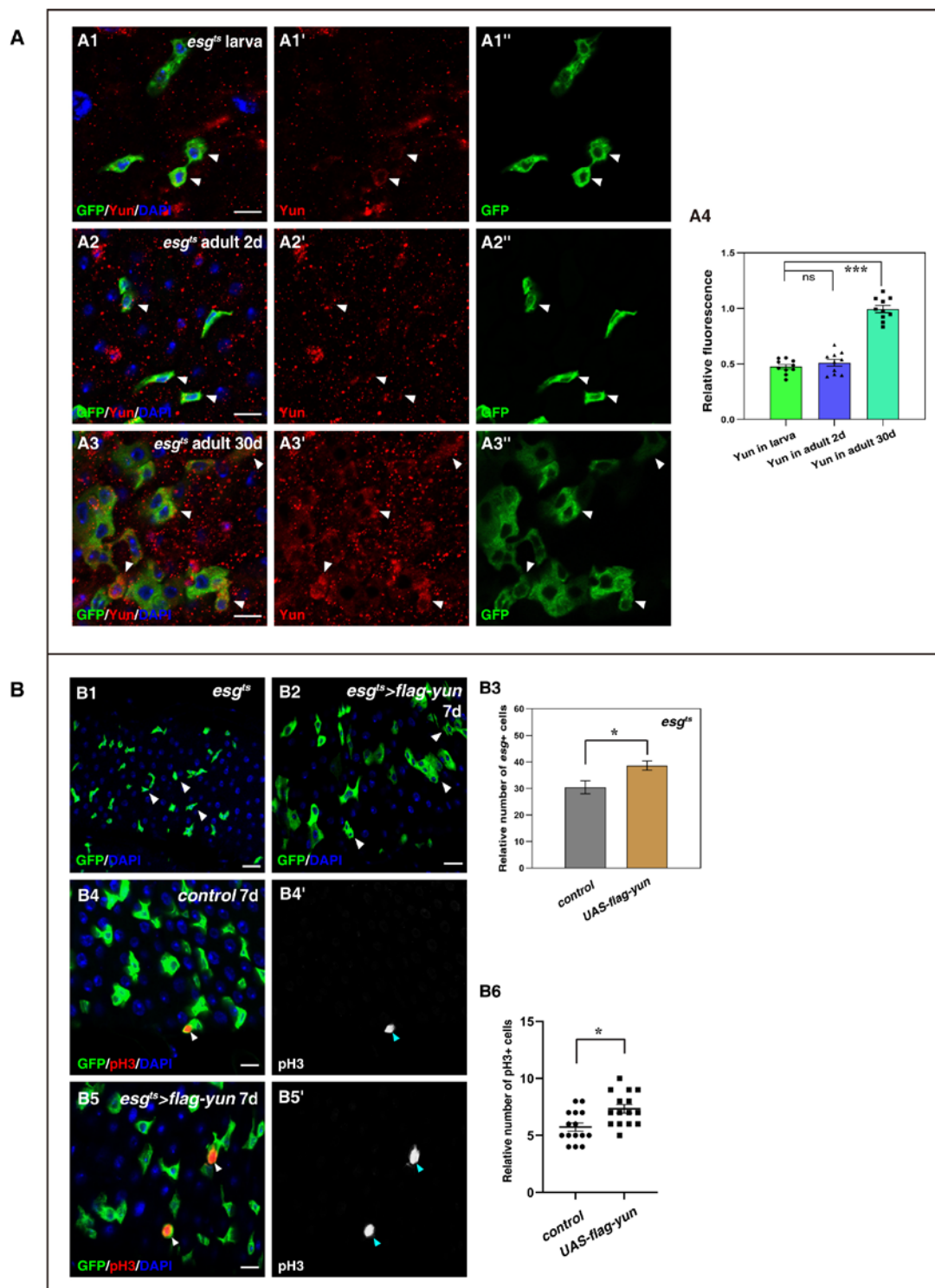


Fig. S10. The levels of Yun increase with age and ectopic expression of Yun results in increased progenitors.

(A) The levels of Yun increase with age. (A1) Yun protein (red) in progenitors of larval intestines (green, by *esg>GFP*) (white arrowheads). Yun and GFP channels are showed

separately. (A2) Yun protein (red) in progenitors of intestines of 2-day-old flies (green, by *esg>GFP*) (white arrowheads). (A3) Yun protein (red) in progenitors of intestines of 30-day-old flies (green, by *esg>GFP*) (white arrowheads). Note that the levels of Yun protein increase with age. (A4) Quantification of the fluorescence intensity of Yun protein in progenitors at different ages. Mean \pm SD is shown. n=10. ^{ns} $P>0.05$; ^{***} $P<0.001$. (B) Ectopic expression of Yun results in modest increase of progenitors. (B1) Progenitors (green, by *esg>GFP*) in control intestines at 29°C for 7 days (white arrowheads). (B2) The number of *esg*⁺ cells (green) is modestly increased in *esg^{ts}>flag-yun* intestines at 29°C for 7 days (white arrowheads). (B3) Quantification of the relative number of *esg*⁺ cells in control and *yun* overexpression intestines. Mean \pm SD is shown. n=20-30. ^{*} $P < 0.05$. (B4) pH3-positive cells (red) in control at 29°C for 7 days (white arrowheads). (B5) pH3-positive cells (red) in *esg^{ts}>flag-yun* at 29°C for 7 days (white arrowheads). (B6) Quantification of the relative number of pH3-positive cells in intestines with indicated genotypes. Mean \pm SD is shown. n=15 intestines. ^{*} $P < 0.05$. In all panels except graphs, GFP is in green and blue indicates DAPI staining for DNA. Scale bars: 20 μ m.

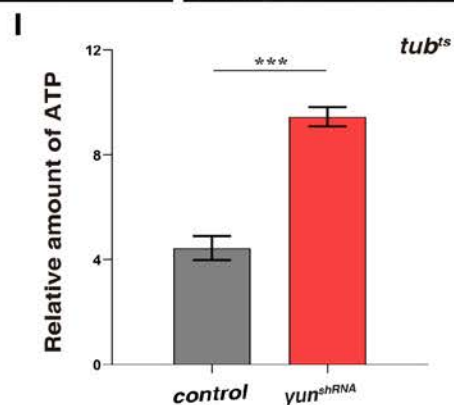
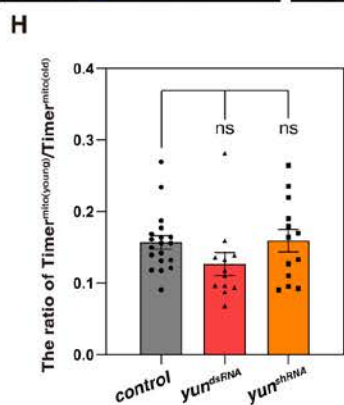
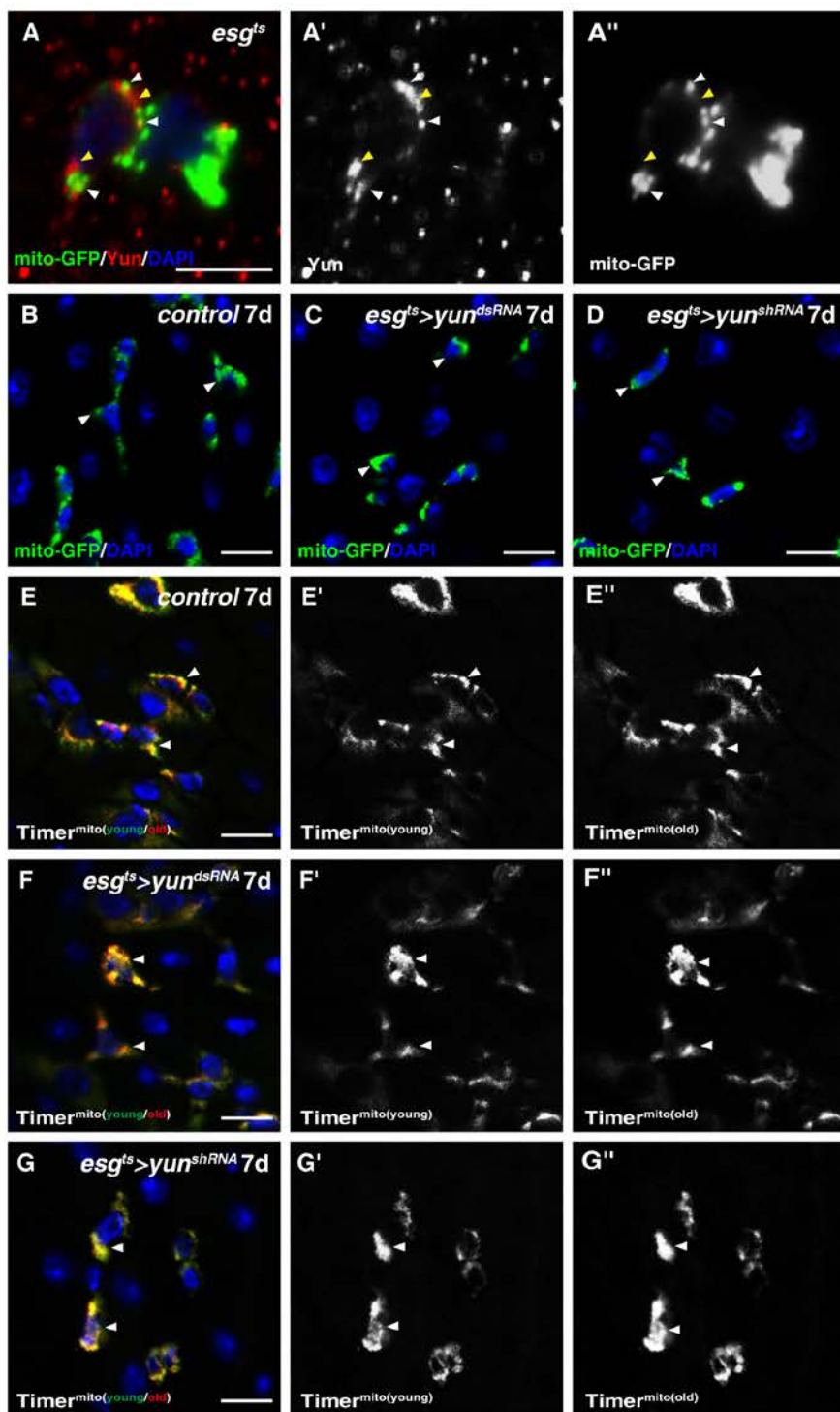


Fig. S11. No obvious mitochondrial morphology and maturation were observed in the absence of *yun*.

(A) Yun (red) and mitochondria (green, by *esg^{ts}>mito-GFP*) in progenitors. Some Yun proteins co-localize with mitochondria (white arrowheads), but the majority of Yun does not co-localize with mitochondria (yellow arrowheads). Yun and mito-GFP channels are showed separately. (B) Mitochondria (green, by *esg^{ts}>mito-GFP*) in control progenitors at 29°C for 7 days (white arrowheads). (C and D) Mitochondria (green, by *esg^{ts}>mito-GFP*) in *esg^{ts}>yun^{RNAi}* progenitors at 29°C for 7 days (white arrowheads) (C: *yun^{dsRNA}*, D: *yun^{shRNA}*). The morphology of mitochondria is largely unaffected by *yun* depletion. (E) Mitochondrial maturation (green and red, by *esg^{ts}>Timer^{mito}*) in control progenitors at 29°C for 7 days (white arrowheads). GFP (young) and RFP (mature) channels are showed separately. (F and G) Mitochondrial maturation (green and red, by *esg^{ts}>Timer^{mito}*) in *esg^{ts}>yun^{RNAi}* progenitors at 29°C for 7 days (white arrowheads) (F: *yun^{dsRNA}*, G: *yun^{shRNA}*). Mitochondrial maturation is largely unaffected by *yun* depletion. (H) Quantification of the ratio of $\text{Timer}^{\text{young}}/\text{Timer}^{\text{old}}$ fluorescence intensity number in control and *esg^{ts}>yun^{RNAi}* intestines. Mean \pm SD is shown. n=10-20. ^{ns}*P*>0.05. (I) Quantification of the relative amount of ATP in control and *tub^{ts}>yun^{shRNA}* flies. Mean \pm SD is shown. n=3. ****P*<0.001. GFP is in green and blue indicates DAPI staining for DNA. Scale bars: 10 μm except A (5 μm).

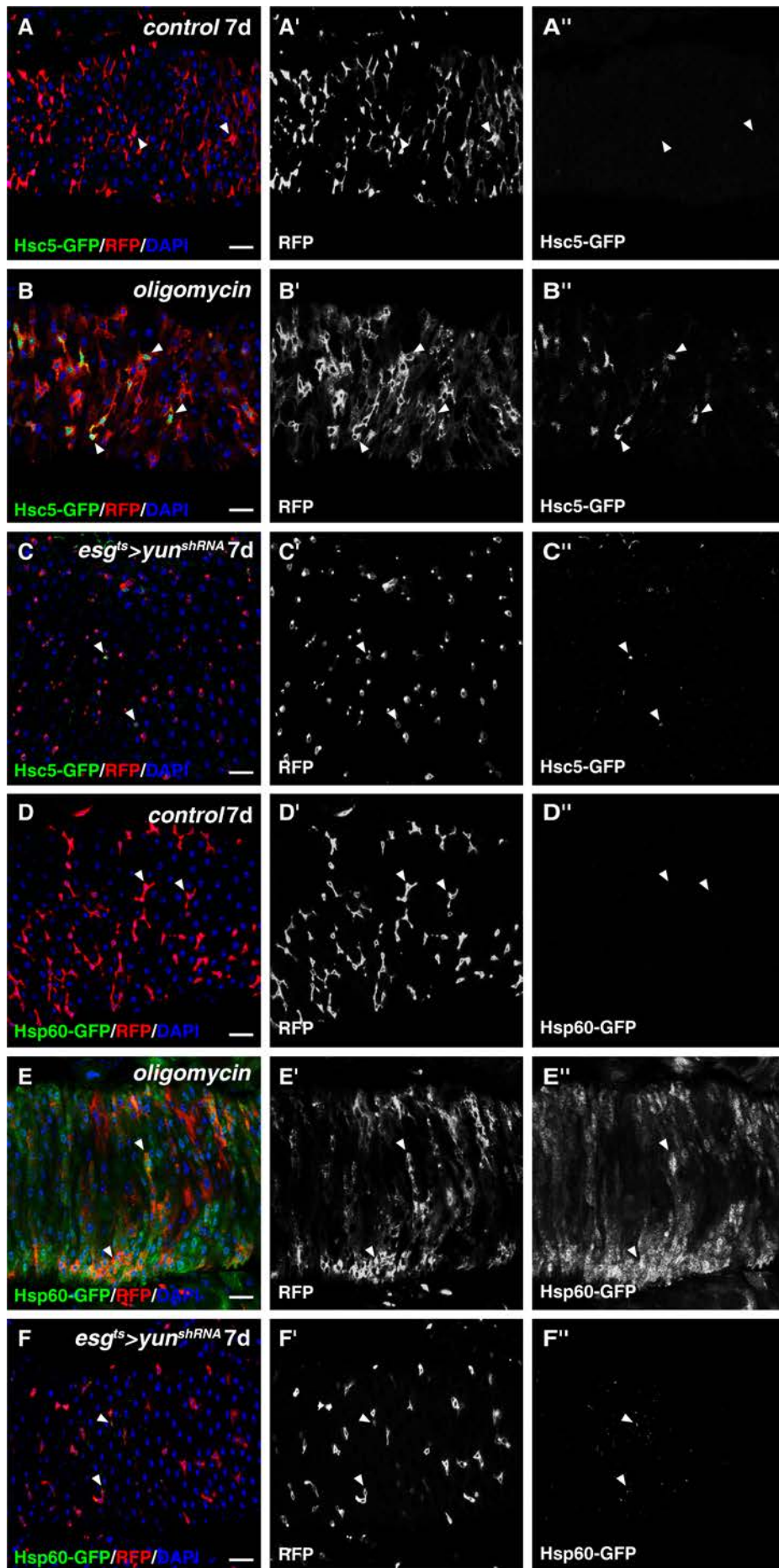


Fig. S12. No Mito^{UPR} is detected in *yun*-defective in progenitors.

(A) No mito^{UPR} (green, by *Hsc5-GFP*) is detected in progenitors (red, by *esg>RFP*) of control flies at 29°C for 7 days (white arrowheads). RFP and Hsc5-GFP/mito^{UPR} channels are showed separately. (B) Mito^{UPR} (green, by *Hsc5-GFP*) could be detected in progenitors (red, by *esg>RFP*) when the flies were fed with mitochondrial drug oligomycin (white arrowheads). (C) Mito^{UPR} (green, by *Hsc5-GFP*) is rarely detectable in progenitors of *esg^{ts}>yun^{shRNA}* flies (red, by *esg>RFP*) (white arrowheads). (D) No mito^{UPR} (green, by *Hsp60-GFP*) is detected in progenitors (red, by *esg>RFP*) of control flies at 29°C for 7 days (white arrowheads). RFP and Hsp60-GFP/mito^{UPR} channels are showed separately. (E) Extensive mito^{UPR} (green, by *Hsp60-GFP*) could be detected in progenitors (red, by *esg>RFP*) when the flies were fed with mitochondrial drug oligomycin (white arrowheads). (F) No mito^{UPR} (green, by *Hsp60-GFP*) is detectable in progenitors of *esg^{ts}>yun^{shRNA}* flies (red, by *esg>RFP*) (white arrowheads). GFP is in green and blue indicates DAPI staining for DNA. Scale bars: 20 μm.

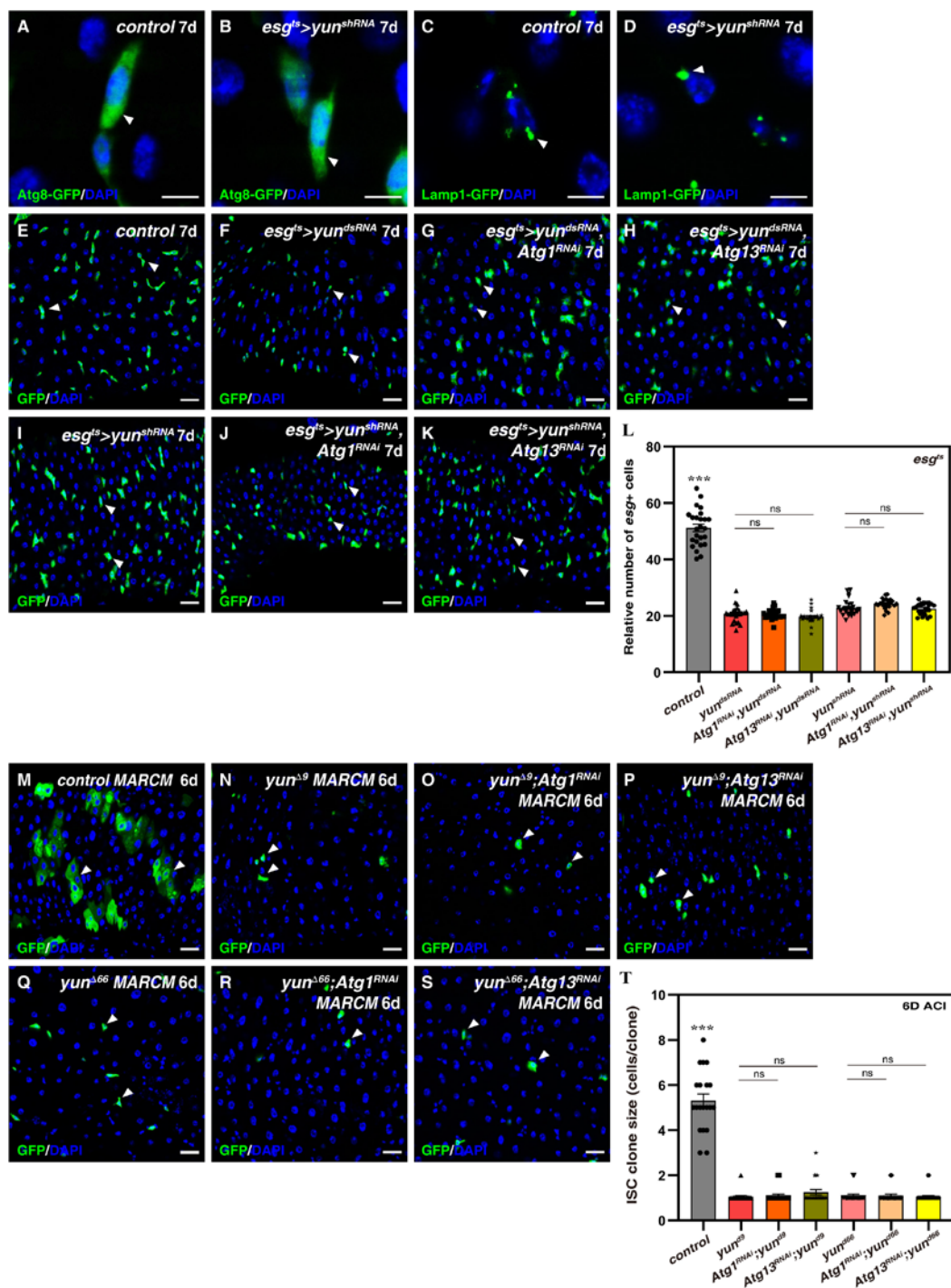


Fig. S13. Autophagy is not the cause of proliferation defects observed in the absence of *yun*.

(A) No autophagosomes (by Atg8-GFP puncta) could be detected in progenitors (green, by *esg*>*Atg8-GFP*) of control flies at 29°C for 7 days (white arrowhead). Note that

Atg8-GFP is uniformly located in progenitors including the nucleus, and will form Atg8-GFP puncta when autophagy is induced. (B) No autophagosomes (by Atg8-GFP puncta) could be detected in progenitors (green, by *esg>Atg8-GFP*) of *esg^{ts}>yun^{shRNA}* flies at 29°C for 7 days (white arrowhead). (C) Lysosomes (green, by *Lamp1-GFP*) in progenitors (green, by *esg>Lamp1-GFP*) of control flies at 29°C for 7 days (white arrowhead). (D) The number and morphology of lysosomes (green, by *Lamp1-GFP*) in progenitors (green, by *esg>Lamp1-GFP*) of *esg^{ts}>yun^{shRNA}* flies are largely unchanged at 29°C for 7 days (white arrowhead). (E) Progenitors (green) in control flies at 29°C for 7 days (white arrowheads). (F) Progenitors (green) in *esg^{ts}>yun^{dsRNA}* flies at 29°C for 7 days (white arrowheads). The number of progenitors is decreased upon *yun* depletion. (G) Progenitors (green) in *esg^{ts}>Atg1^{RNAi}; yun^{dsRNA}* flies at 29°C for 7 days (white arrowheads). The number of progenitors does not increase upon co-depletion of *Atg1* and *yun*. (H) Progenitors (green) in *esg^{ts}>Atg13^{RNAi}; yun^{dsRNA}* flies at 29°C for 7 days (white arrowheads). The number of progenitors does not increase upon co-depletion of *Atg13* and *yun*. (I) Progenitors (green) in *esg^{ts}>yun^{shRNA}* flies at 29°C for 7 days (white arrowheads). The number of progenitors is decreased upon *yun* depletion. (J) Progenitors (green) in *esg^{ts}>Atg1^{RNAi}; yun^{shRNA}* flies at 29°C for 7 days (white arrowheads). The number of progenitors does not increase upon co-depletion of *Atg1* and *yun*. (K) Progenitors (green) in *esg^{ts}>Atg13^{RNAi}; yun^{shRNA}* flies at 29°C for 7 days (white arrowheads). The number of progenitors does not increase upon co-depletion of *Atg13* and *yun*. (L) Quantification of the relative number of *esg⁺* cells in flies with indicated genotypes. Mean \pm SD is shown. n=26 intestines. ^{ns}*P*>0.05; ****P*<0.001. (M)

Control *FRT* ISC MARCM clones (green) (6D ACI) (white arrowheads). (N) *yun^{Δ9}* ISC MARCM clones (green) (6D ACI) (white arrowheads). (O) *yun^{Δ9}; Atg1^{RNAi}* ISC MARCM clones (green) (6D ACI) (white arrowheads). (P) *yun^{Δ9}; Atg13^{RNAi}* ISC MARCM clones (green) (6D ACI) (white arrowheads). (Q) *yun^{Δ66}* ISC MARCM clones (green) (6D ACI) (white arrowheads). (R) *yun^{Δ66}; Atg1^{RNAi}* ISC MARCM clones (green) (6D ACI) (white arrowheads). (S) *yun^{Δ66}; Atg13^{RNAi}* ISC MARCM clones (green) (6D ACI) (white arrowheads). (T) Quantification of ISC MARCM clone size in flies with indicated genotypes. Mean ± SD is shown. n=26 intestines. ^{ns}*P*>0.05; ****P*<0.001. GFP is in green and blue indicates DAPI staining for DNA. Scale bars: 20 μm except A-D (5 μm).

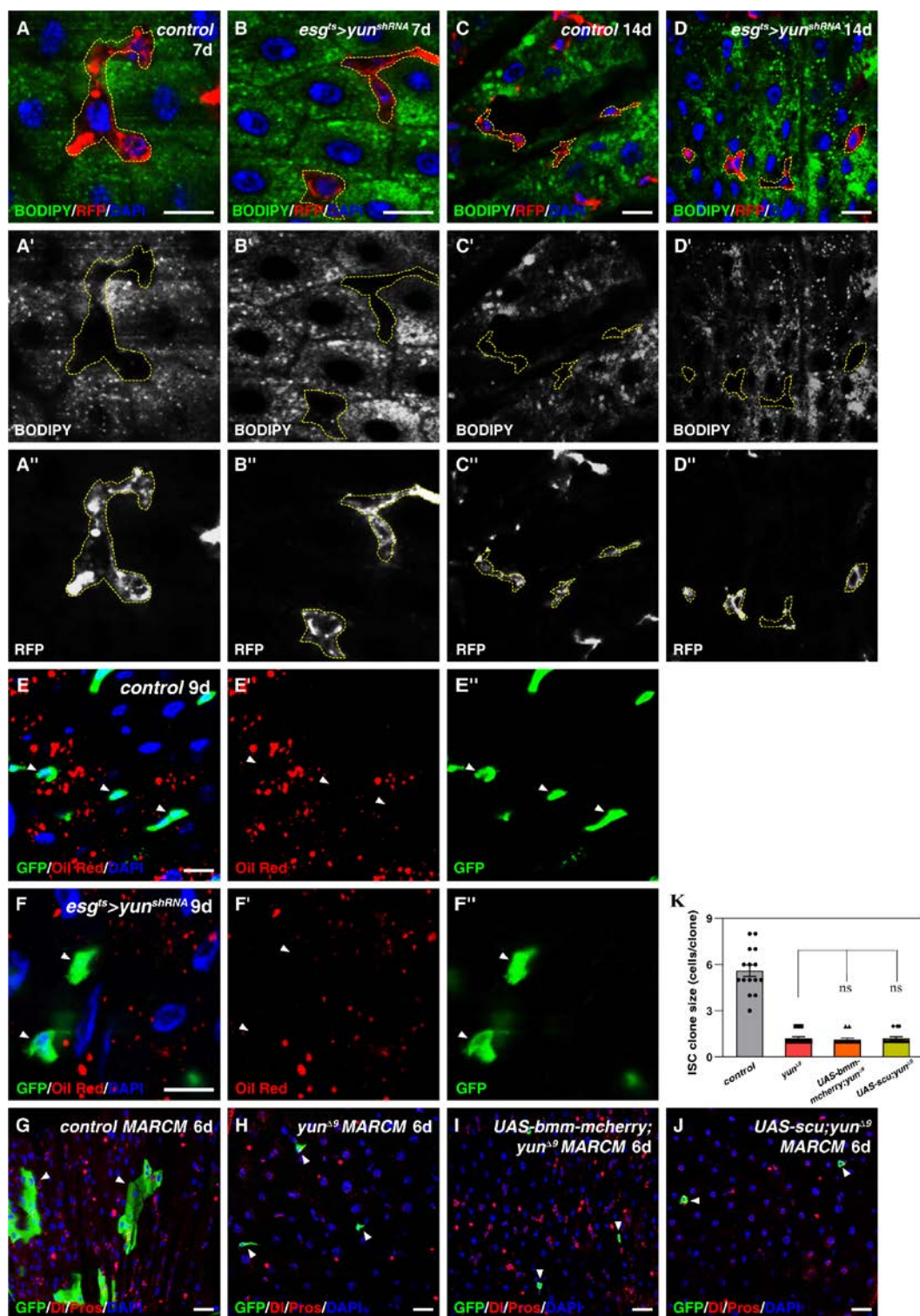


Fig. S14. Yun depletion does not lead to increased lipid storage.

(A) BODIPY staining (green) in control flies at 29°C for 7 days. Progenitors (red, by *esg>RFP*) are outlined with yellow dash lines. BODIPY and RFP channels are showed

separately in black-white. (B) BODIPY staining (green) in *esg^{ts}>yun^{shRNA}* flies at 29°C for 7 days. Progenitors (red, by *esg>RFP*) are outlined with yellow dash lines. No change of lipid droplets is observed. (C) BODIPY staining (green) in control flies at 29°C for 14 days. Progenitors (red, by *esg>RFP*) are outlined with yellow dash lines. BODIPY and RFP channels are showed separately in black-white. (D) BODIPY staining (green) in *esg^{ts}>yun^{shRNA}* flies at 29°C for 14 days. Progenitors (red, by *esg>RFP*) are outlined with yellow dash lines. No change of lipid droplets is observed. (E) Oil red staining (red) in control flies at 29°C for 9 days. Progenitors (green, by *esg>GFP*) are indicated with white arrowheads. Oil red and GFP channels are showed separately. (F) Oil red staining (red) in *esg^{ts}>yun^{shRNA}* flies at 29°C for 9 days. Progenitors (green, by *esg>GFP*) are indicated with white arrowheads. No change of lipid droplets is observed. (G) Control *FRT* ISC MARCM clones (green) (6D ACI) (white arrowheads). Dl and Pros in red. (H) *yun^{Δ9}* ISC MARCM clones (green) (6D ACI) (white arrowheads). Dl and Pros in red. (I) *UAS-bmm-cherry; yun^{Δ9}* ISC MARCM clones (green) (6D ACI) (white arrowheads). Dl and Pros in red. (J) *UAS-scu; yun^{Δ9}* ISC MARCM clones (green) (6D ACI) (white arrowheads). Dl and Pros in red. (K) Quantification of ISC MARCM clone size in flies with indicated genotypes. Mean ± SD is shown. n=15-25 intestines. ^{ns}*P*>0.05. Blue indicates DAPI staining for DNA. Scale bars: 10 μm (A-F) and 20 μm (G-J).

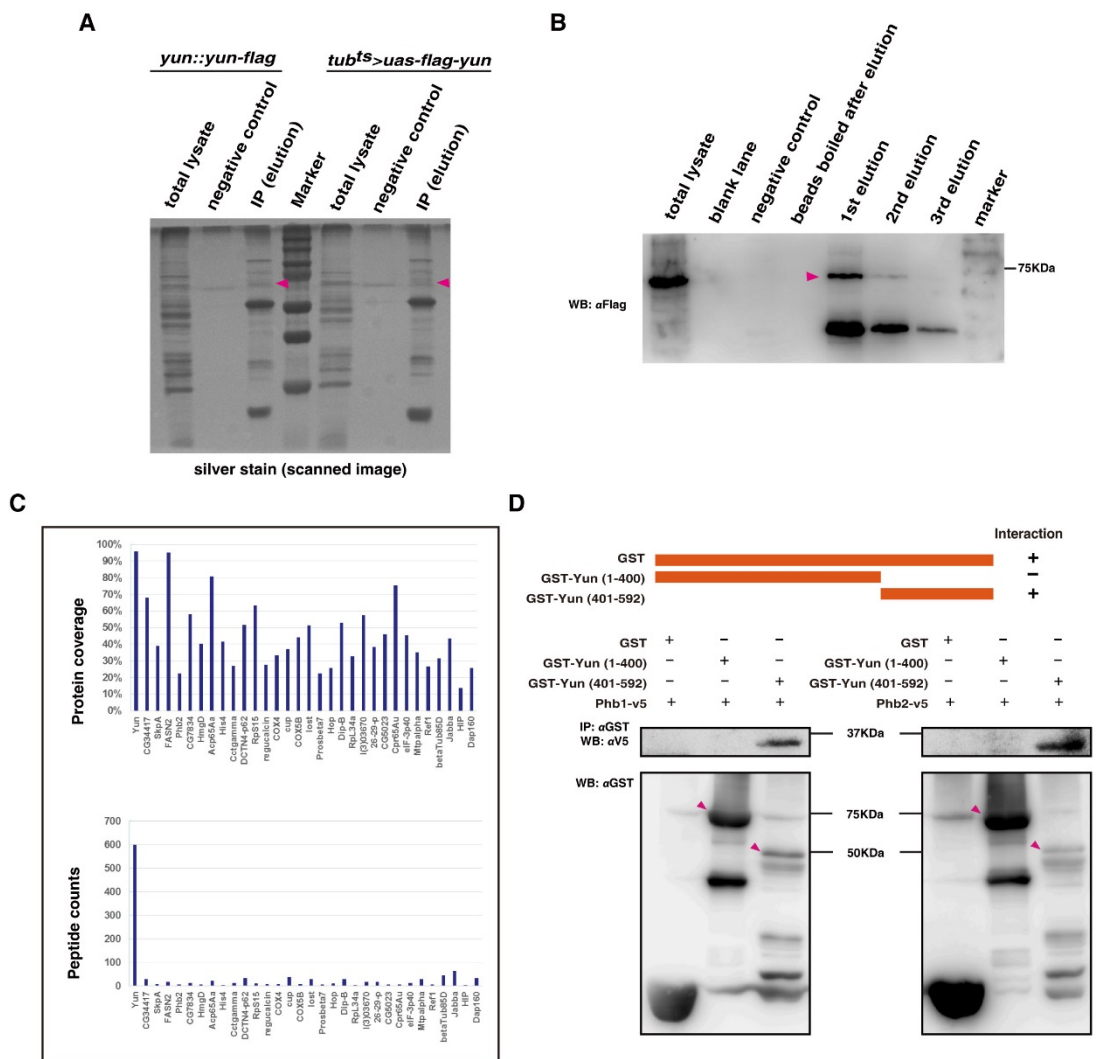


Fig. S15. Identification of Yun interacting proteins by LC-MS.

(A) Silver stained gel of co-IP samples. Pink arrowheads indicate the Yun band. (B) Western blot result of co-IP experiments. Pink arrowhead indicates the Yun band. (C) Protein coverage and peptide counts of some selected proteins from IP-MS results. (D) Co-IP experiment results using purified GST-Yun variants to precipitate endogenous Phb1-V5 or Phb2-V5 from whole fly lysates. Pink arrowheads indicate different Yun variants. The results show that the C-terminus of Yun interacts with both Phb1 and Phb2.

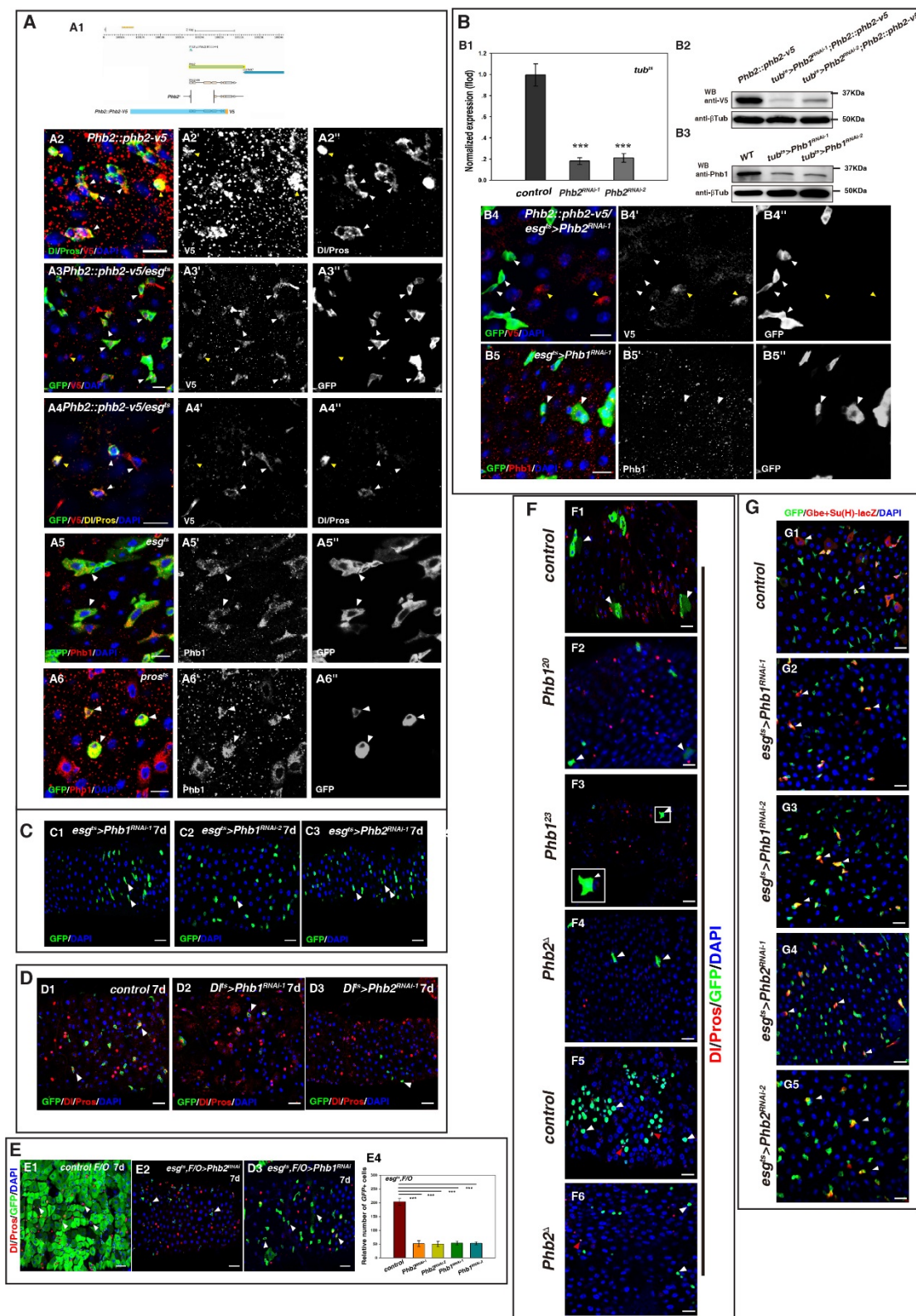


Fig. S16. Phb2 and Phb1 are required for progenitor proliferation.

(A) The expression pattern and subcellular localization of Phb2 and Phb1 in intestines.

(A1) Schematic diagram of *Phb2* mutants and reagents generated in this study. See Methods for detailed information. (A2) D1 and Pros (green) and V5 (red) double labeling of *Phb2::phb2-v5* intestine. Phb2 is expressed in both progenitors (by D1 and GFP) and EE cells (by Pros) (white and yellow arrowheads, respectively). Phb2 localizes mainly in the cytosol but can also be detected in the nuclei of progenitors and EE cells. V5 and D1/Pros channels are shown separately in black-white. (A3) Phb2 (red, by *Phb2::phb2-v5*) is expressed in progenitors (green, by *esg>GFP*) (white arrowheads). V5 and GFP channels are shown separately in black-white. (A4) D1 and Pros (yellow) and V5 (red) double labeling of *Phb2::phb2-v5/esg^{ts}* intestine. Phb2 is expressed in both progenitors (by D1) and EE cells (by Pros) (white and yellow arrowheads, respectively). Phb2 localizes mainly in the cytosol but can also be detected in the nuclei of progenitors and EE cells. V5, D1/Pros, and GFP channels are shown separately in black-white. (A5) Phb1 (red) is expressed in progenitors (green, by *esg>GFP*) (white arrowheads). Phb1 and GFP channels are shown separately in black-white. (A6) Phb1 (red) is also expressed in EE cells (green, by *pros>GFP*) (white arrowheads). Phb1 and GFP channels are shown separately in black-white. Scale bars: 10 μm . (B) Examination of *Phb2^{RNAi}* and *Phb1^{RNAi}* lines used in this study. (B1) The knockdown efficiency of *Phb2^{RNAi}* lines was determined by qRT-PCR quantification from *tub^{ts}>Phb2^{RNAi}* flies (ovaries were not included). Ribosomal gene *RpL11* was used as a normalization control. Means \pm SD are shown. *** $P < 0.001$. (B2 and B3) Phb2 and Phb1 protein levels are significantly reduced upon expression of RNAi constructs. Note that *tubGal4* is not expressed in female germline cells and ovaries are included in

the samples. β Tubulin is used as a loading control. (B4) Phb2 protein in progenitors (red, by *Phb2::phb2-v5*) is decreased upon Phb2 depletion by inducing *Phb2^{RNAi-1}* construct (white arrowheads). V5 and GFP channels are shown separately in black-white. (B5) Phb1 protein levels in progenitors are decreased upon Phb1 depletion by inducing *Phb1^{RNAi-1}* construct (white arrowheads). Phb1 and GFP channels are shown separately in black-white. Scale bars: 10 μ m. (C) Phb1 and Phb2 are required for progenitor proliferation. (C1 and C2) The number of *esg⁺* cells (green) is significantly decreased in *esg^{ts}>Phb1^{RNAi}* intestines at 29°C for 7 days (C1: *Phb1^{RNAi-1}*, C2: *Phb1^{RNAi-2}*) (white arrowheads). See Figure 1A for comparison. (C3) The number of *esg⁺* cells (green) is significantly decreased in *esg^{ts}>Phb2^{RNAi-1}* intestines at 29°C for 7 days (white arrowheads). (D) The PHB complex is required in ISCs. (D1) ISCs (green, by *Dl>GFP*) in control intestines at 29°C for 7 days (white arrowheads). (D2) The number of ISCs (*Dl>GFP* positive cells, green) is significantly decreased in *Dl^{ts}>Phb1^{RNAi-1}* intestines at 29°C for 7 days (white arrowheads). (D3) The number of ISCs (*Dl>GFP* positive cells, green) is significantly decreased in *Dl^{ts}>Phb2^{RNAi-1}* intestines at 29°C for 7 days (white arrowheads). Scale bars: 20 μ m. (E) Lineage tracing experiment results. (E1) Control *esg^{ts},F/O* midguts at 29°C for 7 days with Dl and Pros staining (red, progenitors are indicated by white arrowheads). (E2 and E3) *Phb2* and *Phb1* knockdown in *esg^{ts},F/O* midguts at 29°C for 7 days with Dl and Pros staining (red, progenitors are indicated by white arrowheads) (E2: *Phb2^{RNAi}*, E3: *Phb1^{RNAi}*). (E4) Quantification of the relative number of GFP-positive cells in different genotypes. Mean \pm SD is shown. n=20-30 intestines. *** $P<0.001$. (F) The PHB complex mainly

regulates progenitor proliferation, but not progeny differentiation. (F1) D1 and Pros staining of *FRT* control ISC MARCM clones (cytoplasmic GFP) - differentiated large ECs in the clones are indicated (white arrowheads). (F2 and F3) *Phb1* mutant MARCM clones (cytoplasmic GFP) (F2: *Phb1*²⁰, F3: *Phb1*²³) (white arrowheads). Large D1⁻ *Phb1* mutant cells (GFP+) (differentiating and mature ECs) can be observed. Boxed region is shown with enlarged magnification for better visualization. (F4) *Phb2*^Δ mutant MARCM clones (cytoplasmic GFP) (white arrowheads). Large D1⁻ *Phb2*^Δ mutant cells (GFP+) (putatively differentiating and mature ECs) can be observed. (F5) D1 and Pros staining of *FRT* control ISC MARCM clones (nuclear GFP) - differentiated large ECs in the clones are indicated (white arrowheads). EE cells in control ISC MARCM clone are indicated with red arrowhead. (F6) *Phb2*^Δ mutant MARCM clones (nuclear GFP) (white arrowheads). Large D1⁻ *Phb2*^Δ mutant cells (GFP+) (putatively differentiating and mature ECs) can be observed. Marked *Phb2*^Δ EE cell can also be observed (red arrowhead). Scale bars: 20 μm. (G) Depletion of *Phb1* and *Phb2* do not affect EB identity (Notch signaling activation). (G1) EBs (by *GBE+Su(H)-lacZ* in red) in control intestines (white arrowheads). (G2 and G3) Although the number of EB cells (by *GBE+Su(H)-lacZ* in red) is significantly decreased in *esg^{ts}>Phb1^{RNAi}* intestines at 29°C for 7 days (G2: *Phb1^{RNAi-1}*, G3: *Phb1^{RNAi-2}*) (white arrowheads), the identity of EBs (Notch activation) is not affected by *Phb1* depletion. (G4 and G5) Similarly, although the number of EB cells (by *GBE+Su(H)-lacZ* in red) is significantly decreased in *esg^{ts}>Phb2^{RNAi}* intestines at 29°C for 7 days (G4: *Phb2^{RNAi-1}*, G5: *Phb2^{RNAi-2}*) (white arrowheads), the identity of EBs (Notch activation) is not affected by *Phb2* depletion.

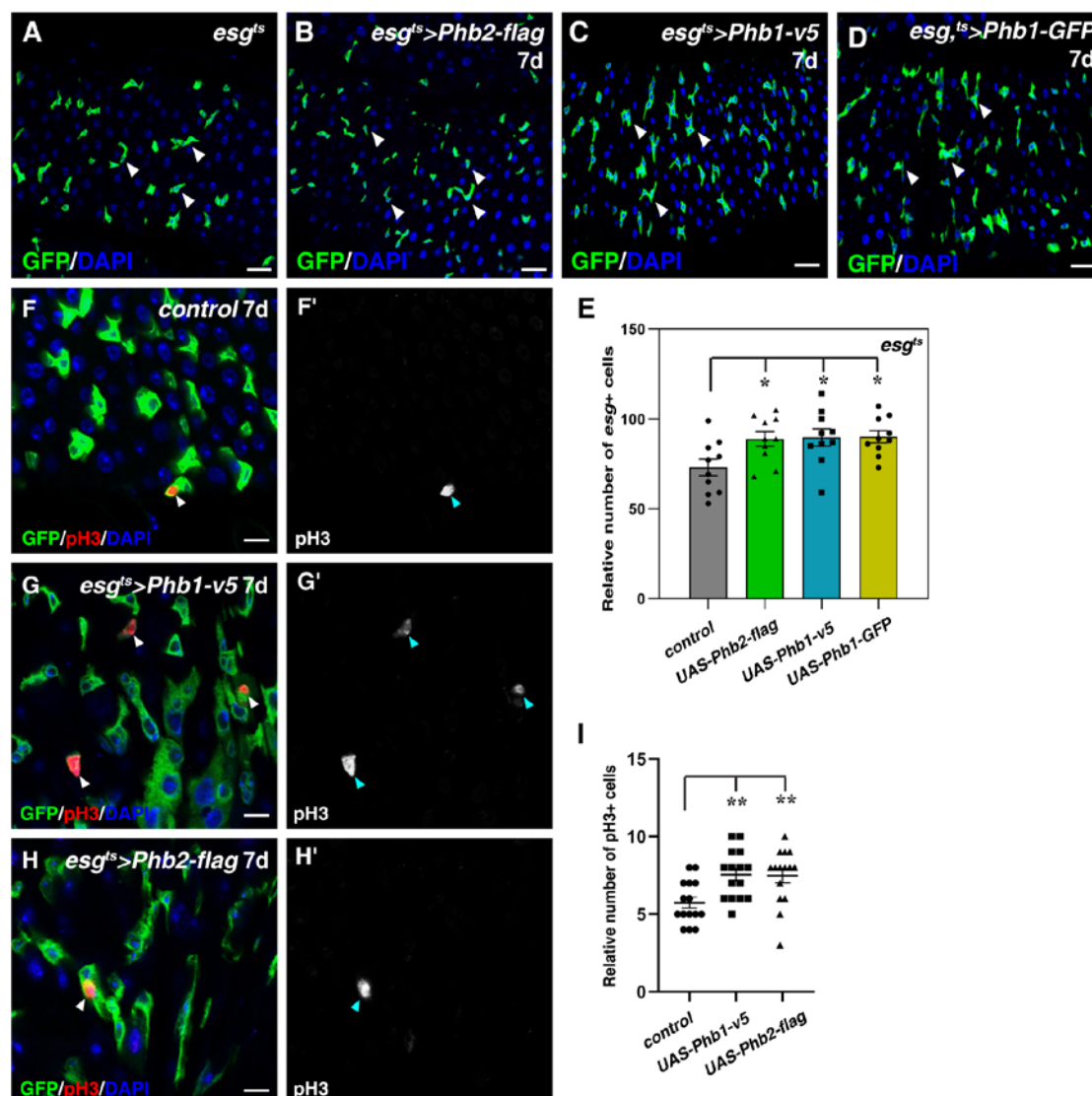
Scale bars: 20 μm .

Fig. S17. Overexpression of the PHB complex increased progenitor proliferation.

(A) Progenitors (green, by *esg*>*GFP*) in control intestines at 29°C for 7 days (white arrowheads). (B) The number of *esg*⁺ cells (green) is mildly increased in *esg*^{ts}>*Phb2-flag* intestines at 29°C for 7 days (white arrowheads). (C) The number of *esg*⁺ cells (green) is mildly increased in *esg*^{ts}>*Phb1-v5* intestines at 29°C for 7 days (white arrowheads). (D) The number of *esg*⁺ cells (green) is mildly increased in *esg*^{ts}>*Phb1-*

GFP intestines at 29°C for 7 days (white arrowheads). (E) Quantification of the relative number of *esg*⁺ cells in flies with indicated genotypes. Mean ± SD is shown. n=10-20. (F) pH3-positive cells (red) in control at 29°C for 7 days (white arrowheads). (G) pH3-positive cells (red) in *esg*^{ts}>*Phb1-v5* at 29°C for 7 days (white arrowheads). (H) pH3-positive cells (red) in *esg*^{ts}>*Phb2-flag* at 29°C for 7 days (white arrowheads). (I) Quantification of the relative number of pH3-positive cells in intestines with indicated genotypes. Mean ± SD is shown. n=15 intestines. **P*<0.05. In all panels except graphs, GFP is in green, blue indicates DAPI staining for DNA. Scale bars: 20 μm.

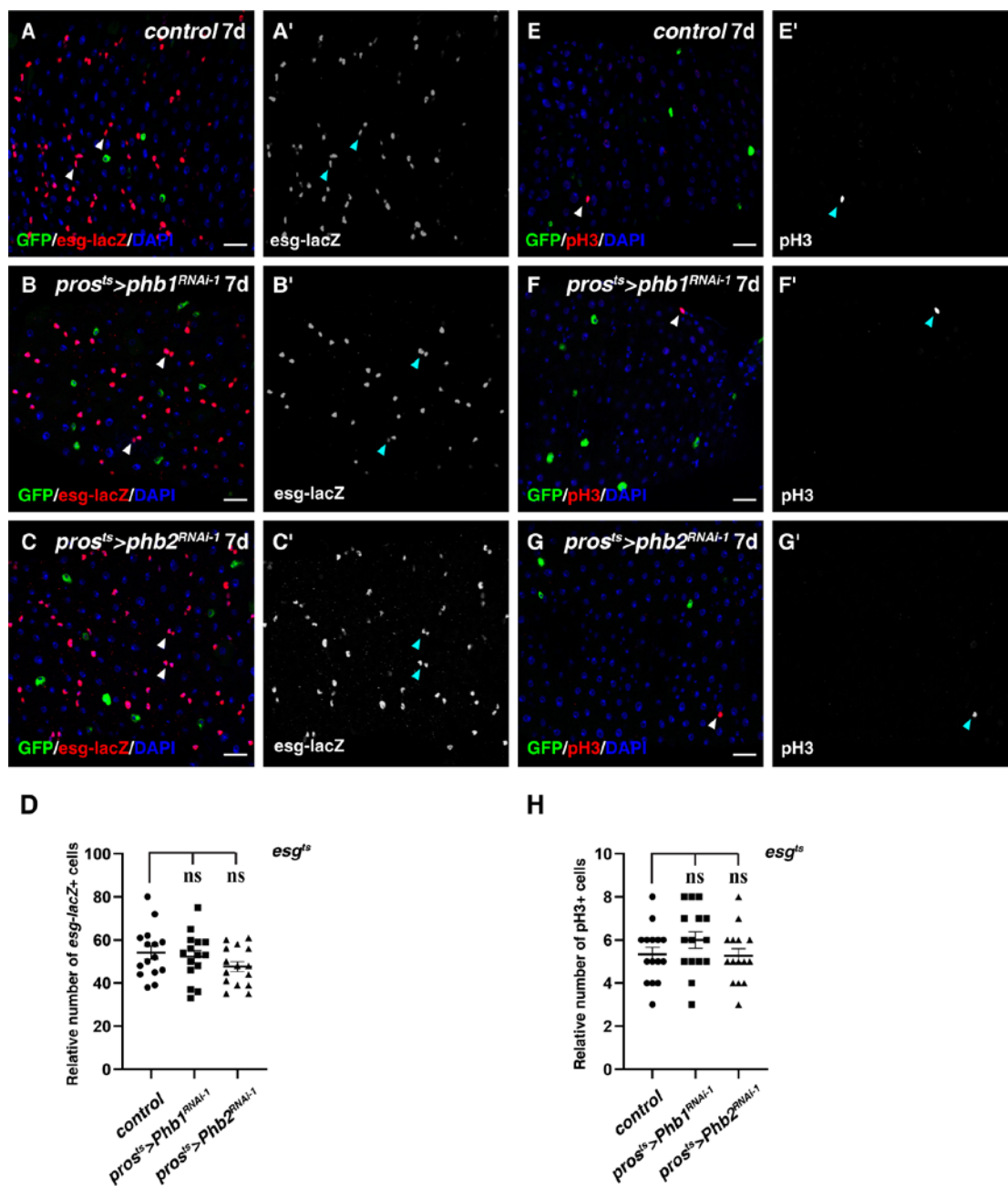


Fig. S18. Intestinal homeostasis is not affected upon depletion of the PHB complex in EEs.

(A-D) The PHB complex in EEs is not required for intestinal homeostasis. (A) Progenitors (red, *e sg-lacZ*) in control intestines at 29°C for 7 days (white arrowheads).

(B) Progenitors (red, *e sg-lacZ*) in *pros^{ts}>Phb1^{RNAi-1}* at 29°C for 7 days (white

arrowheads). (C) Progenitors (red, *esg-lacZ*) in *pros^{ts}>Phb2^{RNAi-1}* at 29°C for 7 days (white arrowheads). (D) Quantification of the relative number of progenitors in intestines with indicated genotypes. Mean \pm SD is shown. n=15 intestines. ^{ns}*P* >0.05. (E-H) Mitosis is not affected in the absence of The PHB complex in EEs. (E) pH3-positive cells (red) in control at 29°C for 7 days (white arrowheads). (F) pH3-positive cells (red) in *pros^{ts}> Phb1^{RNAi-1}* at 29°C for 7 days (white arrowheads). (G) pH3-positive cells (red) in *pros^{ts}> Phb2^{RNAi-1}* at 29°C for 7 days (white arrowheads). (H) Quantification of the relative number of pH3-positive cells in intestines with indicated genotypes. Mean \pm SD is shown. n=15 intestines. ^{ns}*P* >0.05. In all panels except graphs, GFP is in green and blue indicates DAPI staining for DNA. Scale bars: 20 μ m.

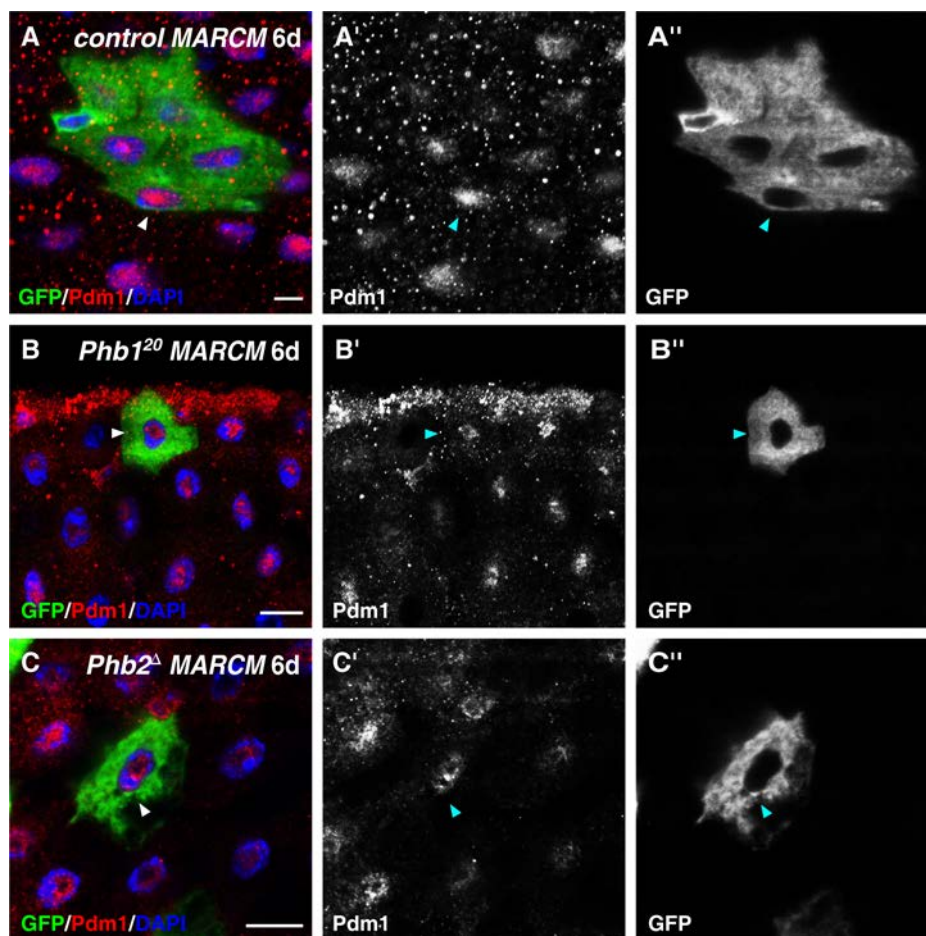


Fig. S19. EC differentiation is unaffected in the absence of the PHB complex.

(A-C) PDM1 (red) in MARCM clones (green) of control (A), *Phb1*²⁰ (B) and *Phb2*^Δ (C)(white arrowheads). PDM1 and GFP channels are showed separately in black-white. GFP is in green, blue indicates DAPI staining for DNA. Scale bars: 10 μm.

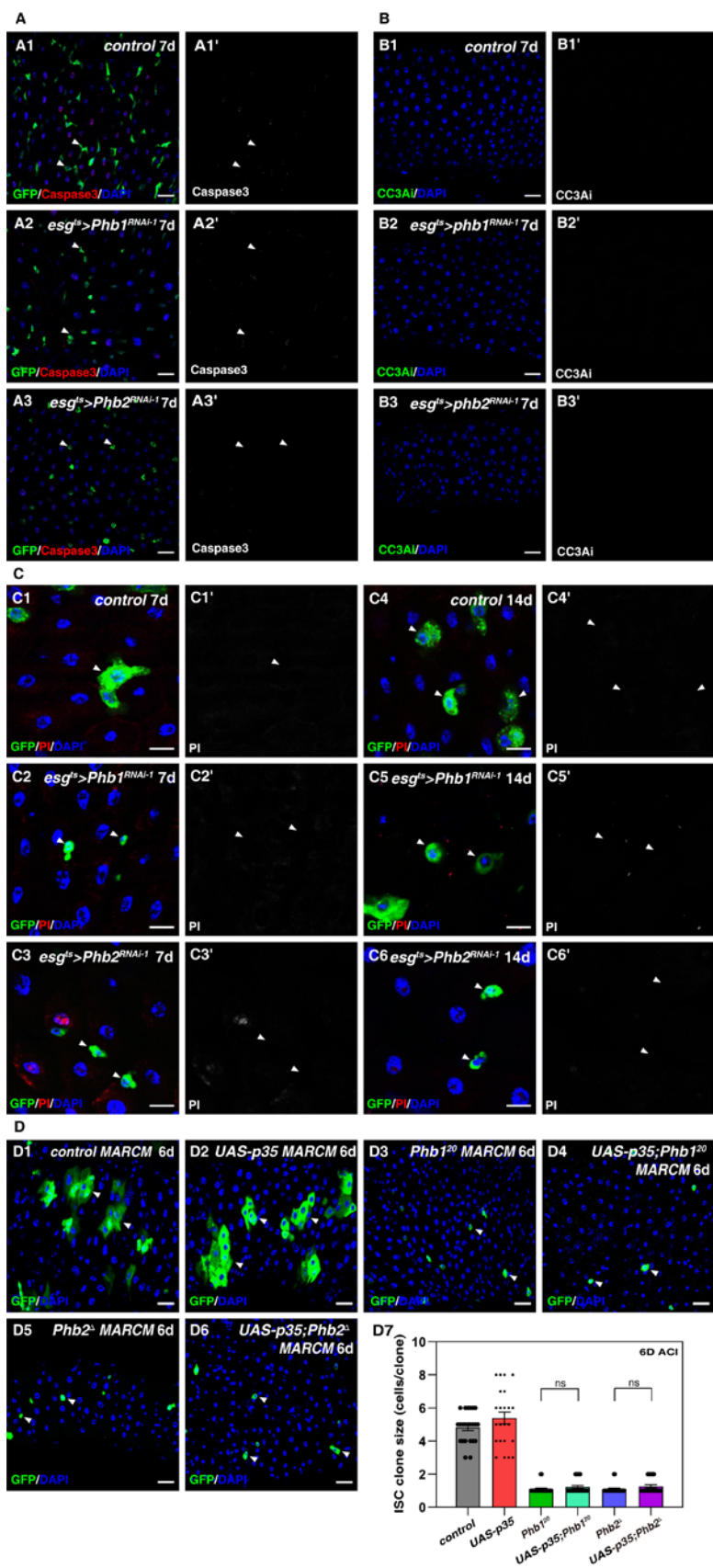


Fig. S20. Progenitor proliferation defects in *Phb*-defective progenitors are not due

to cell death.

(A and B) No increase of apoptosis is observed in *Phb*-depleted progenitors. (A1) Apoptosis (red, by active Caspase 3) in control progenitors at 29°C for 7 days (white arrowheads). Split channel for GFP and active Caspase 3 is showed separately (white arrowheads). (A2) Active Caspase 3 staining (red) in *esg^{ts}>Phb1^{RNAi-1}* intestines at 29°C for 7 days (progenitors by white arrowheads). Split channel for GFP and active Caspase 3 is showed separately (white arrowheads). (A3) Active Caspase 3 staining (red) in *esg^{ts}>Phb2^{RNAi-1}* intestines at 29°C for 7 days (progenitors by white arrowheads). Split channel for GFP and active Caspase 3 is showed separately (white arrowheads). (B1) No apoptosis (by *esg^{ts}>CC3Ai*) is observed in progenitors of control progenitors at 29°C for 7 days. Split channel for CC3Ai is showed separately. (B2) No apoptosis (by CC3Ai) in *esg^{ts}>Phb1^{RNAi-1}* intestines at 29°C for 7 days. Split channel for CC3Ai is showed separately. (B3) No apoptosis (by CC3Ai) in *esg^{ts}>Phb2^{RNAi-1}* intestines at 29°C for 7 days. Split channel for CC3Ai is showed separately. (C) *Phb1*- and *Phb2*-deficient progenitors do not undergo necrosis. (C1) PI staining (red) in control intestines at 29°C for 7 days (progenitors by white arrowheads). No cell necrosis is observed. Split channel for PI and GFP is showed separately (white arrowheads). (C2) PI staining (red) in *esg^{ts}>Phb1^{RNAi-1}* intestines at 29°C for 7 days (progenitors by white arrowheads). No cell necrosis is observed. Split channel for PI and GFP is showed separately (white arrowheads). (C3) PI staining (red) in *esg^{ts}>Phb2^{RNAi-1}* intestines at 29°C for 7 days (progenitors by white arrowheads). No cell necrosis is observed. Split channel for PI and GFP is showed separately (white arrowheads). (C4) PI staining (red) in control

intestines at 29°C for 14 days (progenitors by white arrowheads). No cell necrosis is observed. Split channel for PI and GFP is showed separately (white arrowheads). (C5) PI staining (red) in *esg^{ts}>Phb1^{RNAi-1}* intestines at 29°C for 14 days (progenitors by white arrowheads). No cell necrosis is observed. Split channel for PI and GFP is showed separately (white arrowheads). (C6) PI staining (red) in *esg^{ts}>Phb2^{RNAi-1}* intestines at 29°C for 14 days (progenitors by white arrowheads). No cell necrosis is observed. Split channel for PI and GFP is showed separately (white arrowheads). (D) Over-expression of p35 could not rescue progenitor proliferation defects observed in *Phb1* and *Phb2* mutants. (D1) *FRT* control ISC MARCM clones (white arrowheads). (D2) The size of *UAS-p35* MARCM clones is increased compared to that of control clones (white arrowheads). (D3) *Phb1²⁰* ISC MARCM clones (white arrowheads). (D4) The size of *UAS-p35, Phb1²⁰* ISC MARCM clones is not changed compared to that of *Phb1²⁰* ISC MARCM clones (white arrowheads). (D5) *Phb2^d* ISC MARCM clones (white arrowheads). (D6) The size of *UAS-p35, Phb2^d* ISC MARCM clones is not changed compared to that of *Phb2^d* ISC MARCM clones (white arrowheads). (D7) Quantification of the size of ISC clones in intestines with indicated genotypes. Mean \pm SD is shown. n=20-25 intestines. In all panels except graphs, GFP is in green, blue indicates DAPI staining for DNA. Scale bars: 10 μ m (C) and 20 μ m (A, B and D).

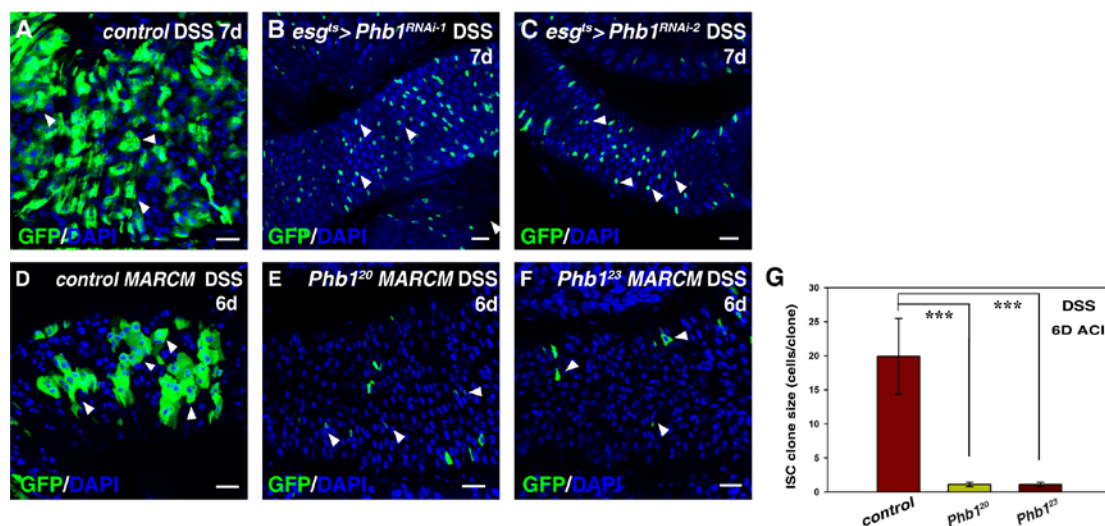


Fig. S21. Phb1 is required for tissue regeneration.

(A) Progenitors (green, arrowheads) proliferate to regenerate midgut after the control flies are treated with DSS at 29°C for 7 days. (B and C) *Phb1*-depleted progenitors (green, arrowheads) do not proliferate to regenerate midgut after the flies are treated with DSS at 29°C for 7 days (B: *Phb1*^{RNAi-1}, C: *Phb1*^{RNAi-2}). (D) Control intestines with FRT ISC MARCM clones (green, arrowheads) can regenerate after treated with DSS (6d ACI). (E and F) *Phb1* mutant MARCM clones (green, arrowheads) do not proliferate to regenerate midgut after the flies are treated with DSS (E: *Phb1*²⁰, F: *Phb1*²³) (6d ACI). (G) Quantification of the size of ISC clones in control and *Phb1* mutant intestines after DSS treatment. Mean \pm SD is shown. n=20-30 intestines. ****P*<0.001. In all panels except graphs, GFP is in green, blue indicates DAPI staining for DNA. Scale bars: 20 μ m.

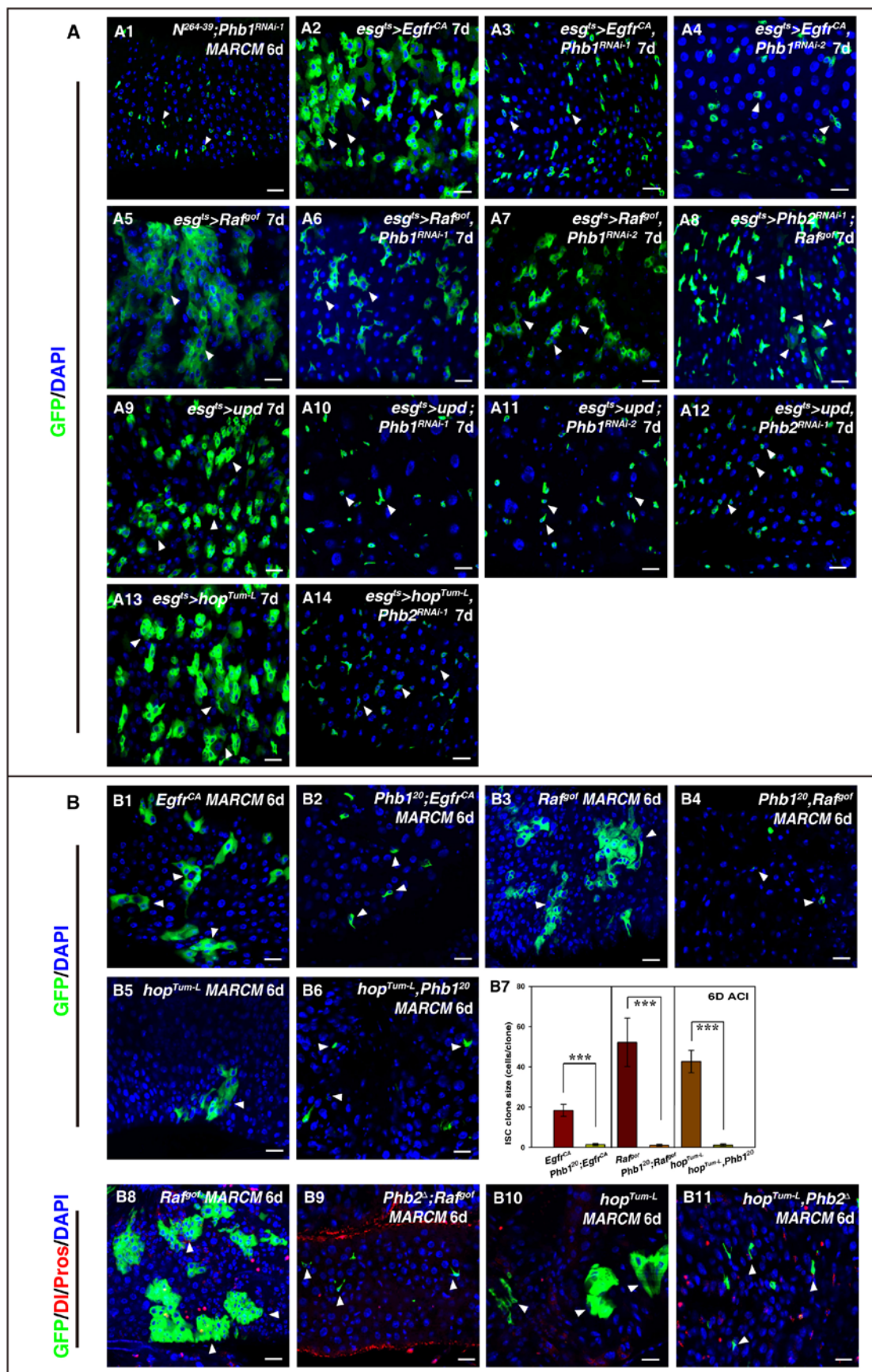


Fig. S22. The PHB complex is required for the proliferation of different

transformed stem cells.

(A) Depleting the PHB complex suppresses the proliferation of transformed stem cells.

(A1) The number of esg^+ cells (green) is dramatically increased in $esg^{ts}>Egfr^{CA}$ intestines at 29°C for 7 days (white arrowheads). See Figure 1A for comparison. (A2 and A3) Depletion of the PHB complex effectively suppresses the increase of esg^+ cells observed in $esg^{ts}>Egfr^{CA}$ intestines at 29°C for 7 days (white arrowheads) (A2: $Phb1^{RNAi-1}$, A3: $Phb1^{RNAi-2}$). (A4) The number of esg^+ cells (green) is dramatically increased in $esg^{ts}>Raf^{gof}$ intestines at 29°C for 7 days (white arrowheads). (A5-A7) Depletion of the PHB complex effectively suppresses the increase of esg^+ cells observed in $esg^{ts}>Raf^{gof}$ intestines at 29°C for 7 days (white arrowheads) (A5: $Phb1^{RNAi-1}$, A6: $Phb1^{RNAi-2}$, and A7: $Phb2^{RNAi}$). (A8) The number of esg^+ cells (green) is dramatically increased in $esg^{ts}>upd$ ($upd1$) intestines at 29°C for 7 days (white arrowheads). (A9-A11) Depletion of the PHB complex effectively suppresses the increase of esg^+ cells observed in $esg^{ts}>upd$ intestines at 29°C for 7 days (white arrowheads) (A9: $Phb1^{RNAi-1}$, A10: $Phb1^{RNAi-2}$, and A11: $Phb2^{RNAi}$). (A12) The number of esg^+ cells (green) is dramatically increased in $esg^{ts}>hop^{Tum-L}$ intestines at 29°C for 7 days (white arrowheads). (A13) Depletion of $Phb2$ effectively suppresses the increase of esg^+ cells observed in $esg^{ts}>hop^{Tum-L}$ intestines at 29°C for 7 days (white arrowheads).

(B) The proliferation of transformed stem cells is suppressed in $Phb1$ mutant. MARCM clones (green) of $Egfr^{CA}$ (B1), $Egfr^{CA};Phb1^{20}$ (B2), Raf^{gof} (B3), $Raf^{gof};Phb1^{20}$ (B4), hop^{Tum-L} (B5) and $hop^{Tum-L};Phb1^{20}$ (B6), stained with DAPI (blue) (25°C, 6D ACI). (B7)

Quantification of ISC clone size of intestines with indicated genotypes. Mean \pm SD is

shown. $n=20-30$. $***P<0.001$. In all panels except graphs, GFP is in green, blue indicates DAPI staining for DNA. Scale bars: 20 μm .

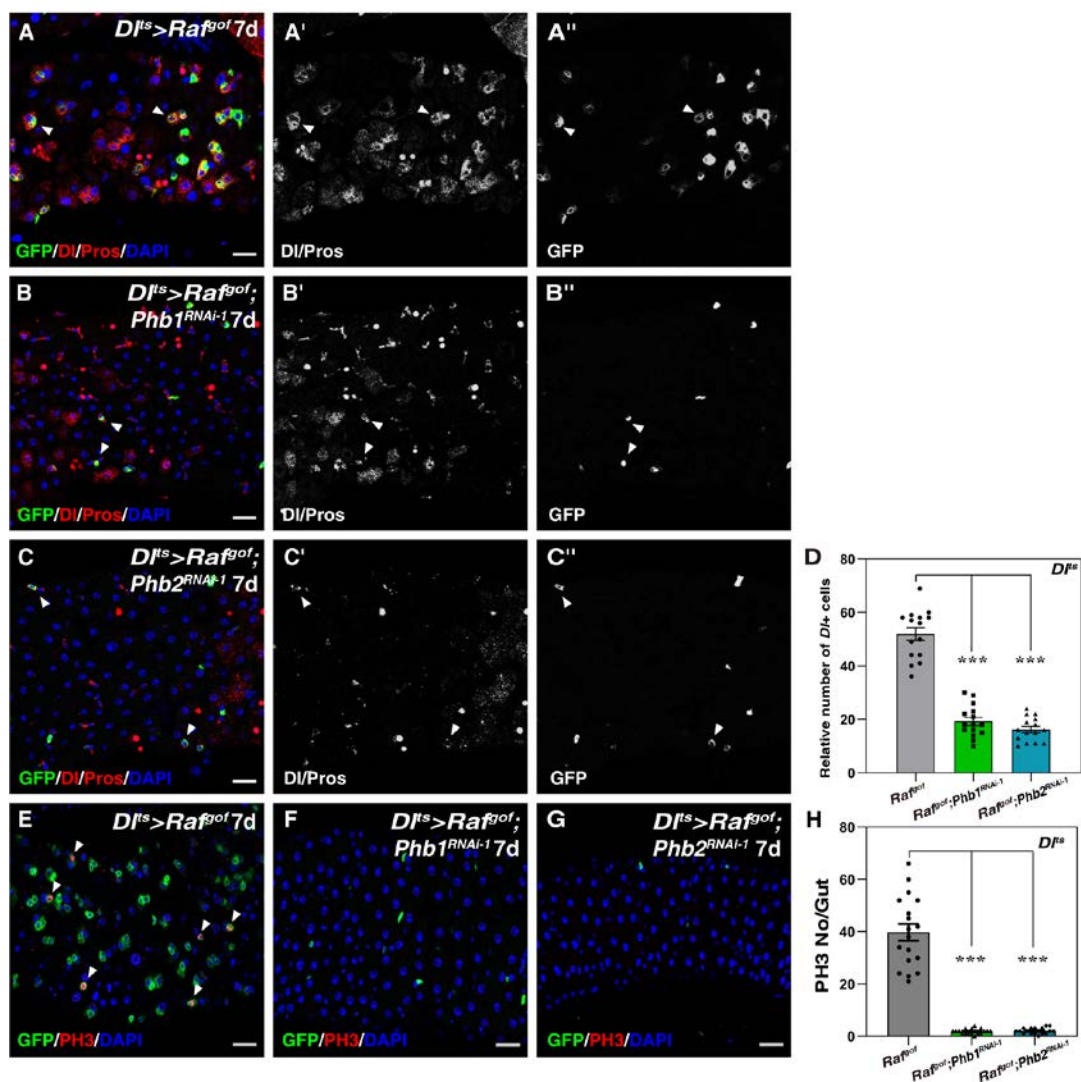


Fig. S23. Phb2 and Phb1 are required for the proliferation of different transformed stem cells.

(A) Activation of *Raf*^{gof} in ISCs (by *Df*^{ts}) results in the accumulation of ISCs (by Df in red and *Df*>*GFP*) at 29°C for 7 days (white arrowheads). Pros in red. Df/Pros and GFP channels are showed separately in black-white. Df and Pros in red. (B) Simultaneous depletion of *Phb1* in *Df*^{ts}>*Raf*^{gof} intestines completely suppresses ISC accumulation at 29°C for 7 days (white arrowheads). Df and Pros in red. (C) Simultaneous depletion of *Phb2* in *Df*^{ts}>*Raf*^{gof} intestines completely suppresses ISC accumulation at 29°C for 7

days (white arrowheads). DI and Pros in red. (D) Quantification of the relative number of ISCs in intestines with indicated genotypes. Mean \pm SD is shown. n=15 intestines. *** P <0.001. (E) pH3 (red, white arrowheads) in $Dl^{ts}>Raf^{gof}$ intestines at 29°C for 7 days (white arrowheads). (F) pH3 in $Dl^{ts}>Phb1^{RNAi-1}; Raf^{gof}$ intestines at 29°C for 7 days. (G) pH3 in $Dl^{ts}>Phb1^{RNAi-1}; Raf^{gof}$ intestines at 29°C for 7 days. (H) Quantification for the number of PH3-positive cells per gut in intestines with indicated genotypes. Mean \pm SD is shown. n=18. *** P <0.001. GFP is in green, blue indicates DAPI staining for DNA. Scale bars: 20 μ m.

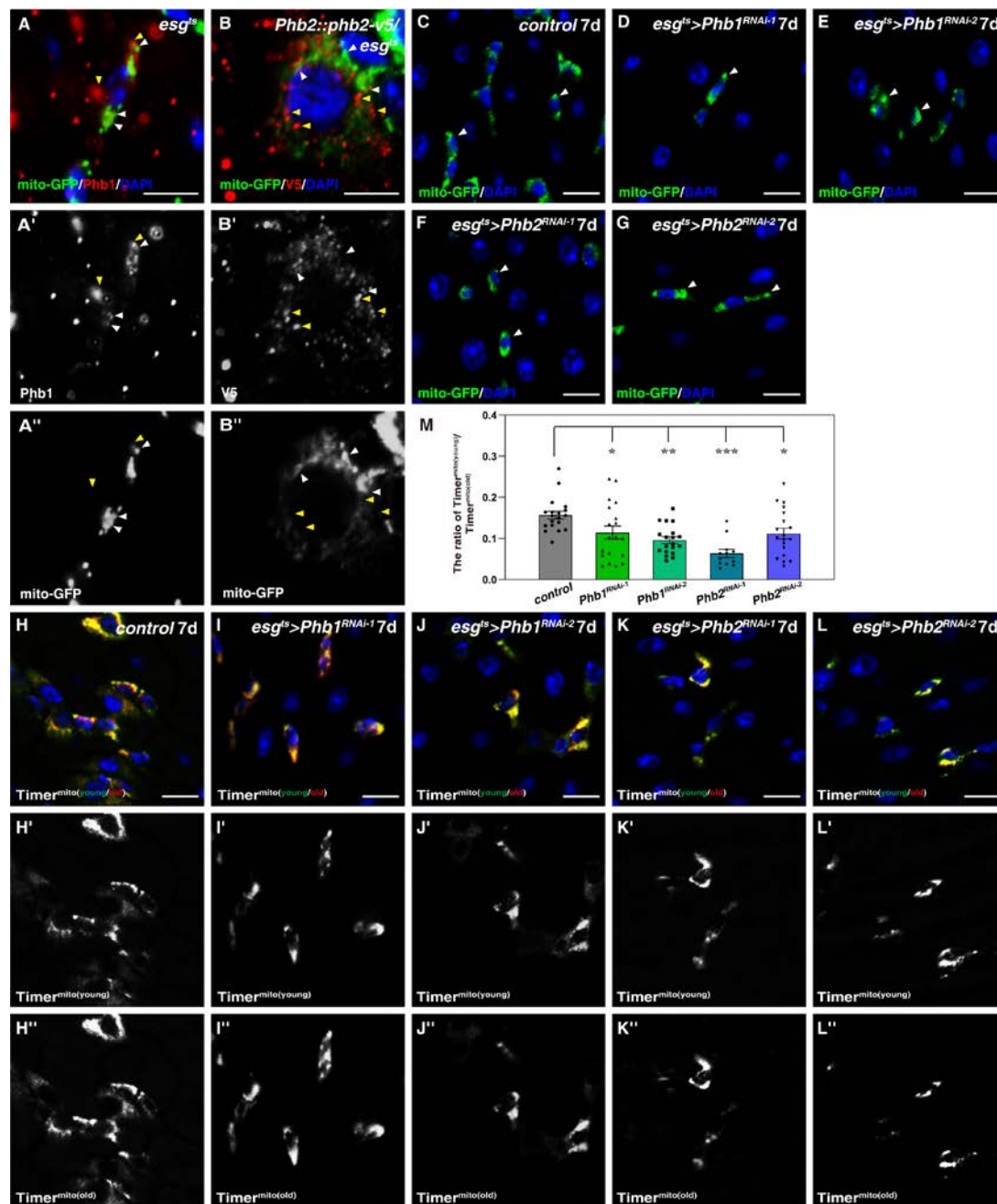


Fig. S24. No obvious mitochondrial defects are observed in *Phb*-defective progenitors.

(A) Phb1 (red) and mitochondria (green, by *esg^{ts}*>*mito-GFP*) in progenitors. Some Phb1 proteins co-localize with mitochondria (white arrowheads), but the majority of Yun does not co-localize with mitochondria (yellow arrowheads). Phb1 and mito-GFP

channels are showed separately. (B) Phb2 (red, by *Phb2::phb2-v5*) and mitochondria (green, by *esg^{ts}>mito-GFP*) in progenitors. Some Phb2 proteins co-localize with mitochondria (white arrowheads), but the majority of Yun does not co-localize with mitochondria (yellow arrowheads). Phb2 and mito-GFP channels are showed separately. (C) Mitochondria (green, by *esg^{ts}>mito-GFP*) in control progenitors at 29°C for 7 days (white arrowheads). (D and E) Mitochondria (green, by *esg^{ts}>mito-GFP*) in *esg^{ts}>Phb1^{RNAi}* progenitors at 29°C for 7 days (white arrowheads) (D: *Phb1^{RNAi-1}*, E: *Phb1^{RNAi-2}*). The morphology of mitochondria is largely unaffected by *Phb1* depletion. (F and G) Mitochondria (green, by *esg^{ts}>mito-GFP*) in *esg^{ts}>Phb2^{RNAi}* progenitors at 29°C for 7 days (white arrowheads) (F: *Phb2^{RNAi-1}*, G: *Phb2^{RNAi-2}*). The morphology of mitochondria is largely unaffected by *Phb2* depletion. (H) Mitochondrial maturation (green and red, by *esg^{ts}>Timer^{mito}*) in control progenitors at 29°C for 7 days (white arrowheads). GFP (young) and RFP (mature) channels are showed separately. (I and J) Mitochondrial maturation (green and red, by *esg^{ts}>Timer^{mito}*) in *esg^{ts}>Phb1^{RNAi}* progenitors at 29°C for 7 days (white arrowheads) (I: *Phb1^{RNAi-1}*, J: *Phb1^{RNAi-2}*). GFP (young) and RFP (mature) channels are showed separately. Mitochondrial maturation is increased in the absence of *Phb1*. (K and L) Mitochondrial maturation (green and red, by *esg^{ts}>Timer^{mito}*) in *esg^{ts}>Phb2^{RNAi}* progenitors at 29°C for 7 days (white arrowheads) (K: *Phb2^{RNAi-1}*, L: *Phb2^{RNAi-2}*). GFP (young) and RFP (mature) channels are showed separately. Mitochondrial maturation is increased in the absence of *Phb2*. (M) Quantification of the ratio of $\text{Timer}^{\text{young}}/\text{Timer}^{\text{old}}$ fluorescence intensity number in intestines with indicated genotypes. Mean \pm SD is shown. n=10-20. * $P<0.05$; ** $P<0.01$;

*** $P < 0.001$. GFP is in green, blue indicates DAPI staining for DNA. Scale bars: 10 μm except A and B (5 μm).

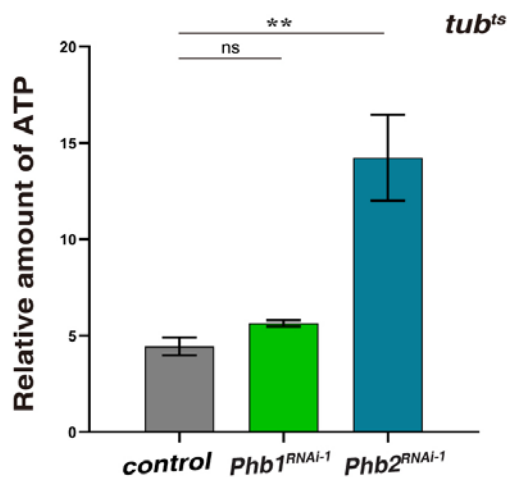


Fig. S25. ATP production is not affected in the absence of Phb2 or Phb1.

yun/Phb was systematically depleted in the animals using *tubulin-Gal4*, combined with *Gal80^{ts}* (*tub^{ts}*). Quantification of the relative amount of ATP in flies with indicated genotypes. Mean \pm SD is shown. $n=3$. ^{ns} $P > 0.05$; ^{**} $P < 0.01$.

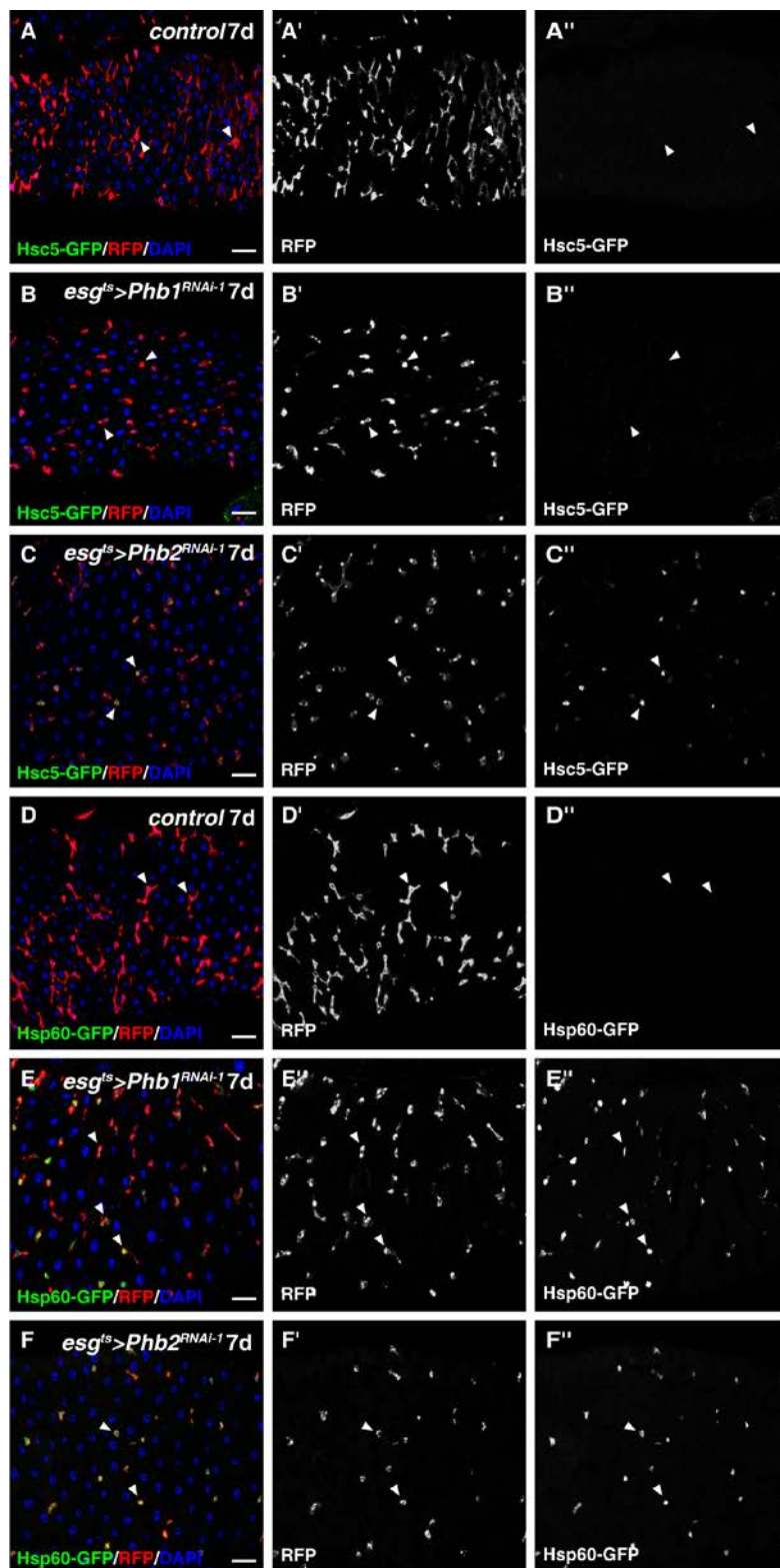


Fig. S26. Different Mito^{UPR} responses were detected in *Phb*-defective progenitors.

(A) No mito^{UPR} (green, by *Hsc5-GFP*) is detected in progenitors (red, by *esg>RFP*) of

control flies at 29°C for 7 days (white arrowheads). RFP and Hsc5-GFP/mito^{UPR} channels are showed separately in black-white. (B) Mito^{UPR} (green, by *Hsc5-GFP*) is not detectable in progenitors of *esg^{ts}>Phb1^{RNAi-1}* flies at 29°C for 7 days (red, by *esg>RFP*) (white arrowheads). RFP and Hsc5-GFP/mito^{UPR} channels are showed separately in black-white. (C) Mito^{UPR} (green, by *Hsc5-GFP*) could be detected in some progenitors of *esg^{ts}>Phb2^{RNAi-1}* flies at 29°C for 7 days (red, by *esg>RFP*) (white arrowheads). RFP and Hsc5-GFP/mito^{UPR} channels are showed separately in black-white. (D) No mito^{UPR} (green, by *Hsp60-GFP*) is detected in progenitors (red, by *esg>RFP*) of control flies at 29°C for 7 days (white arrowheads). RFP and Hsp60-GFP/mito^{UPR} channels are showed separately in black-white. (E) Mito^{UPR} (green, by *Hsp60-GFP*) is detectable in progenitors of *esg^{ts}>Phb1^{RNAi-1}* flies (red, by *esg>RFP*) (white arrowheads). RFP and Hsp60-GFP/mito^{UPR} channels are showed separately in black-white. (F) Mito^{UPR} (green, by *Hsp60-GFP*) is detectable in progenitors of *esg^{ts}>Phb2^{RNAi-1}* flies (red, by *esg>RFP*) (white arrowheads). RFP and Hsp60-GFP/mito^{UPR} channels are showed separately in black-white. GFP is in green, blue indicates DAPI staining for DNA. Scale bars: 20 μm.

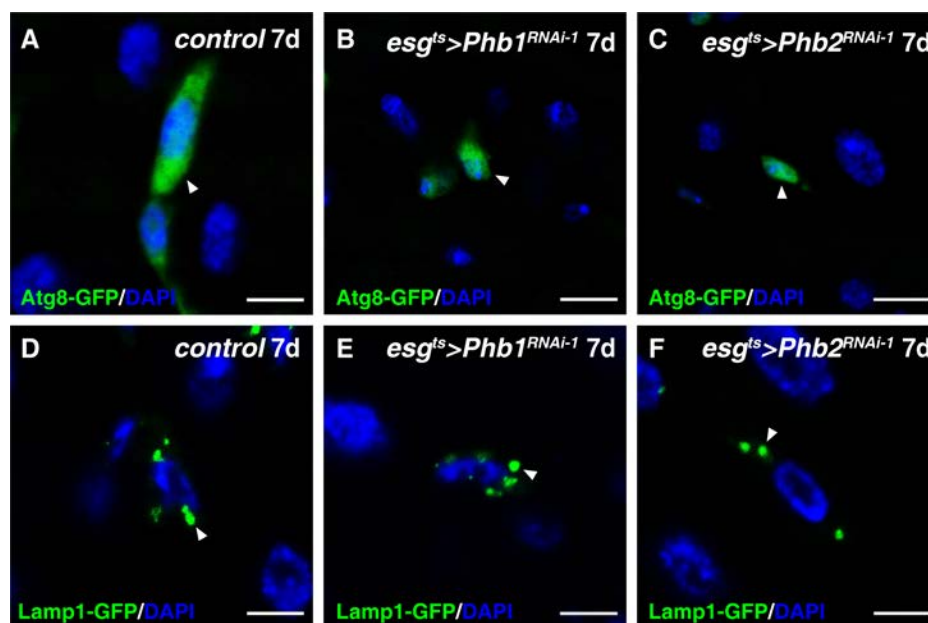


Fig. S27. The PHB complex does not involve in autophagy.

(A) No autophagosomes (by Atg8-GFP puncta) could be detected in progenitors (green, by *esg>Atg8-GFP*) of control flies at 29°C for 7 days (white arrowhead). Note that Atg8-GFP is uniformly located in progenitors including the nucleus, and will form Atg8-GFP puncta when autophagy is induced. (B) No autophagosomes (by Atg8-GFP puncta) could be detected in progenitors (green, by *esg>Atg8-GFP*) of *esg^{ts}>Phb1^{RNAi-1}* flies at 29°C for 7 days (white arrowhead). (C) No autophagosomes (by Atg8-GFP puncta) could be detected in progenitors (green, by *esg>Atg8-GFP*) of *esg^{ts}>Phb2^{RNAi-1}* flies at 29°C for 7 days (white arrowhead). (D) Lysosomes (green, by *Lamp1-GFP*) in progenitors (green, by *esg>Lamp1-GFP*) of control flies at 29°C for 7 days (white arrowhead). (E) The number and morphology of lysosomes (green, by *Lamp1-GFP*) in progenitors (green, by *esg>Lamp1-GFP*) of *esg^{ts}>Phb1^{RNAi-1}* flies are largely unchanged at 29°C for 7 days (white arrowhead). (F) The number and morphology of

lysosomes (green, by *Lamp1-GFP*) in progenitors (green, by *esg>Lamp1-GFP*) of *esg^{ts}>Phb1^{RNAi-1}* flies are largely unchanged at 29°C for 7 days (white arrowhead). GFP is in green, blue indicates DAPI staining for DNA. Scale bars: 5 μm.

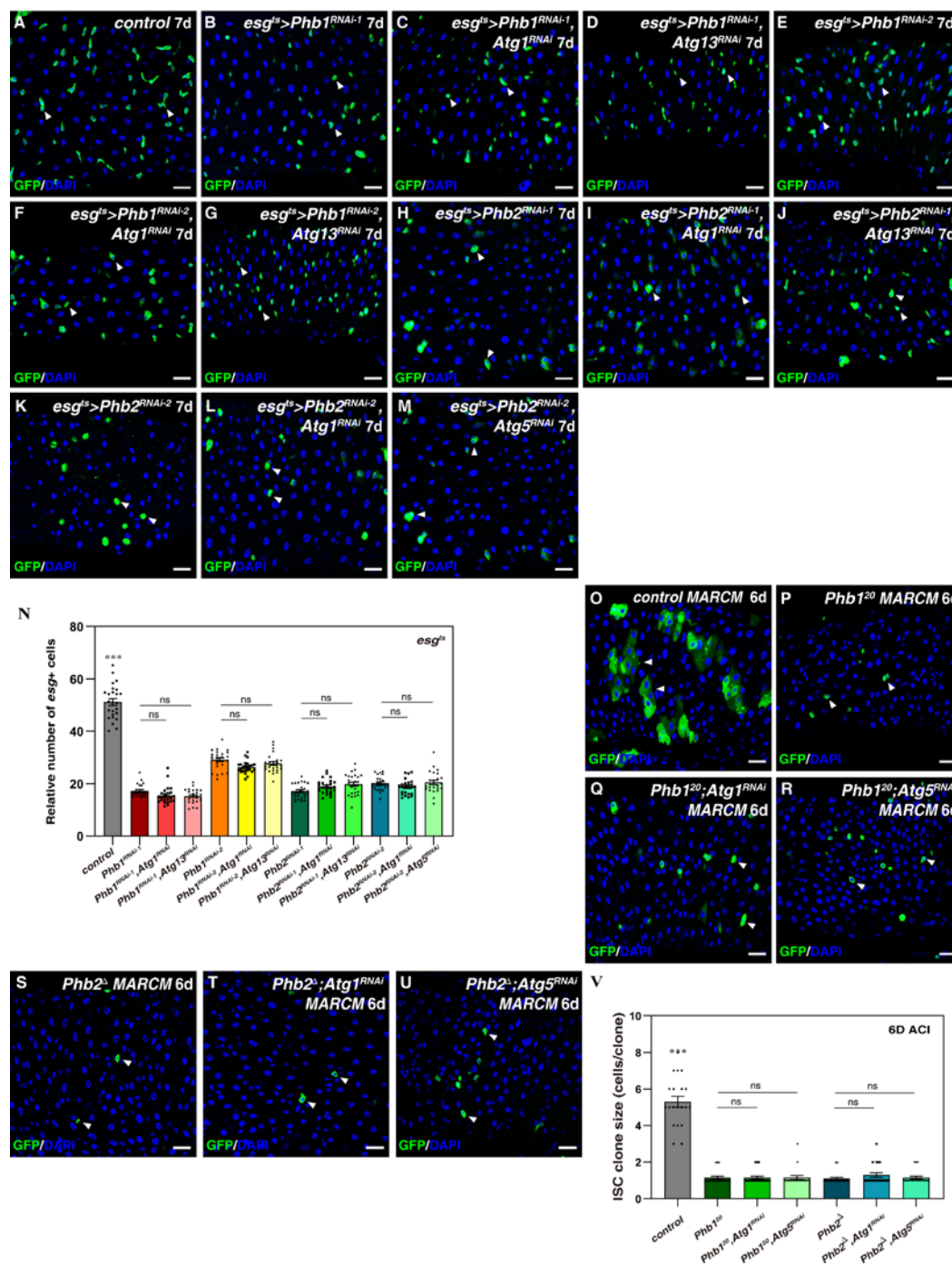


Fig. S28. Autophagy is not involved in proliferation defects in *Phb*-defective progenitors.

(A) Progenitors (green) in control flies at 29°C for 7 days (white arrowheads). (B) Progenitors (green) in $esg^{ts}>Phb1^{RNAi-1}$ flies at 29°C for 7 days (white arrowheads). The number of progenitors is decreased upon *Phb1* depletion. (C) Progenitors (green) in $esg^{ts}>Atg1^{RNAi}; Phb1^{RNAi-1}$ flies at 29°C for 7 days (white arrowheads). The number of progenitors does not increase upon co-depletion of *Atg1* and *Phb1*. (D) Progenitors (green) in $esg^{ts}>Atg13^{RNAi}; Phb1^{RNAi-1}$ flies at 29°C for 7 days (white arrowheads). The number of progenitors does not increase upon co-depletion of *Atg13* and *Phb1*. (E) Progenitors (green) in $esg^{ts}>Phb1^{RNAi-2}$ flies at 29°C for 7 days (white arrowheads). The number of progenitors is decreased upon *Phb1* depletion. (F) Progenitors (green) in $esg^{ts}>Atg1^{RNAi}; Phb1^{RNAi-2}$ flies at 29°C for 7 days (white arrowheads). The number of progenitors does not increase upon co-depletion of *Atg1* and *Phb1*. (G) Progenitors (green) in $esg^{ts}>Atg13^{RNAi}; Phb1^{RNAi-2}$ flies at 29°C for 7 days (white arrowheads). The number of progenitors does not increase upon co-depletion of *Atg13* and *Phb1*. (H) Progenitors (green) in $esg^{ts}>Phb2^{RNAi-1}$ flies at 29°C for 7 days (white arrowheads). The number of progenitors is decreased upon *Phb2* depletion. (I) Progenitors (green) in $esg^{ts}>Atg1^{RNAi}; Phb2^{RNAi-1}$ flies at 29°C for 7 days (white arrowheads). The number of progenitors does not increase upon co-depletion of *Atg1* and *Phb2*. (J) Progenitors (green) in $esg^{ts}>Atg13^{RNAi}; Phb2^{RNAi-1}$ flies at 29°C for 7 days (white arrowheads). The number of progenitors does not increase upon co-depletion of *Atg13* and *Phb2*. (K) Progenitors (green) in $esg^{ts}>Phb2^{RNAi-2}$ flies at 29°C for 7 days (white arrowheads). The number of progenitors is decreased upon *Phb2* depletion. (L) Progenitors (green) in $esg^{ts}>Atg1^{RNAi}; Phb2^{RNAi-2}$ flies at 29°C for 7 days (white arrowheads). The number of

progenitors does not increase upon co-depletion of *Atg1* and *Phb2*. (M) Progenitors (green) in *esg^{ts}>Atg5^{RNAi}; Phb2^{RNAi-2}* flies at 29°C for 7 days (white arrowheads). The number of progenitors does not increase upon co-depletion of *Atg13* and *Phb2*. (N) Quantification of the relative number of *esg*⁺ cells in flies with indicated genotypes. Mean ± SD is shown. n=25-30 intestines. ^{ns}*P*>0.05; ****P*<0.001. (O) Control *FRT* ISC MARCM clones (green) (6d ACI) (white arrowheads). (P) *Phb1²⁰* ISC MARCM clones (green) (6d ACI) (white arrowheads). (Q) *Phb1²⁰; Atg1^{RNAi}* ISC MARCM clones (green) (6d ACI) (white arrowheads). (R) *Phb1²⁰; Atg5^{RNAi}* ISC MARCM clones (green) (6d ACI) (white arrowheads). (S) *Phb2^A* ISC MARCM clones (green) (6d ACI) (white arrowheads). (T) *Phb2^A; Atg1^{RNAi}* ISC MARCM clones (green) (6d ACI) (white arrowheads). (U) *Phb2^A; Atg5^{RNAi}* ISC MARCM clones (green) (6d ACI) (white arrowheads). (V) Quantification of ISC MARCM clone size in flies with indicated genotypes. Mean ± SD is shown. n=20 intestines. ^{ns}*P*>0.05; ****P*<0.001. GFP is in green, blue indicates DAPI staining for DNA. Scale bars: 20 μm.

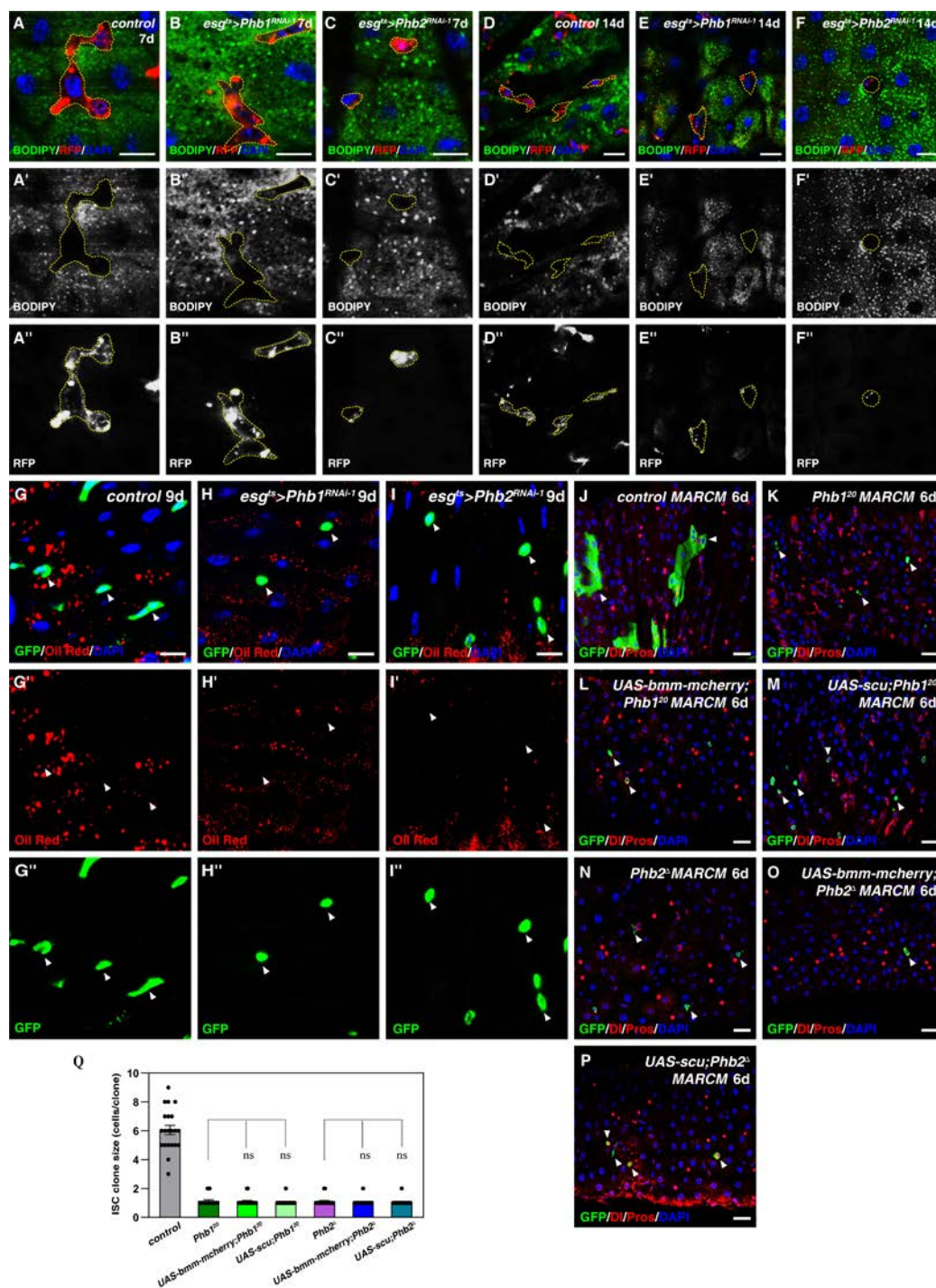


Fig. S29. No increased lipid storage upon PHB depletion.

(A) BODIPY staining (green) in control flies at 29°C for 7 days. Progenitors (red, by *esg>RFP*) are outlined with yellow dash lines. BODIPY and RFP channels are showed separately in black-white. (B) BODIPY staining (green) in *esg^{ts}>Phb1^{RNAi-1}* flies at

29°C for 7 days. Progenitors (red, by *esg>RFP*) are outlined with yellow dash lines. BODIPY and RFP channels are showed separately in black-white. No change of lipid droplets is observed. (C) BODIPY staining (green) in *esg^{ts}>Phb2^{RNAi-1}* flies at 29°C for 7 days. Progenitors (red, by *esg>RFP*) are outlined with yellow dash lines. BODIPY and RFP channels are showed separately in black-white. No change of lipid droplets is observed. (D) BODIPY staining (green) in control flies at 29°C for 14 days. Progenitors (red, by *esg>RFP*) are outlined with yellow dash lines. BODIPY and RFP channels are showed separately in black-white. (E) BODIPY staining (green) in *esg^{ts}>Phb1^{RNAi-1}* flies at 29°C for 14 days. Progenitors (red, by *esg>RFP*) are outlined with yellow dash lines. BODIPY and RFP channels are showed separately in black-white. No change of lipid droplets is observed. (F) BODIPY staining (green) in *esg^{ts}>Phb2^{RNAi-1}* flies at 29°C for 14 days. Progenitors (red, by *esg>RFP*) are outlined with yellow dash lines. BODIPY and RFP channels are showed separately in black-white. No change of lipid droplets is observed. (G) Oil red staining (red) in control flies at 29°C for 9 days. Progenitors (green, by *esg>GFP*) are indicated with white arrowheads. Oil red and GFP channels are showed separately. (H) Oil red staining (red) in *esg^{ts}>Phb1^{RNAi-1}* flies at 29°C for 9 days. Progenitors (green, by *esg>GFP*) are indicated with white arrowheads. Oil red and GFP channels are showed separately. No change of lipid droplets is observed. (I) Oil red staining (red) in *esg^{ts}>Phb2^{RNAi-1}* flies at 29°C for 9 days. Progenitors (green, by *esg>GFP*) are indicated with white arrowheads. Oil red and GFP channels are showed separately. No change of lipid droplets is observed. (J) Control *FRT* ISC MARCM clones (green) (6d ACI) (white arrowheads). DI and Pros are in red.

(K) *Phb1*²⁰ ISC MARCM clones (green) (6d ACI) (white arrowheads). D1 and Pros in red. (L) *UAS-bmm-cherry; Phb1*²⁰ ISC MARCM clones (green) (6d ACI) (white arrowheads). D1 and Pros are in red. (M) *UAS-scu; Phb1*²⁰ ISC MARCM clones (green) (6d ACI) (white arrowheads). D1 and Pros are in red. (N) *Phb2*^Δ ISC MARCM clones (green) (6d ACI) (white arrowheads). D1 and Pros in red. (O) *UAS-bmm-cherry; Phb2*^Δ ISC MARCM clones (green) (6d ACI) (white arrowheads). D1 and Pros are in red. (P) *UAS-scu; Phb2*^Δ ISC MARCM clones (green) (6d ACI) (white arrowheads). D1 and Pros are in red. Note that some *Phb2*^Δ marked cells are Pros⁺, indicating that Phb2 is largely dispensable for progeny differentiation. (Q) Quantification of ISC MARCM clone size in flies with indicated genotypes. Mean ± SD is shown. n=15-25 intestines. ^{ns}*P*>0.05. Blue indicates DAPI staining for DNA. Scale bars: 10 μm (A-I) and 20 μm (J-P).

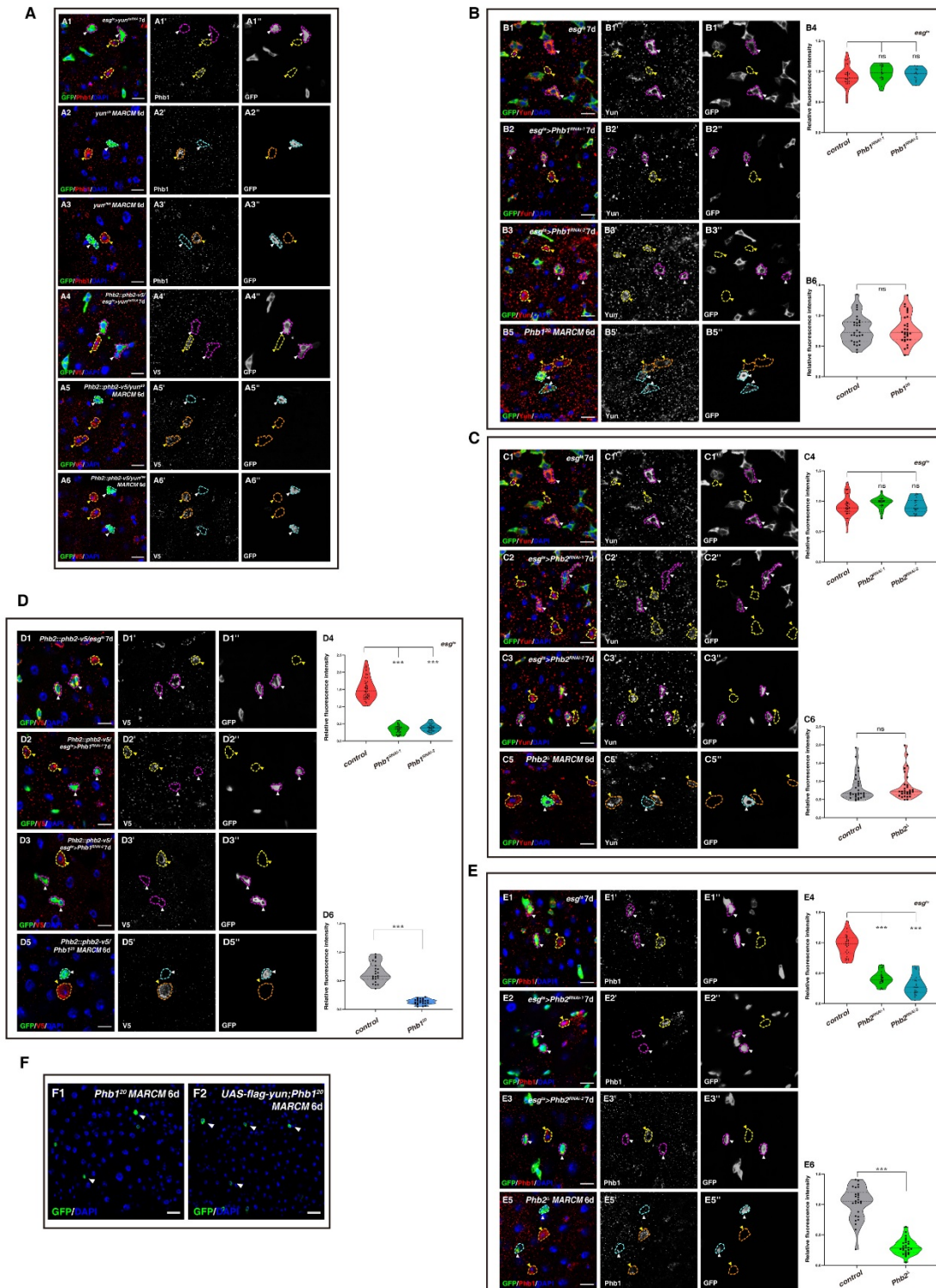


Fig. S30. Yun functions as a scaffold for the PHB complex.

(A) Yun affects the levels of the PHB complex. (A1) The levels of Phb1 protein (red) are decreased in *yun*-depleted progenitor cells (green, GFP⁺ cells with purple dotted

lines)(white arrowheads). Phb1 protein in EE cells (with dotted lines, yellow arrowheads) is not affected, which is used as internal control. Phb1 and GFP channels are shown separately in black-white. (A2 and A3) The levels of Phb1 protein (red) are decreased in *yun* mutant cells (green, GFP⁺ cells with light blue dotted lines) (white arrowheads) (A2: *yun*^{A9}, A3: *yun*^{A66}). Phb1 protein in EE cells (with dotted lines, yellow arrowheads) is not affected, which is used as internal control. (A4) The levels of Phb2 protein (red, by *Phb2::phb2-v5*) are decreased in *yun*-depleted progenitor cells (green, GFP⁺ cells with light blue dotted lines) (white arrowheads). Phb2 protein in EE cells (with dotted lines, yellow arrowheads) is not affected, which is used as internal control. Phb2 and GFP channels are shown separately in black-white. (A5 and A6) The levels of Phb2 protein (red, by *Phb2::phb2-v5*) are decreased in *yun* mutant cells (green, GFP⁺ cells with light blue dotted lines) (white arrowheads) (A5: *yun*^{A9}, A6: *yun*^{A66}). Phb2 protein in EE cells (with dotted lines, yellow arrowheads) is not affected and used as internal control. (B) Phb1 does not affect the levels of Yun. (B1) Yun (red) localization in control intestines at 29°C for 7 days. Yun expresses in progenitors (green, by *esg>GFP* indicated with purple dotted lines) and EE cells (GFP⁻ cells with yellow dotted lines) (white and yellow arrowheads, respectively). Yun and GFP channels are shown separately in black-white. (B2 and B3) The levels of Yun protein (red) are not affected in *Phb1*-depleted progenitor cells (green, GFP⁺ cells with dotted lines) (white arrowheads) at 29°C for 7 days (B2: *Phb1*^{RNAi-1}, B3: *Phb1*^{RNAi-2}). (B4) Quantification of the relative fluorescence intensity of Yun in control and *Phb1* knockdown intestines. The signals in mutant cells are normalized to signals in EE cells. Mean ± SD is shown.

n=15-30. ^{ns} $P>0.05$. (B5) The levels of Yun protein (red) are not affected in *Phb1*²⁰ mutant cells (green, GFP⁺ cells with yellow dotted lines) (white arrowheads) (6D ACI). (B6) Quantification of the relative fluorescence intensity of Yun in control and *Phb1*²⁰ mutant cells. The signals in mutant cells are normalized to signals in neighboring wildtype cells. Mean \pm SD is shown. n=30. ^{ns} $P>0.05$. (C) Phb2 does not affect the levels of Yun. (C1) Yun (red) localization in control intestines at 29°C for 7 days. Yun expresses in progenitors (green, by *esg>GFP* indicated with purple dotted lines) and EE cells (GFP⁻ cells with yellow dotted lines) (white and yellow arrowheads, respectively). Yun and GFP channels are shown separately in black-white. (C2 and C3) The levels of Yun protein (red) are not affected in *Phb2*-depleted progenitor cells (green, GFP⁺ cells with purple dotted lines) (white arrowheads) at 29°C for 7 days (C2: *Phb2*^{RNAi-1}, C3: *Phb2*^{RNAi-2}). (C4) Quantification of the relative fluorescence intensity of Yun in control and *Phb2* knockdown intestines. The signals in mutant cells are normalized to signals in EE cells. Mean \pm SD is shown. n=25-40. ^{ns} $P>0.05$. (C5) The levels of Yun protein (red) are not affected in *Phb2*^Δ mutant cells (green, GFP⁺ cells with yellow dotted lines)(white arrowheads) (6D ACI). Yun protein in neighboring wildtype cells (with cyan dotted lines, yellow arrowheads) is used as internal control. (C6) Quantification of the relative fluorescence intensity of Yun in control and *Phb2*^Δ mutant cells. The signals in mutant cells are normalized to signals in neighboring wildtype cells. Mean \pm SD is shown. n=29. ^{ns} $P>0.05$. (D) Phb1 affects the levels of Phb2. (D1) Phb2 (red, by V5 in *Phb2::phb2-v5*) localization in control intestines at 29°C for 7 days. Phb2 expresses in progenitors (green, by *esg>GFP* indicated with

purple dotted lines) and EE cells (GFP⁻ cells with yellow dotted lines) (white and yellow arrowheads, respectively). V5 and GFP channels are shown separately in black-white. (D2 and D3) The levels of Phb2 protein (red) are decreased in *Phb1*-depleted progenitor cells (green, GFP⁺ cells with purple dotted lines) (white arrowheads) at 29°C for 7 days (D2: *Phb1^{RNAi-1}*, D3: *Phb1^{RNAi-2}*). Phb2 protein in EE cells (with yellow dotted lines, yellow arrowheads) is used as internal control. (D4) Quantification of the relative fluorescence intensity of Phb2 in control and *Phb1* knockdown intestines. The signals in mutant cells are normalized to signals in EE cells. Mean ± SD is shown. n=40-60. ****P*<0.001. (D5) The levels of Phb2 protein (red, V5 in *Phb2::phb2-v5*) are decreased in *Phb1²⁰* mutant cells (green, GFP⁺ cells with cyan dotted lines) (white arrowheads) (6D ACI). Phb2 protein in neighboring wildtype cells (with yellow dotted lines, yellow arrowheads) is used as internal control. (D6) Quantification of the relative fluorescence intensity of Phb2 in control and *Phb1²⁰* mutant cells. The signals in mutant cells are normalized to signals in neighboring wildtype cells. Mean ± SD is shown. n=23. ****P*<0.001. (E) Phb2 affects the levels of Phb1. (E1) Phb1 (red) localization in control intestines at 29°C for 7 days. Phb1 expresses in progenitors (green, by *esg>GFP* indicated with purple dotted lines) and EE cells (GFP⁻ cells with yellow dotted lines) (white and yellow arrowheads, respectively). Phb1 and GFP channels are shown separately in black-white. (E2 and E3) The levels of Phb1 protein (red) are decreased in *Phb2*-depleted progenitor cells (green, GFP⁺ cells with purple dotted lines) (white arrowheads) at 29°C for 7 days (E2: *Phb2^{RNAi-1}*, E3: *Phb2^{RNAi-2}*). Phb1 protein in EE cells (with yellow dotted lines, yellow arrowheads) is used as internal control. (E4)

Quantification of the relative fluorescence intensity of Phb1 in control and *Phb2* knockdown intestines. The signals in mutant cells are normalized to signals in EE cells. Mean \pm SD is shown. n=25-35. *** P <0.001. (E5) The levels of Phb1 protein (red) are decreased in *Phb2^d* mutant cells (green, GFP⁺ cells with cyan dotted lines)(white arrowheads) (6D ACI). Phb1 protein in neighboring wildtype cells (with yellow dotted lines, yellow arrowheads) is used as internal control. Phb1 and GFP channels are shown separately in black-white. (E6) Quantification of the relative fluorescence intensity of Phb1 in control and *Phb2^d* mutant cells. The signals in mutant cells are normalized to signals in neighboring wildtype cells. Mean \pm SD is shown. n=26. *** P <0.001. (F) Yun genetically functions upstream of the PHB complex. (F1) *Phb1²⁰* ISC MARCM clones (green) (white arrowheads) (6D ACI). (F2) Expression of *flag-yun* cannot rescue progenitor proliferation defects observed in *Phb1²⁰* mutant (white arrowheads) (6D ACI). In all panels except graphs, GFP is in green, blue indicates DAPI staining for DNA. Scale bars: 10 μ m except *F* (20 μ m).

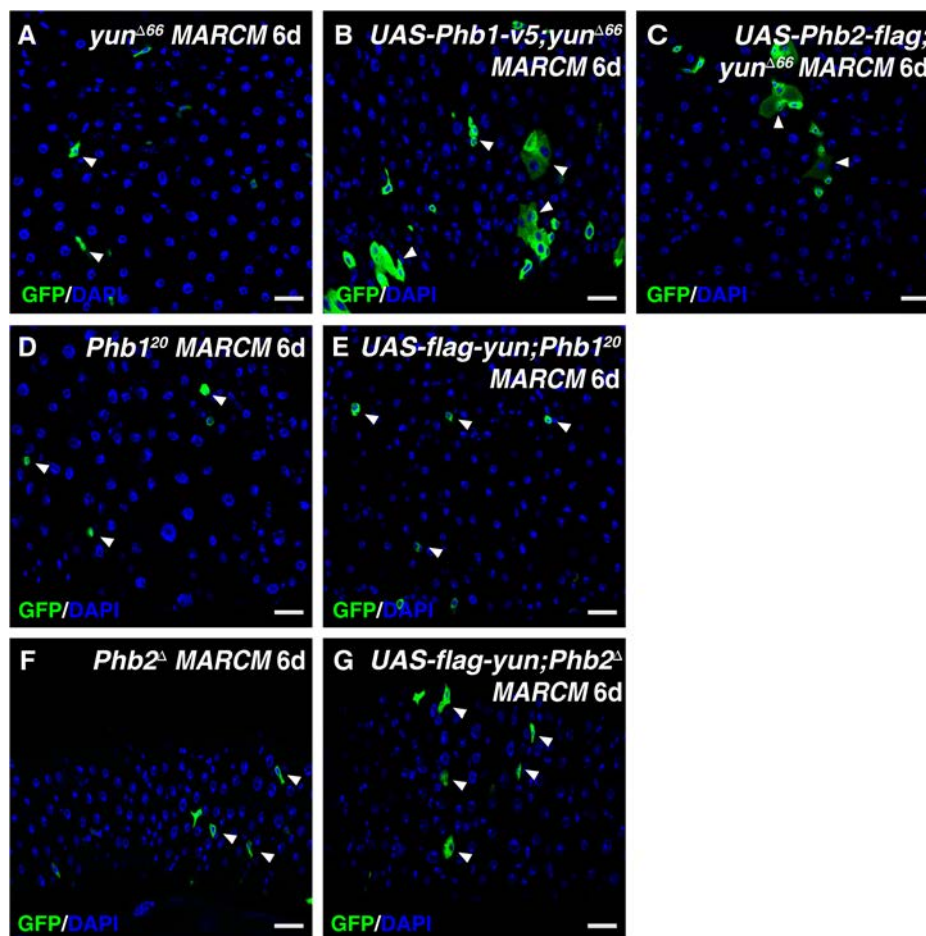


Fig. S31. Yun genetically functions upstream of the PHB complex.

(A) ISC MARCM clones of *yun*^{Δ66} (green)(white arrowheads). (B and C) Expression of *Phb1* (B) and *Phb2* (C) could almost completely rescue ISC proliferation defects observed in *yun*^{Δ66} (white arrowheads). (D) *Phb1*²⁰ ISC MARCM clones (green) (white arrowheads) (6D ACI). (E) Expression of *flag-yun* cannot rescue progenitor proliferation defects observed in *Phb1*²⁰ mutant (white arrowheads) (6D ACI). (F) *Phb2*^Δ ISC MARCM clones (green) (white arrowheads) (6D ACI). (G) Expression of *flag-yun* cannot rescue progenitor proliferation defects observed in *Phb2*^Δ mutant (white arrowheads) (6D ACI). GFP is in green, blue indicates DAPI staining for DNA.

Scale bars: 20 μm.

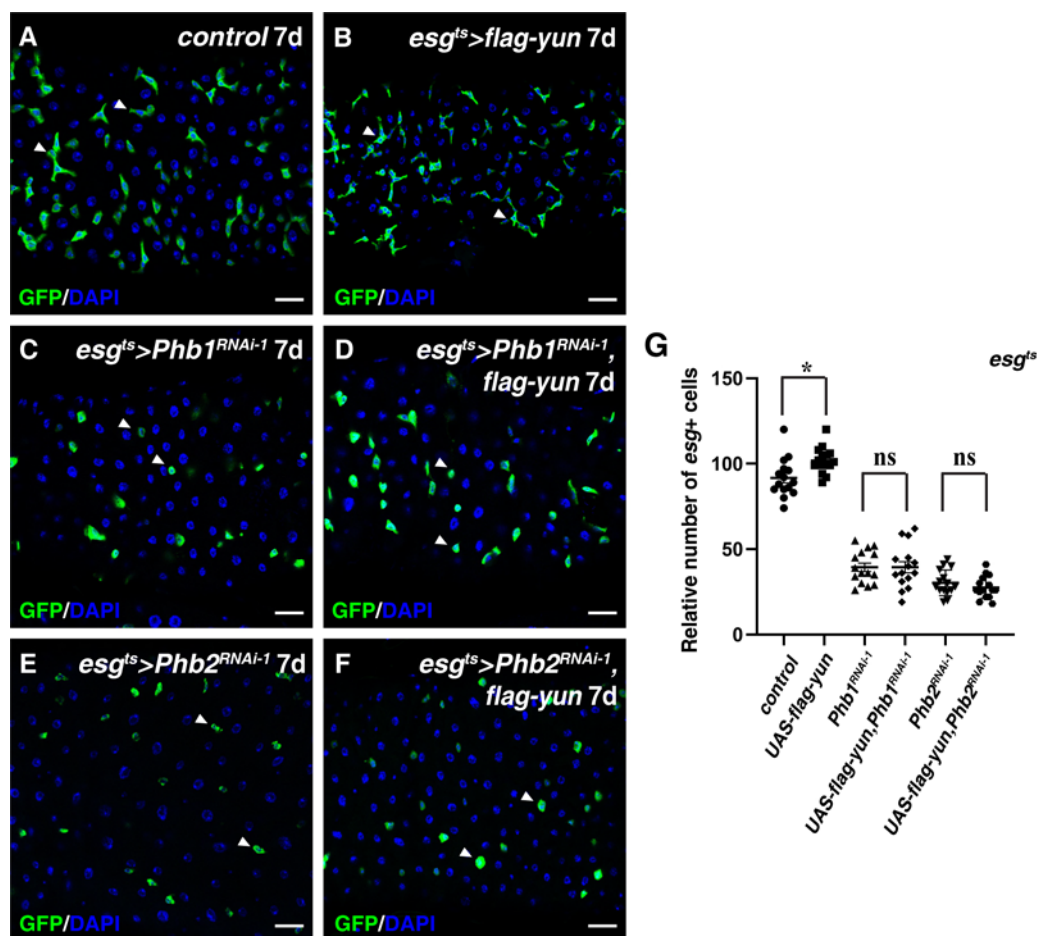


Fig. S32. Yun genetically functions upstream of the PHB complex.

(A) Progenitors (green, by *esg*>*GFP*) in control intestines at 29°C for 7 days (white arrowheads). (B) The number of *esg*⁺ cells (green) is mildly increased in *esg*^{ts}>*flag-yun* intestines at 29°C for 7 days (white arrowheads). (C) Progenitors (green) in *esg*^{ts}>*Phb1*^{RNAi-1} intestines at 29°C for 7 days (white arrowheads). (D) The number of *esg*⁺ cells (green) is not rescued in *esg*^{ts}>*Phb1*^{RNAi-1}, *flag-yun* intestines at 29°C for 7 days (white arrowheads). (E) Progenitors (green) in *esg*^{ts}>*Phb2*^{RNAi-1} intestines at 29°C for 7 days (white arrowheads). (F) The number of *esg*⁺ cells (green) is not rescued in *esg*^{ts}> *Phb2*^{RNAi-1}, *flag-yun* intestines at 29°C for 7 days (white arrowheads). (G) Quantification of the relative number of *esg*⁺ cells in flies with indicated genotypes. Mean ± SD is shown. n=15. **P*<0.05, ^{ns}*P*>0.05. In all panels except graphs, GFP is in

green, blue indicates DAPI staining for DNA. Scale bars: 20 μ m.

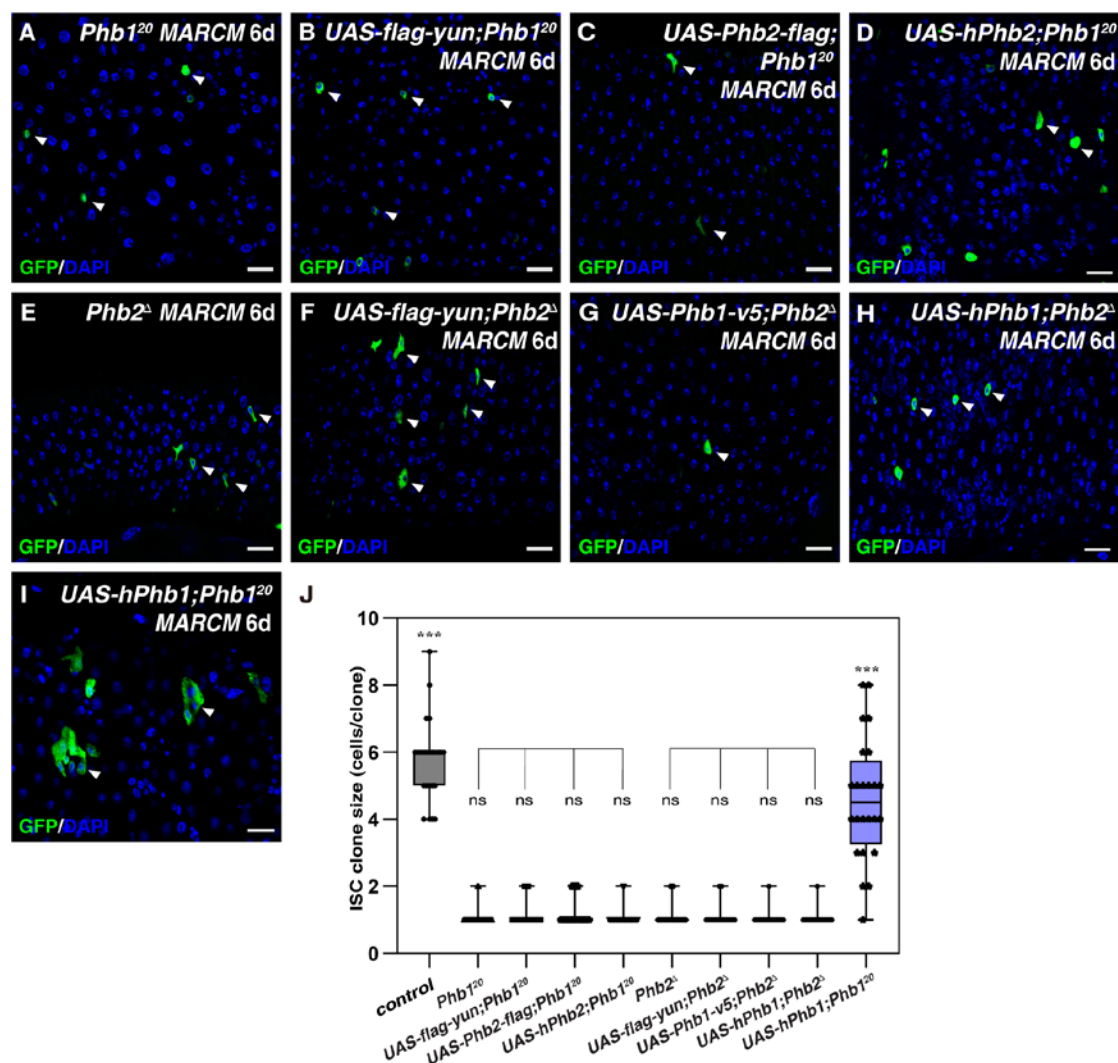


Fig. S33. Phb1 and Phb2 function at the same level.

(A) ISC MARCM clones of *Phb1*²⁰ (green) (white arrowheads) (6D ACI). (B) Expression of *yun* does not rescue ISC proliferation defects observed in *Phb1*²⁰ (white arrowheads) (6D ACI). (C) Expression of *Phb2* does not rescue ISC proliferation defects observed in *Phb1*²⁰ (white arrowheads) (6D ACI). (D) Expression of human *Phb2* does not rescue ISC proliferation defects observed in *Phb1*²⁰ (white arrowheads) (6D ACI). (E) ISC MARCM clones of *Phb2*^Δ (green) (white arrowheads) (6D ACI). (F)

Expression of *yun* does not rescue ISC proliferation defects observed in *Phb2^d* (white arrowheads) (6D ACI). (G) Expression of *Phb1* does not rescue ISC proliferation defects observed in *Phb2^d* (white arrowheads) (6D ACI). (H) Expression of human *Phb1* does not rescue ISC proliferation defects observed in *Phb2^d* (white arrowheads) (6D ACI). (I) Expression of human *Phb1* can rescue ISC proliferation defects observed in *Phb1²⁰* (white arrowheads) (6D ACI). (J) Quantification of ISC clone size in flies with indicated genotypes. Mean \pm SD is shown. n=10-20. *** P <0.001, ^{ns} P >0.05. In all panels except graphs, GFP is in green, blue indicates DAPI staining for DNA. Scale bars: 20 μ m.

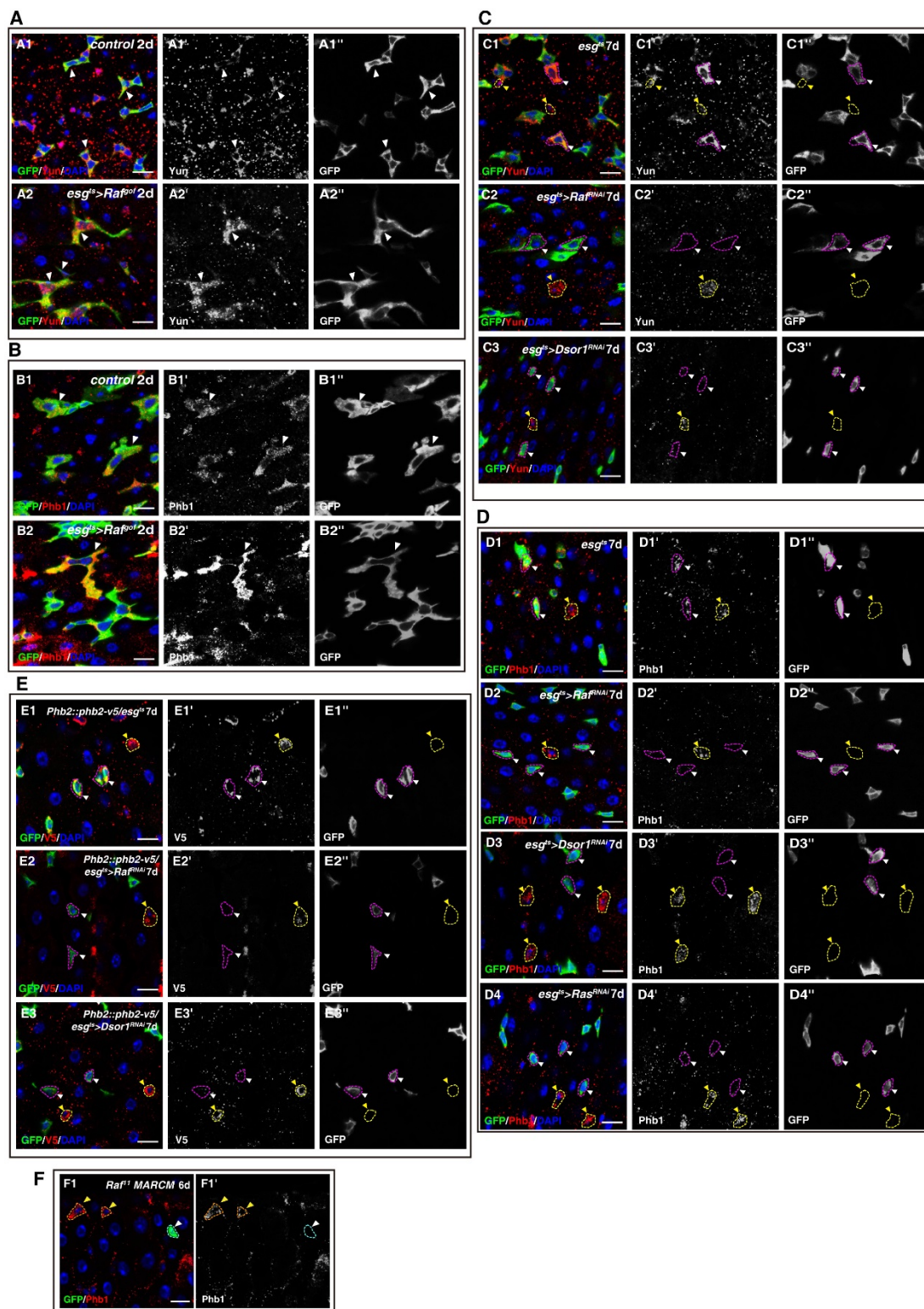


Fig. S34. The Yun/PHB complex is positively regulated by EGFR signaling.

(A) Yun is positively regulated by EGFR signaling. (A1) Yun protein (red) in

progenitors (green, by *esg>GFP*) of 2-day old control flies (white arrowheads). Yun and GFP channels are shown separately in black-white. (A2) The levels of Yun protein (red) are significantly increased in progenitors of *esg^{ts}>Raf^{gof}* intestines at 29°C for 2 days (white arrowheads). (B) Phb1 is positively regulated by EGFR signaling. (B1) Phb1 protein (red) in progenitors (green, by *esg>GFP*) of 2-day old control flies (white arrowheads). Phb1 channel is shown separately in black-white. (B2) The levels of Phb1 protein (red) are significantly increased in progenitors of *esg^{ts}>Raf^{gof}* intestines at 29°C for 2 days (white arrowheads). (C) Yun protein level is significantly decreased upon inhibition of EGFR signaling. (C1) Yun (red) localization in control intestines at 29°C for 7 days. Yun expresses in progenitors (green, by *esg>GFP* indicated with purple dotted lines) and EE cells (GFP⁻ cells with yellow dotted lines) (white and yellow arrowheads respectively). Yun and GFP channels are shown separately in black-white. (C2 and C3) The levels of Yun protein (red) are decreased in progenitors upon depletion of *Raf* (C2) and *Dsor1* (C3) (green, GFP⁺ cells with purple dotted lines) (white arrowheads) at 29°C for 7 days. (D) Phb1 protein level is significantly decreased upon inhibition of EGFR signaling. (D1) Phb1 (red) localization in control intestines at 29°C for 7 days. Phb1 is expressed in progenitors (green, by *esg>GFP* indicated with purple dotted lines) and EE cells (GFP⁻ cells with yellow dotted lines) (white and yellow arrowheads, respectively). Phb1 and GFP channels are shown separately in black-white. (D2-D4) The levels of Phb1 protein (red) are decreased in progenitors upon depletion of *Raf* (D2), *Dsor1* (D3) and *Ras* (D4) (green, GFP⁺ cells with purple dotted lines) (white arrowheads) at 29°C for 7 days. (E) Phb2 protein is significantly decreased upon

inhibition of EGFR signaling. (*E1*) Phb2 (red, by *Phb2::phb2-v5*) localization in control intestines at 29°C for 7 days. Phb2 is expressed in progenitors (green, by *esg>GFP* indicated with purple dotted lines) and EE cells (GFP⁻ cells with yellow dotted lines) (white and yellow arrowheads, respectively). V5 and GFP channels are shown separately in black-white. (*E2* and *E3*) The levels of Phb2 protein (red, by *Phb2::phb2-v5*) are decreased in progenitors upon depletion of *Raf* (*E2*) and *Dsor1* (*E3*) (green, GFP⁺ cells with purple dotted lines) (white arrowheads) at 29°C for 7 days. (*F*) The levels of Phb1 protein (red) are decreased in the absence of *Raf* (white arrowheads). Selected mutant and wildtype cells are outlined with dotted lines. Phb1 channels are shown separately in black-white. In all panels except graphs, GFP is in green, blue indicates DAPI staining for DNA. Scale bars: 10 μm.

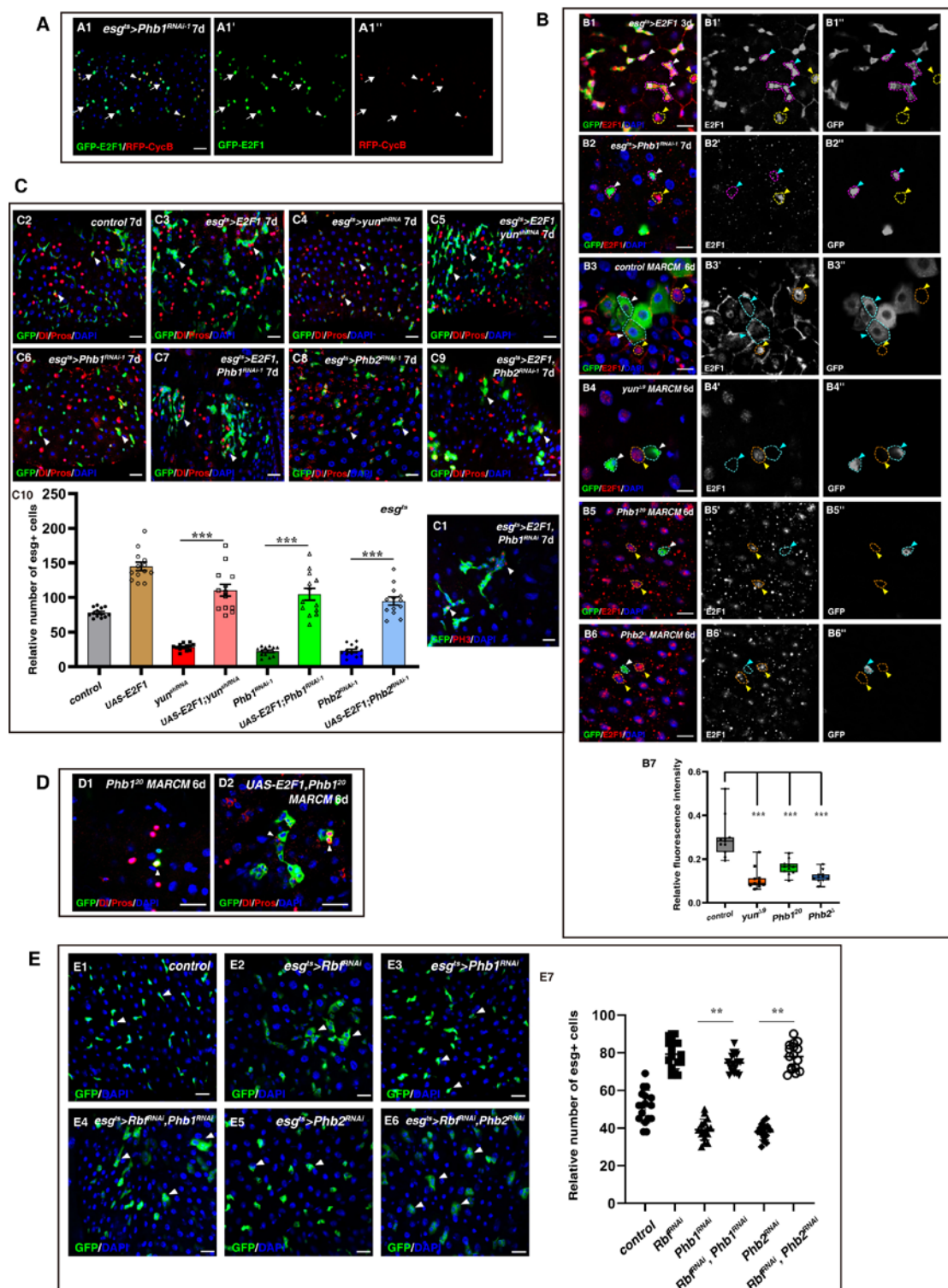


Fig. S35. E2F1 acts downstream of the Yun/PHB complex to regulate ISC proliferation.

(A) Fly-FUCCI cell-cycle distribution of progenitors in *esg^{ts}>Phb1^{RNAi}* intestines. GFP

and RFP channels are shown separately. (B) Yun affects the stability of E2F1 protein. (B1) The levels of E2F1 (red) are dramatically increased in progenitors of *esg^{ts}>E2F1*, *Dp* intestines at 29°C for 3 days. (B2) The levels of E2F1 (red) are decreased in *Phb1*-depleted progenitors at 29°C for 7 days (green, by *esg>GFP*, indicated with purple dotted lines) (white arrowheads). (B3) E2F1 (red) in *FRT* control ISC MARCM clones (green, indicated with cyan dotted lines, white arrowheads) (6D ACI). EC cells are indicated with yellow dotted lines (yellow arrowheads). E2F1 and GFP channels are shown separately in black-white. (B4) The levels of E2F1 (red) are decreased in *yun^Δ* mutant cells (green, indicated with cyan dotted lines) (white arrowheads). EC cells are indicated with yellow dotted lines (yellow arrowhead). (B5) The levels of E2F1 (red) are decreased in *Phb1²⁰* mutant cells (green, indicated with cyan dotted lines) (white arrowheads). EC cells are indicated with yellow dotted lines (yellow arrowhead). (B6) The levels of E2F1 (red) are decreased in *Phb2^Δ* mutant cells (green, indicated with cyan dotted lines) (white arrowheads). EC cells are indicated with yellow dotted lines (yellow arrowhead). (B7) Quantification of the relative fluorescence intensity of E2F1 in control, *yun^Δ*, *Phb1²⁰*, and *Phb2^Δ* mutant cells. The signals in progenitor cells are normalized to signals in EC cells. Mean ± SD is shown. n=10. ****P*<0.001. (C) E2F1 acts downstream of Yun/Phb1/Phb2 to regulate progenitor proliferation. (C1) pH3 (red) in *esg^{ts}>E2F1*, *Dp*; *Phb1^{RNAi}* flies at 29°C for 7 days (white arrowheads). (C2) Progenitors (green, by *esg>GFP*) in control flies at 29°C for 7 days (white arrowheads). DI and Pros are in red. (C3) The number of *esg⁺* cells is dramatically increased in *esg^{ts}>E2F1*, *Dp* flies at 29°C for 7 days (white arrowheads). (C4) The number of *esg⁺*

cells is decreased in $esg^{ts}>yun^{shRNA}$ flies at 29°C for 7 days (white arrowheads). (C5) The number of esg^+ cells is dramatically increased in $esg^{ts}>E2F1, Dp; yun^{shRNA}$ flies at 29°C for 7 days (white arrowheads) and is similar to $esg^{ts}>E2F1, Dp$ intestines. (C6) The number of esg^+ cells is decreased in $esg^{ts}>Phb1^{RNAi-1}$ flies at 29°C for 7 days (white arrowheads). (C7) The number of esg^+ cells is dramatically increased in $esg^{ts}>E2F1, Dp; Phb1^{RNAi-1}$ flies at 29°C for 7 days (white arrowheads) and is similar to $esg^{ts}>E2F1, Dp$ intestines. (C8) The number of esg^+ cells is decreased in $esg^{ts}>Phb2^{RNAi-1}$ flies at 29°C for 7 days (white arrowheads). (C9) The number of esg^+ cells is dramatically increased in $esg^{ts}>E2F1, Dp; Phb2^{RNAi-1}$ flies at 29°C for 7 days (white arrowheads) and is similar to $esg^{ts}>E2F1, Dp$ intestines. (C10) Quantification of the relative number of esg^+ cells in flies with indicated genotypes. Mean \pm SD is shown. n=13 intestines. *** $P<0.001$. (D) E2F1 acts downstream of the Yun/PHB complex to regulate progenitor proliferation. (D1 and D2) Expression of *E2F1* partially rescued ISC proliferation defects observed in *Phb1²⁰* (white arrowheads). (E) Rbf acts downstream of Phb1/Phb2 to regulate progenitor proliferation. (E1) Progenitors (green, by $esg>GFP$) in control flies (white arrowheads). (E2) The number of esg^+ cells is significantly increased in $esg^{ts}>Rbf^{RNAi}$ flies (white arrowheads). (E3) The number of esg^+ cells is decreased in $esg^{ts}>Phb1^{RNAi-1}$ flies (white arrowheads). (E4) The number of esg^+ cells is significantly increased in $esg^{ts}>Rbf^{RNAi}; Phb1^{RNAi-1}$ flies (white arrowheads) and is similar to $esg^{ts}>Rbf^{RNAi}$ intestines. (E5) The number of esg^+ cells is decreased in $esg^{ts}>Phb2^{RNAi-1}$ flies (white arrowheads). (E6) The number of esg^+ cells is significantly increased in $esg^{ts}>Rbf^{RNAi}; Phb2^{RNAi-1}$ flies (white arrowheads) and is

similar to $esg^{ts}>Rbf^{RNAi}$ intestines. (E7) Quantification of the relative number of esg^{+} cells in flies with indicated genotypes. Mean \pm SD is shown. $n=15-20$ intestines. $**P<0.01$. In all panels except graphs, GFP is in green, blue indicates DAPI staining for DNA. Scale bars: 20 μm (A, C and E), 10 μm (B1, B2, B3, B5, B6 and D), 5 μm (B4).

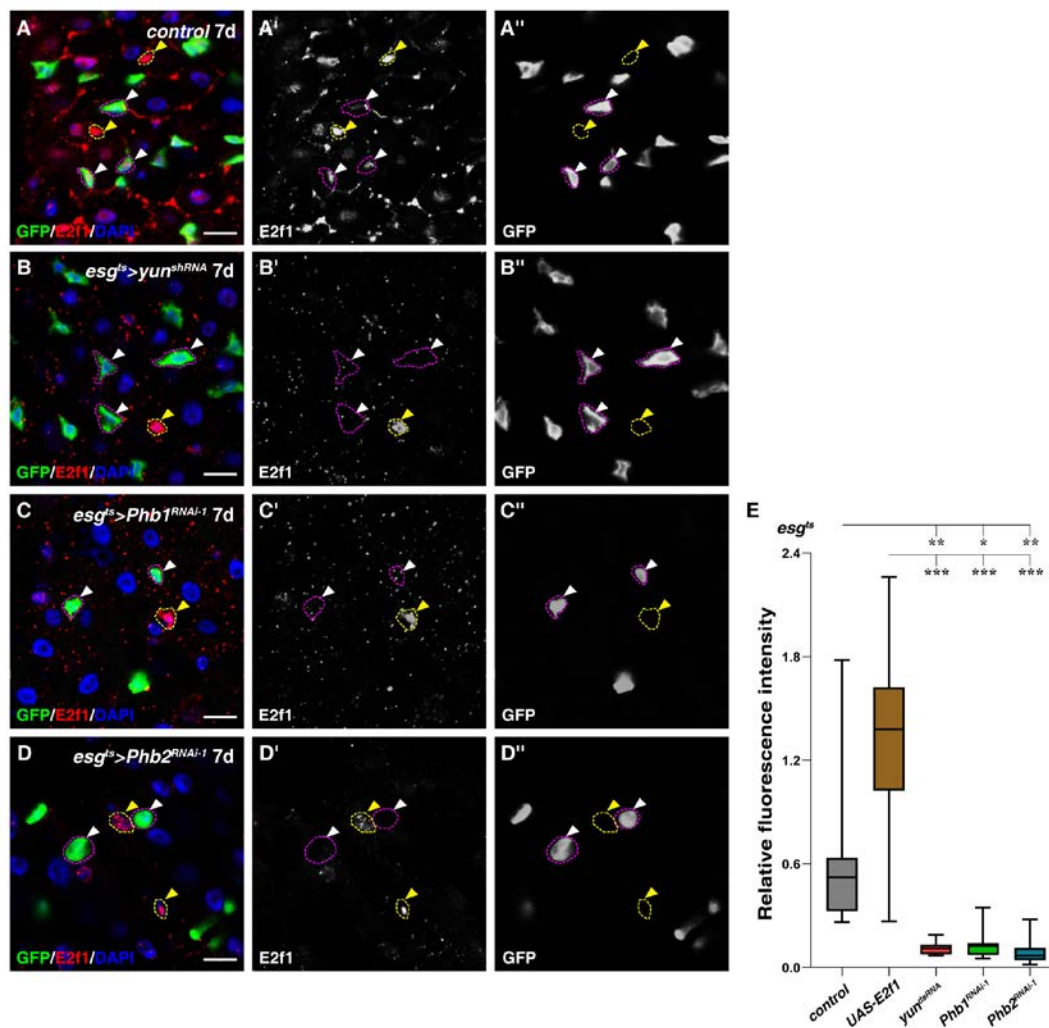


Fig. S36. The Yun/PHB complex affects the levels of E2F1 in progenitors.

(A) Progenitors (green, by $esg>GFP$) in control flies (white arrowheads). (B) The levels of E2F1 are significantly decreased in $esg^{ts}>yun^{shRNA}$ flies (white arrowheads). (C) The levels of E2F1 are significantly decreased in $esg^{ts}>Phb1^{RNAi-1}$ flies (white arrowheads).

(D) The levels of E2F1 are significantly decreased in *esg^{ts}>Phb2^{RNAi-1}* flies (white arrowheads). (E) Quantification of the IOD of E2F1. Mean \pm SD is shown. $n \geq 12$. $*P < 0.05$; $**P < 0.01$; $***P < 0.001$. In all panels except graphs, GFP is in green, E2F1 is in red, blue indicates DAPI staining for DNA. Scale bars: 10 μ m.

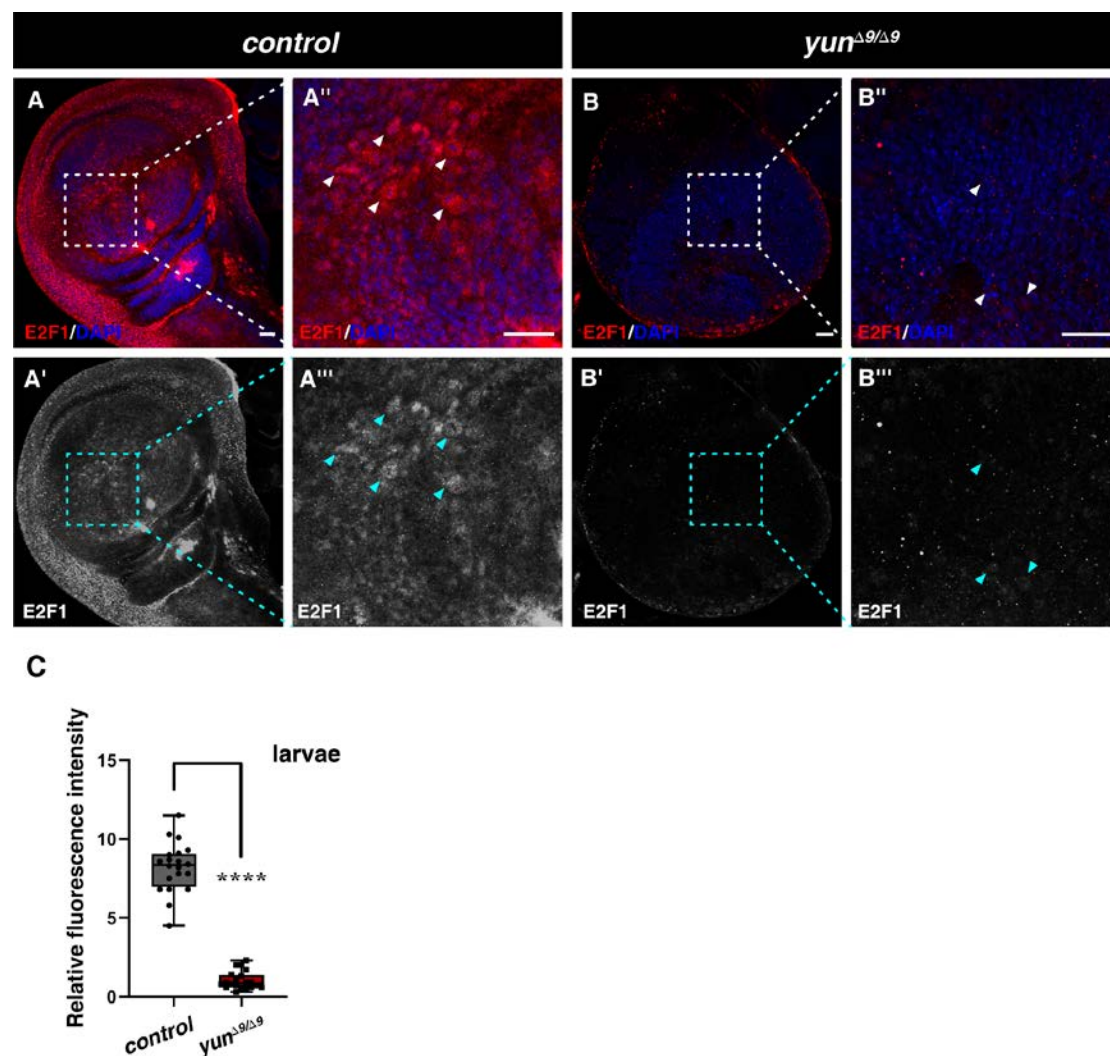


Fig. S37. Yun affects the levels of E2F1 in imaginal wing discs.

(A-A''') E2F1 (red) in control imaginal wing disc. E2F1 channel is showed separately in black-white. (B-B''') The levels of E2F1 are dramatically decreased in *yun^{Δ9}* homozygous imaginal wing disc at the same developmental stage. Please note that the *yun* homozygous mutant discs are smaller than control discs at the same developmental

stages, indicating that *yun* is required for cell proliferation in imaginal wing discs as well. (C) Quantification of E2F1 IOD in control and *yun*⁴⁹ homozygous imaginal wing discs. Mean \pm SD is shown. $n \geq 20$. **** $P < 0.0001$. Scale bars: 20 μ m.

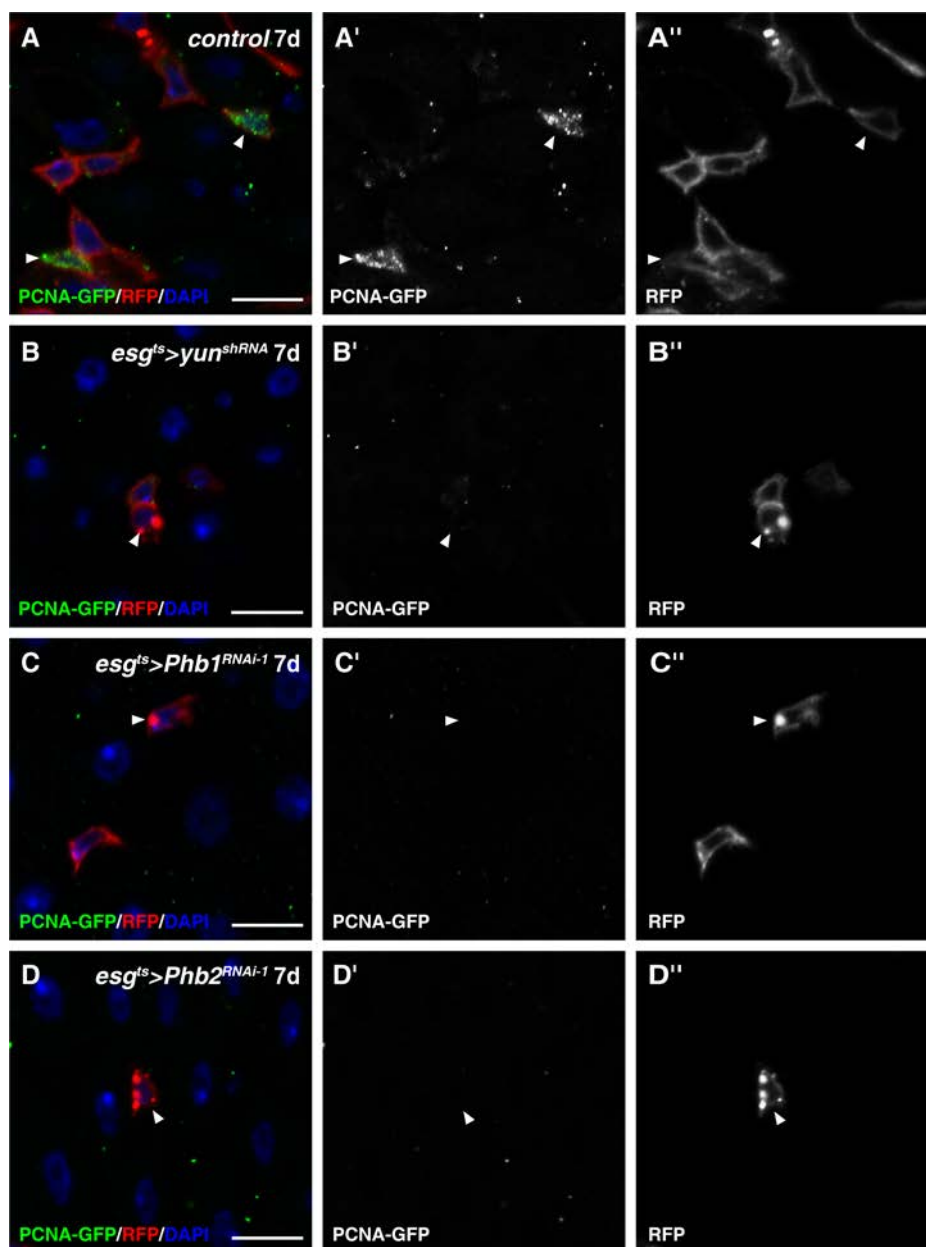


Fig. S38. The expression of PCNA-GFP is dramatically reduced in *yun/Phb*-defective progenitors.

(A) Progenitors (red, by *esg*>*RFP*) in control flies (white arrowheads). (B) The levels of PCNA-GFP are diminished in *esg*^{ts}>*yun*^{shRNA} flies (white arrowheads). (C) The

levels of PCNA-GFP are diminished in *esg^{ts}>Phb1^{RNAi-1}* flies (white arrowheads). (D) The levels of PCNA-GFP are diminished in *esg^{ts}>Phb2^{RNAi-1}* flies (white arrowheads). PCNA-GFP is in green, RFP is in red, blue indicates DAPI staining for DNA. Scale bars: 10 μ m.

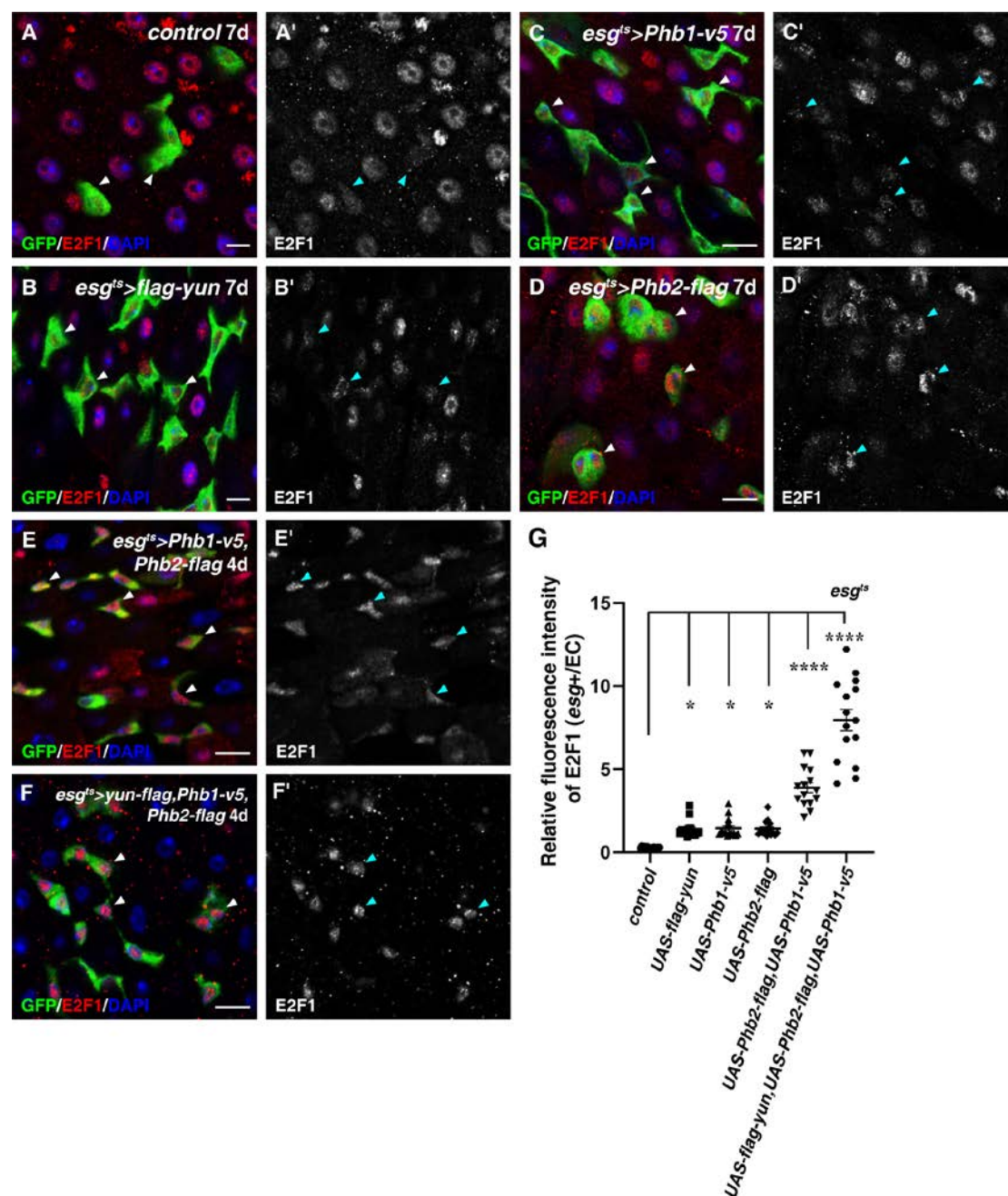


Fig. S39. Ectopic expression of *yun/Phb* increased E2F1 levels.

(A) Progenitors (green, by *esg>GFP*) in control flies (white arrowheads). (B) The levels of E2F1 are mildly increased in *esg^{ts}>flag-yun* flies (white arrowheads). (C) The levels of E2F1 are mildly increased in *esg^{ts}>Phb1-v5* flies (white arrowheads). (D) The levels of E2F1 are mildly increased in *esg^{ts}>Phb2-flag* flies (white arrowheads). (E) The levels of E2F1 are significantly increased in *esg^{ts}>Phb1-v5*, *Phb2-flag* flies (white arrowheads). (F) The levels of E2F1 are significantly increased in *esg^{ts}>flag-yun*, *Phb2-flag*, *Phb1-v5* flies (white arrowheads). (G) Quantification of E2F1 IOD in progenitors in intestines with indicated genotypes. Mean \pm SD is shown. $n \geq 12$. * $P < 0.05$; *** $P < 0.001$. GFP is in green, E2F1 is in red, blue indicates DAPI staining for DNA. Scale bars: 10 μ m.

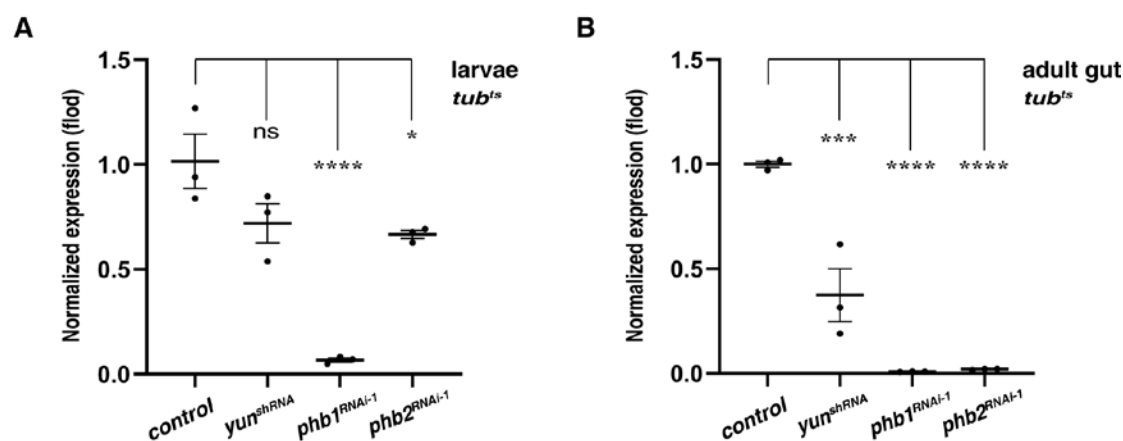


Fig. S40. The Yun/PHB complex affects the levels of E2F1 transcripts.

(A) E2F1 mRNA levels in larvae of control, *tub^{ts}>yun^{shRNA}*, *tub^{ts}>Phb1^{RNAi-1}* and *tub^{ts}>Phb2^{RNAi-1}*. (B) E2F1 mRNA levels in adult guts of control, *tub^{ts}>yun^{shRNA}*, *tub^{ts}>Phb1^{RNAi-1}* and *tub^{ts}>Phb2^{RNAi-1}*. Ribosomal gene *RpL11* was used as a

normalization control. Means \pm SD are shown. ^{ns} $P > 0.05$, $*P < 0.05$, $***P < 0.001$, $****P < 0.0001$.

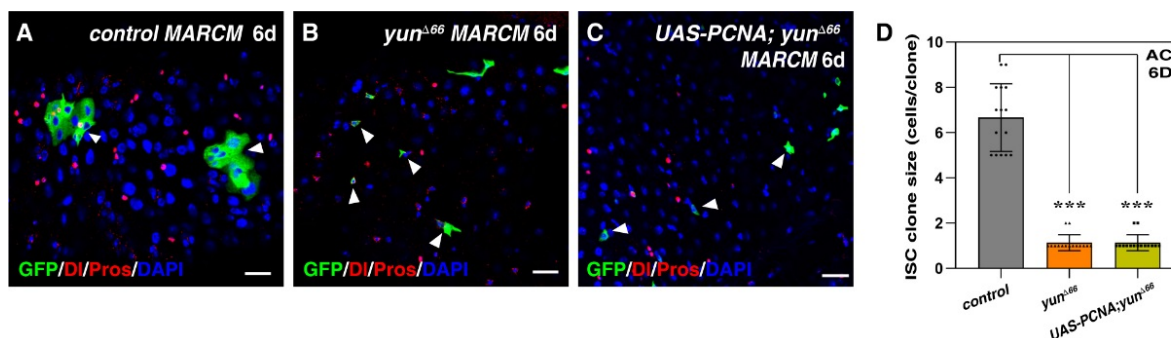


Fig. S41. PCNA overexpression could not rescue progenitor proliferation defects observed in *yun* mutant.

(A) *FRT* control ISC MARCM clones (green, white arrowheads). D1 and Pros in red.

(B) *yun*^{Δ66} mutant ISC MARCM clones (green, white arrowheads). D1 and Pros in red.

(C) Overexpression of *PCNA* could not rescue progenitor proliferation defects observed in *yun*^{Δ66} mutant (green, white arrowheads). D1 and Pros in red. (D) Quantification for

the ISC clone sizes of intestines with indicated genotypes. Mean \pm SD is shown. $n=15-25$. ^{ns} $P > 0.05$; $***P < 0.001$. In all panels except graphs, GFP is in green, blue indicates

DAPI staining for DNA. Scale bars: 20 μ m.

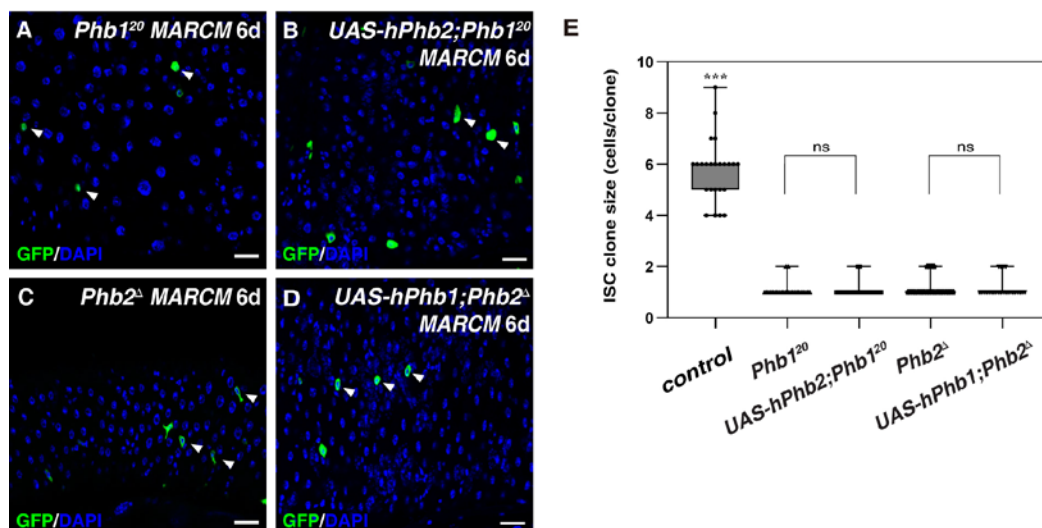


Fig. S42. *hPhb1/2* could not rescue the proliferation defects observed in *dmPhb2/1* mutant clones.

(A) ISC MARCM clones of *Phb1²⁰* (green) (white arrowheads). (B) Expression of human *Phb2* (*hPhb2*) could not rescue ISC proliferation defects observed in *Phb1²⁰* mutant cells (white arrowheads). (C) ISC MARCM clones of *Phb2^Δ* (green) (white arrowheads). (D) Expression of human *Phb1* (*hPhb1*) could significantly rescue ISC proliferation defects observed in *Phb2^Δ* mutant cells (white arrowhead). (E) Quantification for the ISC clone sizes of intestines with indicated genotypes. Mean \pm SD is shown. $n=24$. ^{ns} $P>0.05$; ^{***} $P<0.001$. In all panels except graphs, GFP is in green, blue indicates DAPI staining for DNA. Scale bars: 20 μ m.

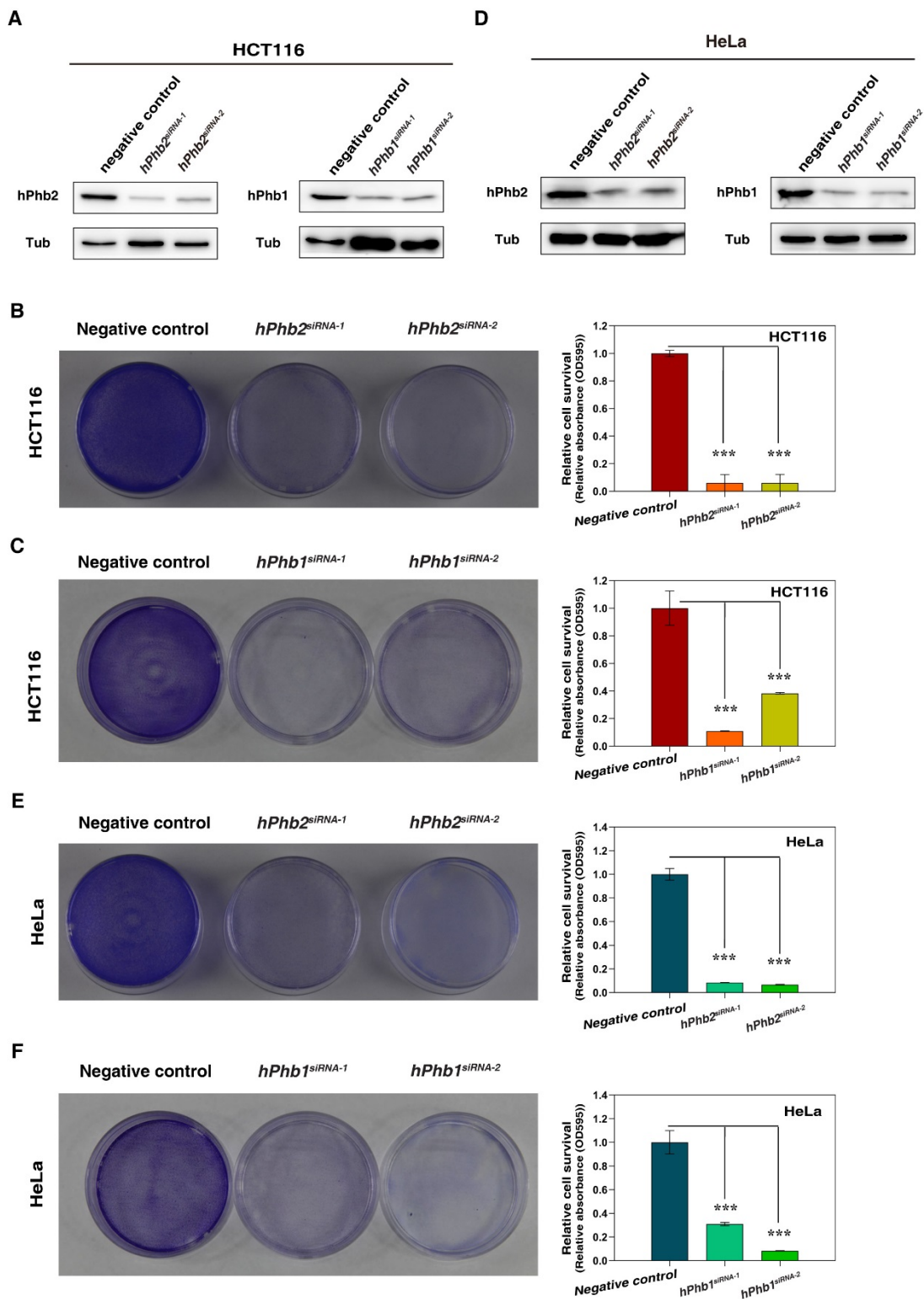


Fig. S43. Human PHB complex is required for the proliferation of different cancer cell lines.

(A) Western blot results showing the knockdown efficacy of siRNAs against human

Phb2 and *Phb1* in HCT116 cell lines respectively. Tubulin antibody is used as a loading control. (B) Depletion of *hPhb2* could significantly inhibit the proliferation/survival of human colorectal cancer cell line HCT116 determined by crystal violet staining. Mean \pm SD is shown. n=3. *** P <0.001. (C) Depletion of *hPhb1* could significantly inhibit the proliferation/survival of human colorectal cancer cell line HCT116. Mean \pm SD is shown. n=3. *** P <0.001. (D) Western blot results indicating the knockdown efficacy of siRNAs against human *Phb2* and *Phb1* in HeLa cell lines, respectively. A Tubulin antibody is used as a loading control. (E) Depletion of *hPhb2* significantly inhibited the proliferation/survival of the human cervical cancer cell line HeLa. Mean \pm SD is shown. n=3. *** P <0.001. (F) Depletion of *hPhb1* significantly inhibited the proliferation/survival of the human cervical cancer cell line HeLa. Mean \pm SD is shown. n=3. *** P <0.001.

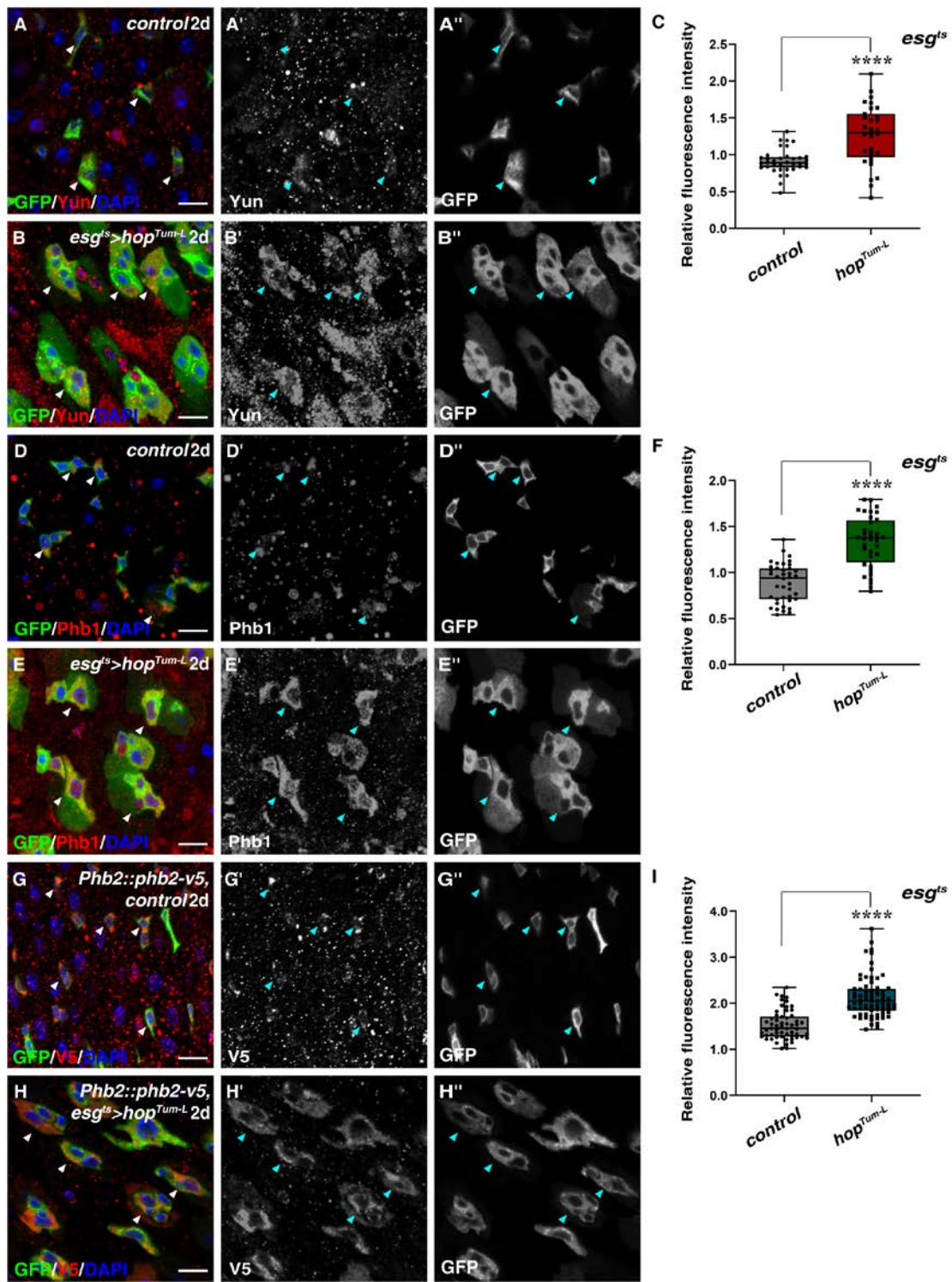


Fig. S44. The protein levels of the Yun/PHB complex are increased upon activation of JAK/STAT signaling.

(A) Yun protein (red) in progenitors (green, by *esg>GFP*) of 2-day old control flies (white arrowheads). Yun and GFP channels are shown separately in black-white. (B)

The levels of Yun protein (red) are significantly increased in progenitors of *esg^{ts}>hop^{Tum-L}* intestines at 29°C for 2 days (white arrowheads). (C) Quantification of the Yun IOD in control and *hop^{Tum-L}* progenitors. The protein levels of Yun in EE cells are used as internal control. Mean \pm SD is shown. $n \geq 30$. **** $P < 0.0001$. (D) Phb1 protein (red) in progenitors (green, by *esg>GFP*) of 2-day old control flies (white arrowheads). Phb1 and GFP channels are shown separately in black-white. (E) The levels of Phb1 protein (red) are significantly increased in progenitors of *esg^{ts}>hop^{Tum-L}* intestines at 29°C for 2 days (white arrowheads). (F) Quantification of the Phb1 IOD in control and *hop^{Tum-L}* progenitors. The protein levels of Phb1 in EE cells are used as internal control. Mean \pm SD is shown. $n \geq 40$. **** $P < 0.0001$. (G) Phb2 (red, by *Phb2::phb2-v5*) protein in progenitors (green, by *esg>GFP*) of 2-day old control flies (white arrowheads). Phb2-V5 and GFP channels are shown separately in black-white. (H) The levels of Phb2 protein (red, by *Phb2::phb2-v5*) are significantly increased in progenitors of *esg^{ts}>hop^{Tum-L}* intestines at 29°C for 2 days (white arrowheads). (I) Quantification of the Phb2-V5 IOD in control and *hop^{Tum-L}* progenitors. The protein levels of Phb2-V5 in EE cells are used as internal control. Mean \pm SD is shown. $n \geq 50$. **** $P < 0.0001$. In all panels except graphs, GFP is in green, blue indicates DAPI staining for DNA. Scale bars: 10 μ m.

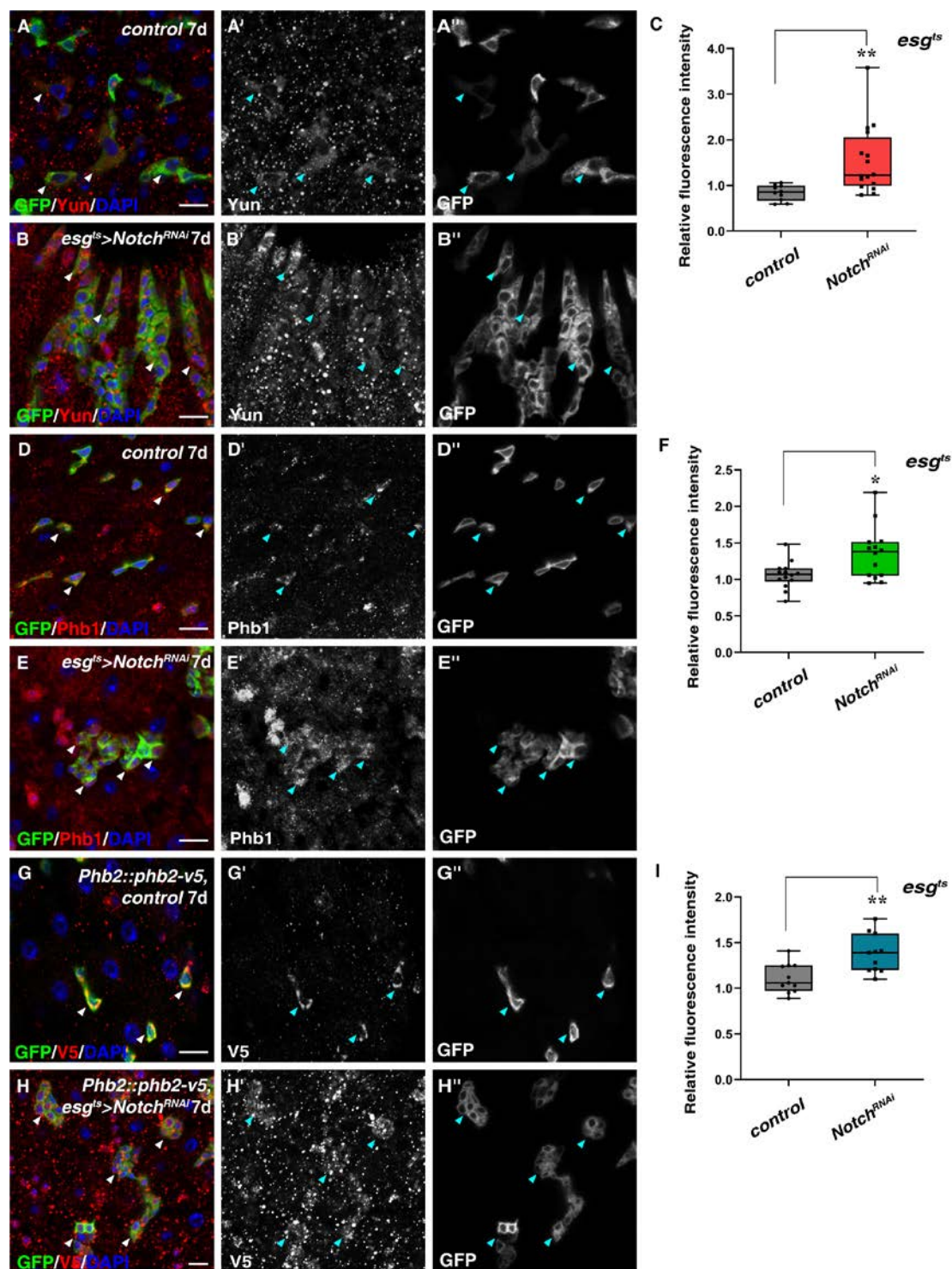


Fig. S45. The protein levels of the Yun/PHB complex are increased in *Notch*-defective progenitors.

(A) Yun protein (red) in progenitors (green, by *esg*>*GFP*) of 7-day old control flies (white arrowheads). Yun and GFP channels are shown separately in black-white. (B)

The levels of Yun protein (red) are significantly increased in progenitors of *esg^{ts}>Notch^{RNAi}* intestines at 29°C for 7 days (white arrowheads). (C) Quantification of the Yun IOD in control and *Notch^{RNAi}* progenitors. The protein levels of Yun in EE cells are used as internal control. Mean \pm SD is shown. $n \geq 10$. $**P < 0.01$. (D) Phb1 protein (red) in progenitors (green, by *esg>GFP*) of 7-day old control flies (white arrowheads). Phb1 and GFP channels are shown separately in black-white. (E) The levels of Phb1 protein (red) are significantly increased in progenitors of *esg^{ts}>Notch^{RNAi}* intestines at 29°C for 7 days (white arrowheads). (F) Quantification of the Phb1 IOD in control and *Notch^{RNAi}* progenitors. The protein levels of Phb1 in EE cells are used as internal control. Mean \pm SD is shown. $n \geq 10$. $*P < 0.05$. (G) Phb2 (red, by *Phb2::phb2-v5*) protein in progenitors (green, by *esg>GFP*) of 7-day old control flies (white arrowheads). Phb2-V5 and GFP channels are shown separately in black-white. (H) The levels of Phb2 protein (red, by *Phb2::phb2-v5*) are significantly increased in progenitors of *esg^{ts}>Notch^{RNAi}* intestines at 29°C for 7 days (white arrowheads). (I) Quantification of the Phb2-V5 IOD in control and *Notch^{RNAi}* progenitors. The protein levels of Phb2-V5 in EE cells are used as internal control. Mean \pm SD is shown. $n \geq 10$. $**P < 0.01$. In all panels except graphs, GFP is in green, blue indicates DAPI staining for DNA. Scale bars: 10 μ m.

3. Supplementary methods

Fly Lines and Husbandry. Flies were maintained on standard media at 25°C. 2-3 day old flies were selected and transferred to 29°C, unless otherwise specified. Flies were transferred to new vials with fresh food every day and dissected at specific time points as indicated. In all experiments, only female posterior midguts were analyzed. Information about alleles and transgenes used in this study can be found either in

FlyBase or as noted: *esgGal4*, *UAS-CD8-GFP*, *tubGal80^{ts}* (*esg^{ts}*), *esgGal4*, *UAS-RFP*, *tubGal80^{ts}*, *esgGal4*, *tubGal80^{ts}*, *UAS-Flp*, *Act>y>Gal4* (*esg^{ts}*, *F/O*), *tubGal80^{ts}*, *tubGal4*, *yun^{dsRNA}* (7705R-3, NIG), *UAS-Egfr^{CA}* (BL9533), *UAS-Raf^{sof}* (BL2033) (1), *UAS-Upd*, *UAS-hop^{Tum-L}*, *10XSTAT-GFP* (gifts from G.H. Baeg) (2), *MyoIAGal4*, *tubGal80^{ts}* (*MyoIA^{ts}*, gift from S. Hou), *esg-lacZ^{B7-2-22}* (BL10927), *P{EP}CG7705^{G18394}* (BL31820), *Df(3R)Exel6180* (BL7659), *P{Δ2-3}* (Kyoto, 106508 and 107128), *esgGal4*, *UAS-CC3Ai* (BL84953)(3), *Phb2^{RNAi-1}* (*l(2)3709*, *VDRC32362*), *P{EP}Phb2^{HP35544}* (BL24459), *Phb2^{RNAi-2}* (HMS02001/BL40835), *Phb1^{RNAi-1}* (HMS702/THU1103), *Phb1^{RNAi-2}* (HMS0399), *Phb2^{HP35544}* (BL24459), *Phb1²⁰* (BL5389), *Phb1²³* (BL5390), *Df(2R)Exel7158* (BL7895), *hsFlp*, *ActGal4*, *UAS-GFP*, *FRT40A-tubGal80* (for MARCM clonal analysis), *hsFlp*, *ActGal4*, *UAS-GFP*, *FRT42D-tubGal80* (for MARCM clonal analysis), *hsFlp*, *ActGal4*, *UAS-GFP*, *FRT19A-tubGal80* (for MARCM clonal analysis), *UAS-GFP-E2F1¹⁻²³⁰*; *UAS-mRFP-CycB¹⁻²⁶⁶* (Fly-FUCCI cell cycle reporter, BL55117 and BL55118, gift from Ruoxi Wang) (4), *UAS-E2F1*, *UAS-Dp* (BL4770 and BL4774, gifts from Xue Lei, Ruoxi Wang, and Xiaolin Bi)(5), *PCNA-GFP* (gift from Xiaolin Bi), *DlGal4*, *tubGal80^{ts}* (*Dl^{ts}*, gift from S. Hou and R.W. Xi), *Su(H)Gal4*, *UAS-GFP*, *tubGal80^{ts}* (*Su(H)^{ts}*)(6), *prosGal4*, *UAS-GFP*, *tubGal80^{ts}* (*pros^{ts}*, gift from Xiaohang. Yang), *FRT19A-N²⁶⁴⁻³⁹* (BL730), *UAS-Ras^{V12}* (BL4847), *Timer^{mito(young/old)}* (BL57323), *UAS-mito-GFP* (BL8442), *UAS-Atg8-GFP* (BL51656 and BL52005) (gift from T. Neufeld) (7), *UAS-GFP-LAMP1* (BL42714), *Atg1^{RNAi}* (HMS02750/THU5552; BL35177/THU0045), *Puc-lacZ* (*E69*), *UAS-Phb1-GFP* (gift from Ronald P. Kühnlein) (8), *Atg13^{RNAi}* (HMS02028, THU4087,

BL40861), *Atg5^{RNAi}* (HMS01244, THU1481, BL34899), *24BGal4*, *tubGal80^{ts}*, *UAS-GFP* (*24B^{ts}*, BL1767), *Ras^{RNAi}* (VDRC28129), *Raf^{RNAi}* (VDRC20909), *Dsor1^{RNAi}* (VDRC40026), *FRT19A-Raf^{fl}* (BL5733), *UAS-bmm-mcherry* and *UAS-scu* (BL8439, gifts from Xun Hunag), *UAS-p35*, *Notch^{RNAi}* (BL7078), *w* (*white*) RNAi (BL33623) was used as RNAi control.

RNAi screen, knockdown and overexpression experiments. To address gene function in progenitors (ISCs+EBs), *esgGal4*, *UAS-GFP*, *tubGal80^{ts}* (*esg^{ts}*) was used. Crosses (unless stated otherwise) were maintained at 18°C to bypass potential requirements during early developmental stages. 2-3 day old progeny with the desired genotypes were collected after eclosion and maintained at 29°C to inactivate Gal80^{ts} before dissection and immunostaining. Flies were transferred to new vials with fresh food every day. More than 11,000 RNAi lines from Vienna *Drosophila* RNAi Center (VDRC), Fly stocks of National Institute of Genetics (NIG-FLY), the Transgenic RNAi Project (TRiP), and Bloomington *Drosophila* Stock Center (BDSC) were screened. Many factors affecting ISC maintenance, viability, proliferation, and differentiation were identified from this screen. Both *UAS-dsRNA* and *UAS-shRNA* transgene stocks were used in this study.

Constructs. *pUAST-flag-yun* was constructed by cloning the *yun* ORF (from cDNA clone LP22035, BDGP/DGRC) into *pUAST-nflag*. *attB-pUAST-Phb2-flag* was

constructed by cloning the *Phb2* PA isoform ORF (from cDNA clone LD46344, BDGP/DGRC) into the EcoRI site of *attB-pUAST-nflag*. *attB-pUAST-hPhb2-V5* was constructed by cloning the human *Phb2* cDNA (from a human cDNA library) into a *attB-pUAST-cV5* vector. *attB-pUAST-Phb1-V5* was constructed by cloning the *Phb1* (*l(2)37Cc*) cDNA into *attB-pUAST-cV5* vector. *attB-pUAST-E2F1-myc* was constructed by cloning the *E2F1* cDNA into an *attB-pUAST-myc* vector. Transgenic flies of *UAS-E2F1-myc* were obtained by standard P-element-mediated germline transformation carrying *attP* site at 86F or 36B. Full-length *yun* ORF was cloned into the BamHI and EcoRI sites of a *pGEX-4T-1* vector to generate *GST-yun* construct. *yun* cDNA fragments of 1-600 bp, 601-1200 bp, and 1201-1776 bp were cloned into the BamHI and EcoRI sites of a *pGEX-4T-1* vector respectively to generate *GST-yun (1-200)*, *GST-yun (201-400)*, and *GST-yun (401-592)* constructs. Full-length *Phb2* ORF was cloned into the BamHI and EcoRI sites of a *pGEX-4T-1* vector to generate *GST-Phb2* construct. *Phb2* PA isoform was cloned into the EcoRI and XbaI sites of a *pMal-c4x* vector to generate *MBP-Phb2* construct. *Phb1* (*l(2)37Cc*) PA isoform was cloned into the EcoRI and XbaI sites of a *pMal-c4x* vector to generate *MBP-Phb1* construct.

Generation of *yun*^{shRNA} transgenic flies. *attB-UAS-yun^{shRNA}* was constructed by cloning the annealed oligos (*yun*-F: 5'-ctagcagt CGCCTATGTGCAGTCACAATata gttatattcaagcataTATTGTGACTGCACATAGGCGgcg-3' and *yun*-R: 5'-aattegcCG CCTATGTGCAGTCACAATAtatgcttgaatataactaTATTGTGACTGCACATAGGCGact g-3') into the EcoRI and NheI sites of an *attB-pWalium20* vector (TRiP). Transgenic

flies were obtained by standard P-element-mediated germline transformation carrying *attP* site at 86F. Depleting *yun* function ubiquitously or in muscle affected the motility of adult flies.

Generation of *yun* and *Phb2* null mutants. *yun* and *Phb2* null mutants were generated by standard P-element-mediated imprecise excision in the presence of $\Delta 2$ -3 transposase of *P{EP}CG7705^{G18394}* (BL31820) and *P{EP}Phb2^{HP35544}* (BL24459). *yun* deletion mutants were identified by PCR using primer pair (*yun*-dF: 5'-AAGACTTCC TGTGCGTGCTATCCT-3' and *yun*-dR: 5'-AGCTGTTCGGCGCAGTGAGG-3'). *Phb2* deletion mutants were identified by PCR using the primer pair *Phb2*-dF: 5'-GTTGTTAGCAAGCACACAAACCG-3' and *Phb2*-dR: 5'-GCGCCGCTTGGGAG TGGTTA-3'. PCR products were sequenced using the corresponding primers to determine the regions deleted. *yun*^{*A66*} and *yun*^{*A9*} mutants carry a 1.8 kb and 2.2 kb deletion from the 5' UTR to the middle of the coding region, respectively (Fig. 1A). *yun*^{*A66*} and *yun*^{*A9*} are functionally null mutants (Fig.S3D). *Phb2*^{*A*}, carrying a 1.3 kb deletion from the 5' UTR to the 3rd coding exon, is likely a functionally null mutant (Fig. 4A).

DSS feeding. Female adult flies at age 3 or 4 days were used to perform DSS feeding experiments. Flies were cultured in an empty vial containing chromatography paper wet with 3% dextran sulfate sodium (MP Biomedicals) in 5% glucose solution with heat inactivated yeast.

MARCM clone analysis. Clonal analyses were achieved using the MARCM system. ISC clones were induced by heat shocking 2-3 day old adult flies at 37°C for 60 minutes. Flies were maintained in a 25°C incubator and transferred to new vials with fresh food daily. Sizes of the marked clones were assayed at 6 days after clone induction (6D ACI, clones from at least 10 midguts for each genotype were assayed).

GST immunoprecipitation. For GST immunoprecipitation experiments, GST-Yun and MBP-Phb2, or GST-Phb2 and MBP-Phb1 proteins were expressed in *E. coli BL21 (DE3)* or *BL21 (DE3) LysS* cells (Transgen Biotech. China). The production of GST-Yun and MBP-Phb2 fusion proteins were induced with 0.1 mM IPTG at 18°C for 16 hr. Fusion proteins were purified according the manufacturer's protocol. The GST immunoprecipitation was performed using standard protocol. Negative control IPs were performed for each immunoprecipitation experiment.

Generation of MARCM drivers for *yun* mutants. To construct a new MARCM driver for *yun* mutants, *aTub84B* promoter (about 2.6 kb) was first cloned into the EcoRI and NotI sites of an *attB-pUAST-nflag* vector using the primer pair (*tub*-F: 5'-cg**GAATTC**GATATCAAGCTTGACAGG-3' and *tub*-R: 5'-ataagaat**GCGGCCGC**GGATCTGATCCCCGGG-3') to generate *attB-tubp*. Then *Gal80* ORF was cloned into the NotI and XbaI sites of *attB-tubp* using the primer pair (*Gal80*-F: 5'-ataagaat**GCGGCCGC**CAACATGGACTACAACAAGAGATC-3' and *Gal80*-R: 5'-gc**TCTAGA**

TTATAAACTATAATGCGAG-3') to generate *attB-tubGal80* construct. Transgenic flies were obtained by standard P-element-mediated germline transformation carrying *attP* site at 86F. *hsFlp*, *ActGal4*, *UAS-GFP/FM7*; *FRT82B-tubGal80^{86F}/TM6*, *Tb* driver was generated for MARCM analysis.

Generation of *yun::yun-flag* transgenic line. To monitor the endogenous expression pattern of *yun*, we cloned a genomic fragment spanning from its endogenous promoter to the last coding exon to be fused with a 3XFlag tag at its C-terminus (Fig. 1A). *yun::yun-flag* vector was constructed by cloning a fragment containing the promoter region (about 2.5 kb upstream of *yun*) and the genomic region of *yun* until the last coding exon (with the stop codon omitted) into the gateway vector *pUASP-W-flag*. Transgenic flies were obtained by standard P-element-mediated germline transformation.

Immunostainings and fluorescence microscopy. For standard immunostainings, intestines were dissected in 1 x PBS (10 mM NaH₂PO₄/Na₂HPO₄, 175 mM NaCl, pH7.4), and fixed in 4% paraformaldehyde for 25 min at room temperature. Samples were washed with 1 x PBT (0.1% Triton X-100 in 1 x PBS) and blocked in 3% BSA in 1 x PBT for 45 min. Primary antibodies were added to the samples and incubated at 4°C overnight. The following primary antibodies were used: mouse mAb anti-Dl (C594.9B, 1:50, developed by S. Artavanis-Tsakonas, Developmental Studies Hybridoma Bank (DSHB)), mouse mAb anti-Prospero (MR1A, 1:100, developed by Chris Doe, DSHB),

rabbit anti-pH3 (pSer10, Millipore, 1:2000), mouse anti-Flag (1:200, Sigma-Aldrich), rabbit anti-V5 (1:200, Abgent), mouse anti-V5 (1:100, HuaxingBio. China), Rabbit anti-Yun (1:1000, this study), Rabbit anti-Phb1 (1:1000, this study), rabbit anti- β -galactosidase (Cappel, 1:5000), mouse anti- β -galactosidase (Cell Signaling, 1:1000), mouse mAb anti-E2F1 (hao4, 1:50, developed by N.J. Dyson, DSHB), rabbit anti-E1F1 (1:200, generous gift from Dr Xiaolin Bi)(9), anti-Caspase3 (1:1000, Cell Signaling), rabbit anti-PDM1 (1:400, generous gifts from Drs Xiaohang Yang and Xiaolin Bi) (10, 11). Primary antibodies were detected by fluorescent-conjugated secondary antibodies from Jackson ImmunoResearch Laboratories. Secondary antibodies were incubated for 2 hrs at room temperature. DAPI (Sigma-Aldrich; 0.1 μ g/ml) was added after secondary antibody staining. Samples were mounted in mounting medium (70% glycerol containing 2.5% DABCO). All images were captured using a Zeiss inverted confocal microscope and were processed in Adobe Photoshop and Illustrator.

Generation of *Phb2::Phb2-V5* transgenic line. To monitor the endogenous expression pattern of *Phb2*, we cloned a genomic fragment containing its endogenous promoter and the coding region to be fused with a V5 tag at its C-terminus (Fig. 4A). *Phb2::Phb2-V5* vector was constructed by cloning a 4.8 kb genomic fragment spanning from 3 kb upstream of *Phb2* transcription start site (TSS) to the last coding exon of the *Phb2* RA isoform (with stop codon omitted) into the XhoI and XbaI sites of a *pUAST-cV5* vector. Transgenic flies were obtained by standard P-element-mediated germline transformation carrying *attP* site at 86F or 36B.

Generation of *Phb1::Phb1-V5* transgenic line. To monitor the endogenous expression pattern of *l(2)37Cc* (*Phb1*), we cloned a genomic fragment containing its endogenous promoter and the coding region to be fused with a V5 tag at its C-terminus (used in Fig. 3H). The *Phb1::Phb1-V5* vector was constructed by cloning a 4.5 kb genomic fragment spanning from 3 kb upstream of *l(2)37Cc* transcription start site (TSS) to the last coding exon of *l(2)37Cc* RA isoform (with stop codon omitted) into the EcoRI and XbaI sites of a *pUAST-cV5* vector. Transgenic flies were obtained by standard P-element-mediated germline transformation.

Generation of anti-Yun antibodies. The rabbit anti-Yun antisera were raised against a GST fusion protein containing the N-terminus region of Yun (1-200aa) with a GST tag at its N terminus. Corresponding cDNA fragment of Yun was amplified and cloned into the BamHI and EcoRI sites of a *pGEX-4T-1* vector, using primers: F: 5'-cgGGATCCATGCAGGAGCTCAAGCAAC G-3' and R: 5'-cgGAATTCCCTACGCATAGTAGGCGCTGTACT-3'. Fusion proteins were purified according to the manufacturer's protocol and immunizations were performed by Animal Facility, Institute of Genetics and Developmental Biology, Chinese Academy of Sciences. Two peptides (EEAFRRRSKQHKERDNF and QKLTVTEAAKKNNSKEL) were also conjugated to KLH and co-injected into two rabbits and affinity purified by BAM Biotech (BAMBIO, China).

Generation of anti-dPhb1 antibodies. The rabbit anti-dPhb1 antisera were raised against a GST fusion protein containing the region of Phb1 (188-275aa) with a GST tag

at its N terminus. Corresponding cDNA fragment of Phb1 was amplified and cloned into the BamHI and EcoRI sites of a *pGEX-4T-1* vector, using primers: F: 5'-CGGGATCCGTGGCCCAGCAGGAGGCGGAG-3' and R: 5'-GGAATTCTACTGCGCGATGGTTCGATGG-3'. Fusion proteins were purified according to the manufacturer's protocol and immunizations were performed by Animal Facility, Institute of Genetics and Developmental Biology, Chinese Academy of Sciences. The peptide injected into two rabbits and affinity purified by BAM Biotech (BAMBIO, China).

Co-Immunoprecipitation and western blotting. Fly tissues were lysed in RIPA buffer [50 mM Tris-HCl, pH 8.0, 150 mM NaCl, 5 mM EDTA, pH 8.0, 0.5% Triton X-100, 0.5% NP-40, 0.5% sodium deoxycholate, and complete protease inhibitor cocktail tablets (Roche)] on ice for 30 minutes. After centrifugation, lysates were then diluted ten-fold with RIPA buffer and subjected to immunoprecipitation using anti-FLAG M2 affinity gel (A2220; Sigma-Aldrich, USA), or rabbit anti-V5 (1:200, Abgent, USA) and rabbit anti-GFP (1:100, Abcam, USA) followed by protein A/G beads. Immunocomplexes were collected by centrifugation and washed with 1 ml of RIPA buffer three times. Negative control IPs were performed for each immunoprecipitation experiment. For western blotting, immunoprecipitated proteins were separated in SDS-PAGE and then blotted onto PVDF membranes. Membranes were stained with primary antibody overnight at 4°C. Followed by washing, PVDF membranes were incubated with secondary antibodies conjugated with HRP, then the membranes were scanned

using Luminescent Image Analyzer (GE, Sweden). Rabbit anti-V5 (1:1000, Abgent, USA), mouse anti-Flag (1:1000, Sigma-Aldrich, USA), rabbit anti-hPhb2 (1:1000, Abcam), mouse anti-hPhb1 (1:100, Abcam), rabbit anti-Phb1 (1:1000, this study), mouse anti-Myc (9E10, 1:1000, Sigma-Aldrich, USA), rabbit anti-GST (1:1000, Abcam), rabbit and mouse anti-MBP (1:1000, HuaxingBio, China), rabbit anti-GFP (1:1000, Abcam, USA), and mouse monoclonal anti- α Tubulin anti- β Tubulin (1:1000, 3G6, Abbkine, USA) antibodies were used.

MS sample preparation. Immunoprecipitated proteins from whole body of *tub^{ts}>yun-Flag* flies were precipitated with 25% trichloroacetic acid (TCA) for at least 30 min on ice. Protein pellets were washed twice with 500 μ l ice-cold acetone, air dried, and then resuspended in 8 M urea, 100 mM Tris, pH 8.5. After reduction (5 mM TCEP, RT, 20 min) and alkylation (10 mM iodoacetamide, RT, 15 min in the dark), the samples were diluted to 2 M urea with 100 mM Tris, pH 8.5 and digested with trypsin at 1/50 (w/w) enzyme/substrate ratio at 37°C for 16-18 hr. Digestion was then stopped by addition of formic acid to 5% (final concentration).

LC-MS/MS analysis. All samples were analyzed using an EASY-nLC 1000 system (Thermo Fisher Scientific, Waltham, MA) interfaced with a Q-Exactive mass spectrometer (Thermo Fisher Scientific). Peptides were loaded on a trap column (75 μ m ID, 4 cm long, packed with ODS-AQ 12 nm-10 μ m beads) and separated on an analytical column (75 μ m ID, 12 cm long, packed with Luna C18 1.9 μ m 100 Å resin)

with a 60 min linear gradient at a flow rate of 200 nl/min as follows: 0-5% B in 2 min, 5-30% B in 43 min, 30-80% B in 5 min, 80% B for 10 min (A = 0.1% FA, B = 100% ACN, 0.1% FA). Spectra were acquired in data-dependent mode: the top ten most intense precursor ions from each full scan (resolution 70,000) were isolated for HCD MS2 (resolution 17,500; NCE 27) with a dynamic exclusion time of 30s. The AGC targets for the MS1 and MS2 scans were 3e6 and 1e5, respectively, and the maximum injection times for MS1 and MS2 were both 60ms. Precursors with 1+, more than 7+ or unassigned charge states were excluded.

Database search. MS data were searched against a Uniprot *Drosophila melanogaster* protein database (database ID number of UP000000803) using ProLuCID with the following parameters: precursor mass tolerance, 3 Da; fragment mass tolerance 20 ppm; peptide length, minimum 6 amino acids and maximum 100 amino acids; enzyme, Trypsin, with up to three missed cleavage sites (12). Results were filtered by DTASelect requiring FDR<1% at the peptide level and spectra count ≥ 2 (13). Proteins identified from the negative control and Flag-Yun IP were contrasted by Contrast (13).

Construction of *yunGal4* transgenic line.

To examine the expression pattern of *yun*, we generated a *yunGal4* line. The primer pair (*yun-p5*: 5'-CACCCGAATTCGC GCTTCTTCCGGTTCCGATG-3' and *yun-p3*: 5'-GGATCCTAAAAATACCGCCAGCATGAGG-3') was used to amplify the *yun* promoter (about 2.5 kb) from genomic DNA (Figure 1E). It was then sub-cloned into

pChs-GAL4 vector (14). Transgenic flies were obtained by standard P-element-mediated germline transformation. The transgenic line was further recombined with *UAS-GFP* to generate *yunGal4, UAS-GFP* driver to monitor endogenous *yun* expression. The *yunGal4* driver is also expressed in progenitors, and interestingly, is not expressed in EE cells, indicating that this transgenic line may not carry all the necessary regulatory elements (Fig. S4 D and E).

Generation of *Hsp60p-GFP* transgenic line.

To evaluate mitochondria stress, we cloned a genomic fragment containing *Hsp60* RA isoform endogenous promoter, followed by a GFP tag. The *Hsp60p-GFP* vector was constructed by cloning a 4.6 kb genomic fragment spanning from 3 kb upstream of *Hsp60* transcription start site (TSS) to the first 21 bp of the first coding exon of *Hsp60* RA isoform into the EcoRI site of a *pUAST-cGFP* vector. Transgenic flies were obtained by standard P-element-mediated germline transformation carrying *attP* site at 86F or 36B.

Generation of *Hsc5p-GFP* transgenic line.

To evaluate mitochondria stress, we cloned a genomic fragment containing *Hsc5* RA isoform endogenous promoter, following a GFP tag. The *Hsc5-GFP* vector was constructed by cloning a 3.3 kb genomic fragment spanning from 3 kb upstream of *Hsp60* transcription start site (TSS) to the first coding exon of *Hsc5* RA isoform into the EcoRI site of the *pUAST-cGFP* vector. Transgenic flies were obtained by standard

P-element-mediated germline transformation carrying *attP* site at 86F or 36B.

Oligomycin feeding.

Oligomycin (Sigma-Aldrich) was dissolved in 100% DMSO at a concentration of 1 mg/ml and stored at -20 °C. Oligomycin was added at a final concentration of 10 µg/ml to the surface of the food. Flies were transferred to fresh vials with drugs supplemented every day. Flies were fed on the food with drug for 3 days before being analyzed.

DHE staining.

DHE was used to detect reactive oxygen species (ROS) as previously described (15). Briefly, intestines were dissected in 1 x PBS and incubated in 30 µM DHE (KeyGEN BioTECH, China) in PBS for 10 min at room temperature in the dark. Samples were washed with 1 x PBS for 5 min twice, then mounted and imaged by confocal microscope.

Propidium iodide staining.

Propidium iodide (PI) was used to evaluate necrosis as previously described (15). Briefly, intestines were dissected in 1 x PBS and incubated in 1.5 µM PI (KeyGEN BioTECH, China) in PBS for 15 min at room temperature, then fixed in 4% paraformaldehyde for 20 min, washed two times in 1 x PBT, stained 0.1 µg/ml DAPI in 1 x PBT for 15 min, rinsed twice with 1 x PBS, mounted and imaged by confocal microscope at last.

Oil red staining.

Oil Red was used to stain lipid droplets. Intestines were dissected in 1 x PBS and fixed in 4% paraformaldehyde for 20 min, rinse 3 times with 1 x PBS, stained Oil Red (Sigma-Aldrich; 0.1% solution in isopropanol) diluted solution (diluted to a 60% solution by distilled water adding 0.1 μ g/ml DAPI), incubated for 20 min, washed 3 times with 60% isopropanol and 2 times with 1 x PBS, mounted, imaged by confocal microscope and processed with Adobe Photoshop.

BODIPY staining.

BODIPY was used to stain lipid droplet. Intestines were dissected in 1 x PBS and fixed in 4% paraformaldehyde for 20 min, rinse twice with 1 x PBS, stained BODIPY (Invitrogen; BODIPYTM 500/510 C1, C12) diluted solution (1:500, diluted by 1 x PBS adding 0.1 μ g/ml DAPI), incubated for 30 min, rinse twice with 1 x PBS, mounted, imaged by confocal microscope.

RT-qPCR.

RNA was extracted from 20 female adults using RNA pre pure kit (TIANGEN) and complementary DNA (cDNA) was synthesized with the M-MLV Reverse transcriptase (Promega). qPCR was performed using GoTaq qPCR Master Mix kit (Promega) on CFX96 Real-time PCR system (Bio-Rad). Experiments were performed in 3 biological independent replicates, each also contained 3 repeats. All the results are shown as mean

\pm SD of the biological replicates. Ribosomal gene *RpL11* was used as normalization control.

Silver staining.

SDS-PAGE gels were stained by Fast Silver Stain Kit (Beyotime, China) according to the manufacturer's instructions.

ATP detection.

Flies of *tub^{ts}* control, *tub^{ts}>yun^{dsRNA}*, *tub^{ts}>phb1^{RNAi-1}* and *tub^{ts}>phb2^{RNAi-1}* were detected three times by Enhanced ATP Assay Kit (Beyotime, China) according to the manufacturer's instructions.

Generation of UAS-Flag-GFP-PCNA transgenic line.

The *UAS-Flag-GFP-PCNA* vector was constructed by cloning the coding region of PCNA into the KpnI and XbaI sites of an *attB UAS-nFlag-GFP* vector (lab made) using the primer pair: PCNA-5: CGGCATGGACGAGCTGTACAAGggtaccATGTTTCG AGGCACGCCTGGGtc and PCNA-3: GTAAGGTTTCCTTCACAAAGATCCtctaga TTATGTCTCGTTGTCCTCGATCTTGG. Transgenic flies were obtained by standard P-element-mediated germline transformation carrying *attP* site at 86F or 36B.

Cell culture.

The human colon cancer cell line HCT116 and cervical cancer cell line HeLa (provided

Dr. Hailong Wang) were cultured in RPMI-1640 (Lonza) supplemented with 10% fetal bovine serum (PAN-Biotech) and 100 units per ml penicillin/streptomycin (Hyclone) at 37 °C in a humidified atmosphere containing 5% CO₂.

shRNA and siRNA against *hPhb2* and *hPhb1*.

shRNA-expressing vectors were constructed by cloning different shRNAs into the BsmBI site of a *pL-shRNA-NoGFP* vector. Nucleotide sequences of shRNA targets used are as follows: *shLuci*: 5'-AACTTACGCTGAGTACTTCGA-3'; *hPhb2-1*: 5'-GTGATTCCTACAGTGTTGTTCCCT-3'; *hPhb2-2*: 5'-AGATTCGAGCAGCCCA GAATATCTC-3'. *hPhb1-1*: 5'-GCGGAGAGAGCCAGATTTG-3'; *hPhb1-2*: 5'-GAC ACATCTGACCTTCGGG-3'. Knockdown cell lines were constructed by transfecting HCT116 and HeLa cells with the respective lentiviral vector in the presence of Polyethylenimine (Sigma-Aldrich). siRNAs against *hPhb2* and *hPhb1* were also generated (synthesized by RiboBio, China). Negative control siRNAs (RiboBio, China) and siRNAs against *hPhb2* and *hPhb1* were transfected into HCT116 and HeLa cells using riboFECT CP kit (RiboBio, China) according to the manufacturer's instructions.

Cell survival assay.

Cells were seeded at 2×10^5 cells per well in 3 cm tissue culture dishes (Thermo Fisher). After transfection, cells were incubated for 2 more days. The surviving cells were stained with Crystal Violet (Beyotime, China). For quantification, the stained cells were solubilized in 1% SDS, and the absorbance at 595 nm was determined.

Sphere formation assay.

Single cells were cultured in a Corning Costar Ultra-Low Attachment Multiple Well Plate (Sigma-Aldrich) in sphere culture medium, consisting of DMEM/F12 (1:1), B27 (Invitrogen), and 20 ng/ml EGF (Invitrogen), with the indicated chemicals. The number of spheres was counted after 10 days of cell culture.

Data analysis.

pH3 numbers were scored manually under a Zeiss Imager Z2/LSM780 microscope. The number of intestines scored is indicated in the text. To determine the relative number of *esg*⁺ cells, confocal images of 40 X lens/1.0 zoom from a defined posterior midgut region (indicated in the main figures) between the hindgut and the copper cells of different genotypes indicated were acquired. The relative number of *esg*⁺ cells was determined from each confocal image using Image-Pro Plus software, manually selecting the “filter” depending on the respective cell size to filter out background signals. Clone sizes were scored manually under Zeiss Imager Z2/LSM780 microscope for indicated genotypes. Fluorescence intensity (IOD), normalized to signals of EE, was measured by ImageJ software for indicated genotypes. At least ten different guts were analyzed for each set. Statistical analysis was done using the Student’s *t*-test. Graphs were further modified using Adobe Photoshop and Illustrator. ^{ns}*P* > 0.05; **P* < 0.05; ***P* < 0.01; *** *P* < 0.001; *****P* < 0.0001.

qRT-PCR primers used:

yun-F: CTGCGGGAGTGCGAGTACTTC

yun-R: CAGATCCTCGCTCAGCTGAG

Phb2-F: TCCGCCGGGATTGGGAATCG

Phb2-R: CATAGATAATGGGATACTGG

RpL11-F: GGTCCGTTCGTTTCGGTATTCGC

RpL11-R: GGATCGTACTTGATGCCAGATCG

4. Full genotypes of flies in Figures

Fig. 1:

Panels A1, B5, and C1: control corresponds to +/+; *esgGal4*, *UAS-GFP*, *tubGal80^{ts}/+*; *w^{RNAi}/+*

Panel A2: *esg^{ts}>yun^{dsRN}* corresponds to +/+; *esgGal4*, *UAS-GFP*, *tubGal80^{ts}/+*; *yun^{dsRNA}/+*

Panels A3, B6, and C3: *esg^{ts}>yun^{shRNA}* corresponds to +/+; *esgGal4*, *UAS-GFP*, *tubGal80^{ts}/+*; *yun^{shRNA}/+*

Panel B1: control MARCM corresponds to *hsFlp*, *ActGal4*, *UAS-GFP/+*; +/+; *FRT82B-TubGal80/FRT82B*

Panel B2: *yun^{A9}* MARCM corresponds to *hsFlp*, *ActGal4*, *UAS-GFP/+*; +/+; *FRT82B-TubGal80/FRT82B-yun^{A9}*

Panel B3: *yun::yun-flag*; *yun^{A9}* corresponds to *hsFlp*, *ActGal4*, *UAS-GFP/+*; +/+; *FRT82B-TubGal80/yun::yun-flag*, *FRT82B-yun^{A9}*

Panel C2: *esg^{ts}>Egfr^{CA}* corresponds to +/+; *esgGal4*, *UAS-GFP*, *tubGal80^{ts}/+*; *Egfr^{CA}/+*

Panel C4: $esg^{ts}>Egfr^{CA}$, yun^{shRNA} corresponds to +/+; $esgGal4$, $UAS-GFP$, $tubGal80^{ts}/+$; $Egfr^{CA}$, $yun^{shRNA}/+$

Panel C6: $N^{264-39}MARCM$ corresponds to $FRT19A-TubGal80/FRT19A-N^{264-39}$; $hsFlp$, $ActGal4$, $UAS-GFP/+$;

Panel C7: N^{264-39} , $yun^{shRNA} MARCM$ corresponds to $FRT19A-TubGal80/FRT19A-N^{264-39}$; $hsFlp$, $ActGal4$, $UAS-GFP/+$; $yun^{shRNA}/+$

Fig. 2:

Panel H: $yun::yun-flag;Phb2::phb2-v5$ corresponds to +/+; +/+; $yun::yun-flag/Phb2::phb2-v5$

Panels I and J: $Phb2::phb2-v5$ corresponds to +/+; +/+; $Phb2::phb2-v5/+$

Fig. 3:

Panels A1 and C1: *control* corresponds to +/+; $esgGal4$, $UAS-GFP$, $tubGal80^{ts}/+$; $w^{RNAi}/+$ *control F/O* corresponds to +/+; $esgGal4$, $UAS-GFP$, $tubGal80^{ts}/+$; $UAS-Flp$, $Act>y>Gal4/w^{RNAi}$

Panels A2 and C2: $esg^{ts}>Phb2^{RNAi-1}$ corresponds to +/+; $esgGal4$, $UAS-GFP$, $tubGal80^{ts}/+$; $Phb2^{RNAi-1}/+$

Panels B1 and C4: *control MARCM* corresponds to $hsFlp$, $ActGal4$, $UAS-GFP/+$; $FRT42D-TubGal80/FRT42D$

Panels B2 and C5: $Phb2^A MARCM$ corresponds to $hsFlp$, $ActGal4$, $UAS-GFP/+$; $FRT42D-TubGal80/FRT42D-Phb2^A$

Panel D1: $esg^{ts}>Egfr^{CA}$ corresponds to +/+; $esgGal4$, $UAS-GFP$, $tubGal80^{ts}/+$; $Egfr^{CA}/+$

Panel D2: $esg^{ts}>Egfr^{CA}$, $Phb2^{RNAi}$ corresponds to +/+; $esgGal4$, $UAS-GFP$, $tubGal80^{ts}/+$; $Phb2^{RNAi}$, $Egfr^{CA}/+$

Panel D4: $N^{264-39}MARCM$ corresponds to $FRT19A-TubGal80/FRT19A-N^{264-39}$; $hsFlp$, $ActGal4$, $UAS-GFP/+$;

Panel D5: N^{264-39} , $Phb2^{RNAi} MARCM$ corresponds to $FRT19A-TubGal80/FRT19A-N^{264-39}$; $hsFlp$, $ActGal4$, $UAS-GFP/+$; $Phb2^{RNAi}/+$

Fig. 4:

Panels A1 and C1: *Phb2::phb2-v5/esg^{ts}* corresponds to +/+; *esgGal4, UAS-GFP, tubGal80^{ts}/+; Phb2::phb2-v5/+*

Panel A2: *Phb2::phb2-v5; esg^{ts}>yun^{shRNAi}* corresponds to +/+; *esgGal4, UAS-GFP, tubGal80^{ts}/ Phb2::phb2-v5; yun^{shRNAi}/+*

Panel B1: *esg^{ts}* corresponds to +/+; *esgGal4, UAS-GFP, tubGal80^{ts}/+;*

Panel B2: *esg^{ts}>Phb2^{RNAi}* corresponds to +/+; *esgGal4, UAS-GFP, tubGal80^{ts}/+; Phb2^{RNAi}/+*

Panel C2: *Phb2::phb2-v5/esg^{ts}>Phb1^{RNAi}* corresponds to +/+; *esgGal4, UAS-GFP, tubGal80^{ts}/ Phb2::phb2-v5; Phb1^{RNAi}/+*

Panel D1: *control MARCM* corresponds to *hsFlp, ActGal4, UAS-GFP/+; +/+; FRT82B-TubGal80/FRT82B*

Panel D2: *yun^{A9}MARCM* corresponds to *hsFlp, ActGal4, UAS-GFP/+; +/+; FRT82B-TubGal80/FRT82B-yun^{A9}*

Panel D3: *UAS-Phb1-v5; yun^{A9} MARCM* corresponds to *hsFlp, ActGal4, UAS-GFP/+; +/+; FRT82B-TubGal80/UAS-Phb1-v5, FRT82B-yun^{A9}*

Panel D4: *UAS-Phb2-flag; yun^{A9}* corresponds to *hsFlp, ActGal4, UAS-GFP/+; UAS-Phb2-flag/+; FRT82B-TubGal80/FRT82B-yun^{A9}*

Panel D5: *UAS-Phb2-flag; Phb1²⁰MARCM* corresponds to *hsFlp, ActGal4, UAS-GFP/+; FRT40A-TubGal80/ UAS-Phb2-flag, FRT40A-Phb1²⁰*

Panel D6: *Phb2^A MARCM* corresponds to *hsFlp, ActGal4, UAS-GFP/+; FRT42D-TubGal80/FRT42D-Phb2^A*

Panel D7: *UAS-flag-yun; Phb2^A MARCM* corresponds to *hsFlp, ActGal4, UAS-GFP/+; FRT42D-TubGal80/ UAS-flag-yun; FRT42D-Phb2^A*

Panel D8: *UAS-Phb1-v5; Phb2^A MARCM* corresponds to *hsFlp, ActGal4, UAS-GFP/+; FRT42D-TubGal80/ FRT42D-Phb2^A; UAS-Phb1-v5/+*

Fig. 5:

Panel A1: *control* corresponds to +/+; *esgGal4, UAS-GFP, tubGal80^{ts}/+; w^{RNAi}/+*

Panel A2: *esg^{ts}>Ras^{v12}* corresponds to +/+; *esgGal4, UAS-GFP, tubGal80^{ts}/+; UAS-Ras^{v12}/+*

Panel A5: *Phb2::phb2-v5/esg^{ts}* corresponds to +/+; *esgGal4, UAS-GFP, tubGal80^{ts}/Phb2::phb2-v5*

Panel A6: *Phb2::phb2-v5; esg^{ts}>Raf^{gof}* corresponds to +/+; *esgGal4, UAS-GFP, tubGal80^{ts}/Phb2::phb2-v5; UAS-Raf^{gof}/+*

Panel B1: *esg^{ts}>Ras^{RNAi}* corresponds to +/+; *esgGal4, UAS-GFP, tubGal80^{ts}/+; UAS-Ras^{RNAi}/+*

Panel B4: *Phb2::phb2-v5/esg^{ts}>Ras^{RNAi}* corresponds to +/+; *esgGal4, UAS-GFP, tubGal80^{ts}/Phb2::phb2-v5; UAS-Ras^{RNAi}/+*

Panels B6 and C1: *Raf^{f1}MARCM* corresponds to *FRT19A-TubGal80/FRT19A-Raf^{f1}; hsFlp, ActGal4, UAS-GFP/+*

Panel B7: *Phb2::phb2-v5/Raf^{f1}MARCM* corresponds to *FRT19A-TubGal80/FRT19A-Raf^{f1}; hsFlp, ActGal4, UAS-GFP/+; Phb2::phb2-v5/+*

Panel C1: *control MARCM* corresponds to *FRT19A-TubGal80/FRT19A; hsFlp, ActGal4, UAS-GFP/+*

Panel C3: *UAS-yun-flag; Raf^{f1}MARCM* corresponds to *FRT19A-TubGal80/FRT19A-Raf^{f1}; hsFlp, ActGal4, UAS-GFP/UAS-yun-flag*

Panel C4: *UAS-Phb1-v5; Raf^{f1}MARCM* corresponds to *FRT19A-TubGal80/FRT19A-Raf^{f1}; hsFlp, ActGal4, UAS-GFP/+; UAS-Phb1-v5/+*

Panel C5: *UAS-Phb2-flag; Raf^{f1}MARCM* corresponds to *FRT19A-TubGal80/FRT19A-Raf^{f1}; hsFlp, ActGal4, UAS-GFP/UAS-Phb2-flag*

Fig. 6:

Panel A1: *control* corresponds to +/+; *esgGal4, tubGal80^{ts}/UAS-NLS-GFP-E2F1¹⁻²³⁰, UAS-NLS-RFP-CycB¹⁻²⁶⁶; w^{RNAi}/+*

Panel A2: *esg^{ts}>yun^{shRNA}* corresponds to +/+; *esgGal4, tubGal80^{ts}/UAS-NLS-GFP-E2F1¹⁻²³⁰, UAS-NLS-RFP-CycB¹⁻²⁶⁶; yun^{shRNA}/+*

Panel A3: *esg^{ts}>Phb2^{RNAi}* corresponds to +/+; *esgGal4, tubGal80^{ts}/UAS-NLS-GFP-E2F1¹⁻²³⁰, UAS-NLS-RFP-CycB¹⁻²⁶⁶; Phb2^{RNAi}/+*

Panels B1 and C1: *control* corresponds to +/+; *esgGal4, UAS-GFP, tubGal80^{ts}/+; w^{RNAi}/+*

Panel B2: *esg^{ts}>yun^{shRNAi}* corresponds to +/+; *esgGal4, UAS-GFP, tubGal80^{ts}/+; yun^{shRNAi}/+*

Panel B3: *esg^{ts}>Phb2^{RNAi}* corresponds to +/+; *esgGal4, UAS-GFP, tubGal80^{ts}/+; Phb2^{RNAi}/+*

Panel C2: *esg^{ts}>E2F1* corresponds to +/+; *esgGal4, UAS-GFP, tubGal80^{ts}/UAS-E2F1, UAS-Dp*

Panel C3: *esg^{ts}>E2F1, yun^{shRNAi}* corresponds to +/+; *esgGal4, UAS-GFP, tubGal80^{ts}/UAS-E2F1, UAS-Dp; yun^{shRNAi}/+*

Panel C4: *esg^{ts}>E2F1, Phb2^{RNAi}* corresponds to +/+; *esgGal4, UAS-GFP, tubGal80^{ts}/UAS-E2F1, UAS-Dp; Phb2^{RNAi}/+*

Panel C6: *control MARCM* corresponds to *hsFlp, ActGal4, UAS-GFP/+; +/+; FRT82B-TubGal80/FRT82B*

Panel C7: *yun⁴⁹ MARCM* corresponds to *hsFlp, ActGal4, UAS-GFP/+; +/+; FRT82B-TubGal80/FRT82B-yun⁴⁹*

Panel C8: *UAS-E2F1, yun⁴⁹ MARCM* corresponds to *hsFlp, ActGal4, UAS-GFP/+; UAS-E2F1, UAS-Dp/+; FRT82B-TubGal80/FRT82B-yun⁴⁹*

Panel C9: *Phb2^A MARCM* corresponds to *hsFlp, ActGal4, UAS-GFP/+; FRT42D-TubGal80/FRT42D-Phb2^A*

Panel C10: *UAS-E2F1, Phb2^A MARCM* corresponds to *hsFlp, ActGal4, UAS-GFP/+; FRT42D-TubGal80/FRT42D-Phb2^A; UAS-E2F1, UAS-Dp/+*

Fig. 7:

Panel A: *Phb1²⁰ MARCM* corresponds to *hsFlp, ActGal4, UAS-GFP/+; FRT40A-TubGal80/FRT40A-Phb1²⁰*

Panel B: *Phb1²⁰, UAS-Phb1-v5 MARCM* corresponds to *hsFlp, ActGal4, UAS-GFP/+; FRT40A-TubGal80/FRT40A-Phb1²⁰; UAS-Phb1-v5/+*

Panel C: *Phb1²⁰, UAS-hPhb1-v5 MARCM* corresponds to *hsFlp, ActGal4, UAS-GFP/+; FRT40A-TubGal80/FRT40A-Phb1²⁰; UAS-hPhb1-v5/+*

Panel D: *Phb2^A MARCM* corresponds to *hsFlp, ActGal4, UAS-GFP/+; FRT42D-TubGal80/FRT42D-Phb2^A*

Panel E: *Phb2^A, UAS-Phb2-flag MARCM* corresponds to *hsFlp, ActGal4, UAS-GFP/+; FRT42D-TubGal80/ UAS-Phb2-flag, FRT42D-Phb2^A*

Panel F: *Phb2^A, UAS-hPhb2-v5 MARCM* corresponds to *hsFlp, ActGal4, UAS-GFP/+; FRT42D-TubGal80/FRT42D-Phb2^A; UAS-hPhb2-v5/+*

5. Supplementary References

1. Brand AH & Perrimon N (1994) Raf acts downstream of the EGF receptor to determine dorsoventral polarity during *Drosophila* oogenesis. *Genes Dev.* 8(5):629-639.
2. Bach EA, *et al.* (2007) GFP reporters detect the activation of the *Drosophila* JAK/STAT pathway *in vivo*. *Gene Expr Patterns* 7(3):323-331.
3. Schott S, *et al.* (2017) A fluorescent toolkit for spatiotemporal tracking of apoptotic cells in living *Drosophila* tissues. *Development* 144(20):3840-3846.
4. Zielke N, *et al.* (2014) Fly-FUCCI: A versatile tool for studying cell proliferation in complex tissues. *Cell Rep* 7(2):588-598.
5. Neufeld TP, de la Cruz AF, Johnston LA, & Edgar BA (1998) Coordination of growth and cell division in the *Drosophila* wing. *Cell* 93(7):1183-1193.
6. Lu Y & Li Z (2015) Notch signaling downstream target *E(spl)mbeta* is dispensable for adult midgut homeostasis in *Drosophila*. *Gene* 560(1):89-95.
7. Juhász G, *et al.* (2008) The class III PI(3)K Vps34 promotes autophagy and endocytosis but not TOR signaling in *Drosophila*. *J Cell Biol* 181(4):655-666.
8. Beller M, *et al.* (2006) Characterization of the *Drosophila* Lipid Droplet Subproteome. *Mol Cel Proteomics* 5(6):1082-1094.
9. Song F, Li D, Wang Y, & Bi X (2018) *Drosophila* Caliban mediates G1-S transition and ionizing radiation induced S phase checkpoint. *Cell Cycle* 17(18):2256-2267.
10. Dai Z, *et al.* (2020) *Drosophila* Caliban preserves intestinal homeostasis and lifespan through regulating mitochondrial dynamics and redox state in enterocytes. *PLoS Genet.* 16(10):e1009140.
11. Yeo SL, *et al.* (1995) On the functional overlap between two *Drosophila* POU homeo domain genes and the cell fate specification of a CNS neural precursor. *Genes Dev* 9(10):1223-1236.
12. Xu T, *et al.* (2015) ProLuCID: An improved SEQUEST-like algorithm with enhanced sensitivity and specificity. *Journal of Proteomics* 129:16-24.
13. Tabb DL, McDonald WH, & Yates JR (2002) DTASelect and Contrast: Tools for Assembling and Comparing Protein Identifications from Shotgun Proteomics. *J. Proteome Res.* 1(1):21-26.
14. Apitz H (2002) pChs-Gal4, a vector for the generation of *Drosophila* Gal4 lines driven by identified enhancer elements *Dros. Inf. Serv.* 85 118-120.
15. Singh SR, *et al.* (2016) The lipolysis pathway sustains normal and transformed stem cells in adult *Drosophila*. *Nature* 538(6):109-115.